Supplementary Information for

Evolutionary Inspired Engineering of Megasynthetases

Kenan A. J. Bozhüyük[1,2,3,&,*], Leonard Präve[1,3,&], Carsten Kegler[1,&], Sebastian Kaiser[4], Yan-Ni Shi[3], Wolfgang Kuttenlochner[5], Leonie Schenk[1,3], Michael Groll[5], Georg K. A. Hochberg[4,6,7], Helge B. Bode[1,3,6,7,8,*]

[1]Max-Planck-Institute for Terrestrial Microbiology, Department of Natural Products in Organismic Interactions, 35043 Marburg, Germany

[2]Myria Biosciences AG, Basel, Switzerland

[3]Molecular Biotechnology, Department of Biosciences, Goethe-University Frankfurt, 60438 Frankfurt, Germany

[4]Evolutionary Biochemistry Group, Max-Planck-Institute for Terrestrial Microbiology, 35043 Marburg, Germany

[5]Center for Integrated Protein Science Munich (CIPSM), Department of Chemistry, Technical University Munich, 85748 Garching, Germany

[6]Center for Synthetic Microbiology (SYNMIKRO), Phillips University Marburg, 35043 Marburg, Germany

[7]Department of Chemistry, Phillips University Marburg, 35043 Marburg, Germany

[8]Senckenberg Gesellschaft für Naturforschung, 60325 Frankfurt, Germany

[&]These authors contributed equally to this work

*Correspondence authors: Kenan.Bozhueyuek@mpi-marburg.mpg.de, helge.bode@mpi-marburg.mpg.de

1. Material and Methods

1.1. Cultivation of strains

All *E. coli* DH10B::*mtaA* cells were cultured either on liquid or solid low salt LB medium ((pH 7.5, 10 g/L tryptone, 5 g/L yeast extract and 5 g/L NaCl). Either kanamycin (50 µg/ml), chloramphenicol (34 µg/ml) or spectinomycin (50 µg/ml) were added as selection markers. Solid media contained 1% (w/v) agar. Cells were cultivated at 37 °C and at 22 °C for peptide production cultures.

1.2. Cloning of biosynthetic gene clusters and NRPS modules

For use as template, genomic DNA (gDNA) was extracted from bacteria indicated in Table S1 by use of the Gentra Puregene Yeast/Bact. Kit (Qiagen) and the Monarch® Genomic DNA Purification Kit (NEB) which in turn was taken as template for the PCR amplification. The proof-reading PCR polymerase Q5® High-Fidelity DNA Polymerase (NEB) and *Phusion* DNA Polymerase (NEB/Thermo Fisher Scientific) in their standard and hot start variations were employed. Oligonucleotides for the PCR and the correct product size are documented in Table S4. In specified cases (Table S4) already cloned NRPS parts were used as template for the PCR. PCR products were agarose gel purified taking the Monarch® DNA Gel Extraction Kit (NEB) to be used as substrate for the Gibson cloning procedure using the Gibson Assembly® Master Mix or the NEBuilder® HiFi DNA Assembly Cloning Kit (NEB). In cases indicated in Table S4 restriction enzyme digests with enzymes indicated were used as one part of the substrate for the Gibson cloning step.

The vector pCK_0407 was cloned in a classic fashion. To this end the plasmid pCK_0407 was linearised using the restriction enzymes AvrII/XbaI and the 1.750 bp fragment ligated to the 1.933 bp fragment of the AvrII/XbaI digest of pCDFDuet (Merck-Novagen).

1.3. Heterologous expression of NRPS constructs and HPLC-MS analysis

After plasmid transformation into *E. coli* DH10B::*mtaA*, cells were grown overnight in LB medium containing all necessary antibiotics (50 µg/ml kanamycin, 34 µg/ml chloramphenicol, 100 µg/ml spectinomycin). 10 ml LB medium containing antibiotics, 0.002 mg/ml L-arabinose and 2 % (v/v) XAD-16 were inoculated with 1 % overnight grown culture. After incubation for 72 h at 22 °C, XAD-16 beads were harvested and one culture volume methanol was added. Methanol extraction was conducted for 60 min at 22 °C. The organic phase was filtrated and diluted 1:10 in methanol. Cleared HPLC-UV-MS analysis was conducted on an UltiMate 3000 system (Thermo Fisher) coupled to an AmaZonX mass spectrometer (Bruker) with an ACQUITY UPLC BEH C18 column

(130 Å, 2.1 mm × 100 mm, 1.7-µm particle size, Waters) at a flow rate of 0.4 ml min−1 (5–95% acetonitrile/water with 0.1% formic acid, vol/vol, 16 min, UV detection wavelength 190–800 nm). HPLC-UV-HRMS analysis was conducted on an UltiMate 3000 system (Thermo Fisher) coupled to an Impact II qTof mass spectrometer (Bruker) with an ACQUITY UPLC BEH C18 column (130 Å, 2.1 mm × 100 mm, 1.7-µm particle size, Waters) at a flow rate of 0.4 ml min−1 16 min, UV detection wavelength 190–800 nm). Evaluation was performed using DataAnalysis 5.3 software (Bruker).

For peptide quantification of NRPS-8- to -20 the production medium was, deviating from above, XPP medium[1] without phenylalanine with 1 mM ß-alanine added.

1.4. Peptide Purification

Compounds **4**, **5**, **7**, **10**, **26**, **41** and **61** were produced in *E. coli* DH10B::*mtaA* expressing the respective NRPS variants. 4L XPP medium containing 34 µg/ml chloramphenicol, 0.002 % L-arabinose and 2 % XAD 16N beads was inoculated with 1 % overnight grown culture as described in section S1.3. The culture was incubated at 180 rpm for 72 h at 22 °C. Subsequently, the XAD 16N beads were extracted 3 times with 500 ml methanol for 30 minutes, stirring. Solvent was fully removed at reduced pressure and the crude extract was completely solved in DMSO in order to purify it by preparative HPLC–MS (LC-MS-System 1260 Infinity II Preparative LC/MSD from Agilent). A C3 column (Agilent ZORBAX 300XB-C3) utilizing a gradient of 40-55 % ACN/H2O (+0.1 % formic acid) was used. The compound was freeze-dried and the purity of the compound was determined by NMR and HPLC-HR-MS.

1.5. Peptide quantification

The absolute production titres were calculated as previously described[2]. Therefore, calibration curves based on pure **1** (for quantification of **1**, **2** and **3**), **4** (**4**, **5**, **15**, **17**, **18**, **32** and **33**), **10** (**6**, **7**, **8**, **9**, **10**, **11** and **16**), **26** (**26**, **27**, **28**, **29**), **34** (**34** and **35**), **36** (**36** and **37**), **38** (**38** and **39**), and **41** (**40**, **41** and **42**), were prepared. The pure compounds were prepared at different concentrations: **1** utilizing a standard curve with concentrations of 5000, 500, 50, 5 and 0.5 µg L^{-1}; **4** utilizing a standard curve with concentrations of 10, 4, 1, 0.4, 0.1, 0.04 and 0.01 mg l^{-1}, **10** utilizing a standard curve with concentrations of 10, 4, 1, 0.4, 0.1 and 0.04 mg l^{-1}, **26** utilizing a standard curve with concentrations of 40, 4, 0.4, 0.04 and 0.004 mg l^{-1}, **34**, **36** and **38** utilizing a standard curve with concentrations of 100, 20, 4, 0.8 and 0.16 mg l^{-1}, **41** utilizing a standard curve with concentrations 10, 5, 2.5, 1.25, 0.625, 0.3125 and 0.1562 mg l^{-1} and measured by LC-MS using HPLC/MS measurements as described above. To ensure sample signals being within the range

of the standard curve they were diluted when necessary. The peak area for each compound at different concentrations was calculated using Compass Data Analysis and used for the calculation of a standard curve passing through the zero point. Triplicates of all *in vivo* experiments were measured. The pure peptide standards **1**, **34**, **36**, **38** were synthesized in-house, **4, 10**, **26** and **41** were purified from production cultures.

1.6. Chemical Synthesis

The linear peptide **1** was synthesized on preloaded resin (0.25 mmol H-Leu-2ClTrt PS resin, Sigma Aldrich, Germany) by solid phase peptide synthesis using standard Fmoc/*t*-Bu chemistry. Fmoc protected amino acids or fatty acids were activated by mixture of 5 eq. Fmoc-AA-OH (or fatty acid), 12 eq. N,N-diisopropylethylamine (DIPEA, Iris Biotech, c = 2.4 M), 5 eq. O-(7-azabenzotriazol-1-yl)-N,N,N′,N′-tetramethyluronium hexafluorophosphate (HATU, Carbolution Chemicals) in 15 ml dimethylformamide (DMF, Carl Roth, Germany). The resin was incubated with the activated amino acid/fatty acid mixture for 2 h at room temperature. After each coupling, the resin was washed with NMP (5 ×), DMF (5 ×) and DCM (5 ×). Finally, the peptide was cleaved by addition of 20 ml of a mixture of Hexafluoroisopropanol (HFIP) and DCM (1:4 v/v). Subsequently, the peptide was deprotected upon addition of 2 ml Trifluoroacetic acid (TFA) incubating for 2 h at room temperature. The linear peptide was dissolved in MeOH in order to purify it by semi-preparative HPLC–MS (Agilent LC-MS-System 1260 Infinity II Analytical-Scale LC/MSD) utilizing a C18 column (Eclipse XDB-C18 (9.4 x 250 mm, 5 µm). The purity was determined by NMR and HPLC-HR-MS analysis.

Chemical synthesis of peptides **34**, **36**, **38** was performed as described previously[2]. The linear sequences were synthesized on preloaded resins (H-AA-2ClTrt PS resin, Sigma Aldrich, Germany) on a 25 µM scale with a Syro Wave peptide synthesizer (Biotage, Sweden) by using standard Fmoc/*t*-Bu chemistry. Fmoc-amino acids were purchased from Carbolution Chemicals (Germany), Iris Biotech (Germany) or Bachem (Switzerland). Therefore, the resin was placed in a plastic reactor vessel with a Teflon frit and an amount of 6 eq. of amino acid derivative (c = 0.2 M) was activated *in situ* at room temperature with 6 eq. of *O*-(6-chlorobenzotriazol-1-yl)-*N*,*N*,*N*′,*N*′-tetramethyluronium hexafluorophosphate (HCTU, Carl Roth, Germany, c = 0.6 M) in dimethylformamide (DMF, Carl Roth, Germany) in the presence of 12 eq. *N,N*-diisopropylethylamine (DIPEA, Iris Biotech, c = 2.4 M) in *N*-methylpyrrolidone (NMP, Iris Biotech) for 50 min. Fmoc-protecting groups were removed with a solution of 40 % piperidine (Iris Biotech) in NMP (v/v %) for 5 min and followed by a second deprotection step with 20 % piperidine in NMP (v/v %) for 10 min. After each coupling and deprotection step, the resin was washed with NMP (4

×). After addition of the final amino acid and deprotection step, the resin was washed with NMP (5 ×), DMF (5 ×) and DCM (5 ×).

For total deprotection or cleavage 0.5 mL 95 % trifluoroacetic acid (TFA, Iris Biotech) and 2.5 % triisopropylsilane (TIS, Sigma Aldrich) in water were added to peptidyl resin and the mixture was agitated for at least 1 h at room temperature. The resin was removed by filtration and washed twice with TFA. Then the cleavage cocktail was evaporated. Linear peptide was dissolved in MeOH in order to purify it by semi-preparative HPLC–MS (Agilent LC-MS-System 1260 Infinity II Analytical-Scale LC/MSD) utilizing a C18 column (Eclipse XDB-C18 (9.4 x 250 mm, 5 µm). The purity was determined by HPLC-HR-MS and NMR.

1.7. Expression and purification of yeast 20 S proteasome

The yeast 20S proteasome was prepared as previously described[3,4].

1.8. IC_{50} value determination with purified yCP

Concentration of purified yeast 20 S proteasome (yCP) was determined spectrophotometrically at 280 nm. yCP (final concentration: 0.05 mg/mL in 100 mM Tris-HCl, pH 7.5) was mixed with DMSO as a control or serial dilutions of fellutamide derivatives in DMSO, thereby not surpassing a final concentration of 10% (v/v) DMSO. After an incubation time of 45 min at RT, fluorogenic substrates Boc-Leu-Arg-Arg-AMC, Z-Leu-Leu-Glu-AMC and Suc-Leu-Leu-Val-Tyr-AMC (final concentration of 200 µM) were added to measure the residual activity of caspase-like (C-L, β1 subunit), trypsin-like (T-L, β2 subunit) and chymotrypsin-like (ChT-L, β5 subunit), respectively. The assay mixture was incubated for another 60 min at RT and afterwards diluted 1:10 in 20 mM Tris-HCl, pH 7.5. The AMC-molecules released by hydrolysis were measured in triplicate with a Varian Cary Eclipse Fluorescence Spectrophotometer (Agilent Technologies) at λ_{exc}=360 nm and λ_{em}=460 nm. Relative fluorescence units were normalized to the DMSO treated control. The calculated residual activities were plotted against the logarithm of the applied inhibitor concentration and fitted with GraphPad Prism 5. Half maximum inhibitory concentration (IC_{50}) values were deduced from the fitted data. They depend on enzyme concentration and are comparable within the same experimental settings.

1.9. Crystallisation and structure determination of the yeast 20S proteasome core particle (yCP) in complex with 41.

Crystals of yCP were grown in hanging drops at 20°C as previously described[3,4]. The protein concentration used for crystallization was 40 mg/mL in Tris / HCl (20 mM, pH 7.5) and EDTA (1

mM). The drops contained 1 µL of protein and 1 µL of the reservoir solution [30 mM magnesium acetate, 100 mM 2-(N-morpholino)ethanesulfonic acid (pH 6.8) and 10% (wt/vol) 2-methyl-2,4-pentanediol]. Crystals appeared after two days and were incubated with a fellutamide derivative at final concentrations of 10 mM for at least 24 h. Droplets were then complemented with a cryoprotecting buffer [30% (wt/vol) 2-methyl-2,4-pentanediol, 15 mM magnesium acetate, 100 mM 2-(N-morpholino)ethanesulfonic acid, pH 6.9] and vitrified in liquid nitrogen. The dataset from the yCP: **41** complex was collected using synchrotron radiation (λ =1.0 Å) at the X06SA-beamline (Swiss Light Source, Villingen, Switzerland). X-ray intensities and data reduction were evaluated using the XDS program package (Table Sx)[5]. Conventional crystallographic rigid body, positional, and temperature factor refinements were carried out with REFMAC5[6] using coordinates of the yCP structure as starting model (PDB ID 5CZ4)[7]. For model building, the programs SYBYL and COOT[8] were used. The final coordinates yielded excellent R factors, as well as geometric bond and angle values. Coordinates were confirmed to fulfill the Ramachandran plot and have been deposited in the RCSB (PDB ID xxxx)

1.10 Evolutionary analysis of ATC tridomains (XUs) from NRPS using PhyML_Multi

The amino acid sequence of NRPS were collected from our *Photorhabdus* and *Xenorhabdus* genome collection. We also included a few NRPS representatives from actinomycetes, cyanobacteria and other proteobacteria in our analysis (sup. x). XUs from NRPS protein sequences were extracted from our NRPS dataset using local BLAST with the second XU from GxpS of Photorhabdus laumondii TT01 as query. XUs were aligned using MUSCLE v3.8.31[9] and trimed with trimAl v1.2[10]. This alignment was used for the evolutionary analysis using the software PhyML_Multi. We specified that PhyML_multi search for two trees under a hidden markov model that together best fit the alignment. Since PhyML_Multi does not have a model finder, the model finder of IQ-tree[10] with the selection of '-msub nuclear' was used. IQ-tree chose JTT as the best fit model which was also used for the analysis with PhyML_Multi with a 4-category gamma distribution of among site rate-variation. Afterwards, the log likelihood of tree 1 was deducted from the log likelihood of tree 2 and plotted.

1.11 Evolutionary analysis of the T domain from NRPS using PhyML_Multi

The T domain dataset covered the amino acid sequence of the A-T-Linker and the T domain. This area was extracted from our NRPS dataset using local BLAST with the third T domain from GxpS of Photorhabdus laumondii TT01 as query. The T domains were aligned using MUSCLE and

carefully trimmed manually to reduce gaps. Afterwards, the software PhyML_Multi was used to detect recombination breakpoints and phylogenetic histories within the T domain.

1.12 Topological comparison of different phylogenetic trees

The four different trees generated by PhyML_Multi were pruned using the software mesquite[11] to reduce the number branches on the trees for visual clarity. Trees were compared using the R package phytools[12].

Table S1. Strains used in this work.

Strain	Genotype/NRPS	Reference
E. coli DH10B	F_mcrA (*mrr-hsd*RMS-*mcr*BC), 80*lacZ*Δ, M15, Δ*lac*X74 *rec*A1 *end*A1 *ara*D 139Δ(*ara*, *leu*)7697 *gal*U *gal*K λ *rps*L (*Strr*) *nup*G / -	[13]
E. coli DH10B::*mta*A	DH10B with *mtaA* from pCK_*mtaA*Δ*entD* / -	[14]
Bacillus subtilis subsp. subtilis str. 168 DSM 402	WT (*srfAB, ppsA*)	DSMZ
M. xanthus DK1622	WT (*MchABC*)	[15, 16]
Pseudomonas lurida sp. MYb11	WT (v*iscA*)	[17]
Serratia sp. SCBI	WT (*swrA*)	[18]
S. marcescens DSM 12481	WT (*swrW*)	DSMZ
P. luminescens subsp. laumondii TT01	WT (*gxpS*, *kolS*)	DSMZ
P. temperata KT122	WT (4325)	[19]
X. bovienii SS-2004	WT (*txlA*)	[20]
X. doucetiae DSM 17909	WT (*xabA, prtA*)	DMSZ
X. indica DSM17382	WT (*xldS*, *xtvB, xeyS, XlNDV2_09420*)	DSMZ
X. innexi DSM 16336	WT (*fitAB*1*)	DSMZ
X. mauleonii DSM 17908	WT (*ftrAB*2*)	DSMZ
X. miraniensis DSM 17902	WT (*ambS*)	DMSZ
X. nematophila ATCC19061	WT (*xtpS*, *PAX*)	ATCC
X. stockiae DSM 17904	WT (*xabA*)	DMSZ
X. szentirmaii DSM 16338	WT (*xabA*)	DMSZ
Xenorhabdus sp. KK7.4	WT (*XEKKV2_12060*)	[20,21]
Chondromyces crocatus Cm c5 DSM 14714	WT (*cpnD*)	DMSZ

Table S2. Protein and nucleic acid references to data bank used for NRPS-constructs.

NRPS-construct	GenPept locus/protein ID	GenBank	locus tag	gene
NRPS-8	PHM30481.1 PHM29999	NIBU01000054.1 NIBU01000077.1	Xinn_03284 Xinn_03635	*fitAB*
NRPS-9	YP_003466710.1	FN667741	XBJ1_0775	*txlA*
NRPS-10	WP_148886166.1	NZ_VNHN01000062.1	LY16_RS14705	*prtA*
NRPS-11	WP_099121989.1	NZ_NJAH01000014.1	Xekk_RS12280	XEKKV2_12060
NRPS-12	MBC8943736.1	NKHP01000001.1	Xind_00118	XINDV2_09420
NRPS-13	AIM23801.1	CP003424.1	SERRSCBI_21215	*swrA*
NRPS-14	WP_187681863	NZ_JACSZU010000009.1	IAI52_RS13305	*viscA*
NRPS-15	WP_012987679	NC_013892.1	XBJ1_1126	*xfpS*
NRPS-16	CAB13717.2	AL009126.3	BSU18340	*ppsA*
NRPS-19	PHM39367.1 PHM39368	NITY01000011.1	Xmau_02974 Xmau_02975	*ftrAB*
NRPS-20	BAD60917.1	AB193098.2	AB193098.2	*swrW*
NRPS-17	ABF89060.1 ABF89457.1	CP000113.1	MXAN_4077 MXAN_4078	*mchAB*
NRPS-18	PHM40846.1	NIUA01000001.1	Xszus_00521	*xabA*

Table S3. Plasmids and corresponding NRPSs used in this work.

NRPS	Plasmids	Genotype	Reference
	pCOLA_ara/ tacI	ori ColA, kanR, *araC*- $P_{BAD,}$ and tacI	[22]
	pCK_0401	ori p15A, cmR, *araC*- $P_{BAD,}$ and tacI	[23]
	pCK_0407	ori ColDF13, specR, *araC*- $P_{BAD,}$ and tacI; mtaA	This work
-1	pLP23	ori ColA, *kan*^{R}, *araC*- $P_{BAD,}$ *xabABC*_C1A1-*gxpS*_T3C/E4A4T4C/E5A5T5TE and *tacI*	This work
-2	pLP24	ori ColA, *kan*^{R}, *araC*- $P_{BAD,}$ *xabABC*_C1A1T1$_{1/2}$-*gxpS*_T3$_{1/2}$C/E4A4T4C/E5A5T5TE and *tacI*	This work
-3	pFP7	ori ColA, *kan*^{R}, *araC*- $P_{BAD,}$ *xabABC*_C1A1T1$_{1/2}$-*gxpS*_T3$_{1/2}$C/E4A4T4C/E5A5T5TE and *tacI*	This work
-4	pFP8	ori ColA, *kan*^{R}, *araC*- $P_{BAD,}$ *xabABC*_C1A1T1$_{1/2}$-*gxpS*_T3$_{1/2}$C/E4A4T4C/E5A5T5TE and *tacI*	This work
-5	pFP9	ori ColA, *kan*^{R}, *araC*- $P_{BAD,}$ *xabABC*_C1A1T1$_{1/2}$-*gxpS*_T3$_{1/2}$C/E4A4T4C/E5A5T5TE and *tacI*	This work
-6	pFP11	ori ColA, *kan*^{R}, *araC*- $P_{BAD,}$ *xabABC*_C1A1T1$_{1/2}$-*gxpS*_T3$_{1/2}$C/E4A4T4C/E5A5T5TE and *tacI*	This work
-7	pLP31	ori ColA, *kan*^{R}, *araC*- $P_{BAD,}$ *xabABC*_C1A1T1-*gxpS*_C/E4A4T4C/E5A5T5TE and *tacI*	This work
-8	pCK_0683	ori p15A, cmR, *araC*- $P_{BAD,}$ *fitAB* 6 modular NRPS *X. mauleonii*	This work
-9a	pCK_0760	ori p15A, cmR, *araC*- P_{BAD}, *txlA* C1A1 – T1 modules 2-6 *fitAB*	This work
-9b	pCK_0761	ori p15A, cmR, *araC*- P_{BAD}, *txlA* C1A1 T1$_{1/2}$ – modules 2-6 *fitAB*	This work
-10a	pCK_0762	ori p15A, cmR, *araC*- P_{BAD}, *prtA* C1A1 – T1 modules 2-6 *fitAB*	This work
-10b	pCK_0762	ori p15A, cmR, *araC*- P_{BAD}, *prtA* C1A1 T1$_{1/2}$ – modules 2-6 *fitAB*	This work
-11a	pCK_0768	ori p15A, cmR, *araC*- P_{BAD}, *xucA** C1A1^{Val} – T1 modules 2-6 *fitAB*	This work
-11b	pCK_0768	ori p15A, cmR, *araC*- P_{BAD}, *xucA** C1A1^{Val} T1$_{1/2}$ – modules 2-6 *fitAB*	This work
-12a	pCK_0820	ori p15A, cmR, *araC*- P_{BAD}, *xucA** C1A1^{Ser} – T1 modules 2-6 *fitAB*	This work
-13a	pCK_0822	ori p15A, cmR, *araC*- P_{BAD}, *xucA** C1A1^{Leu} – T1 modules 2-6 *fitAB*	This work
-13b	pCK_0823	ori p15A, cmR, *araC*- P_{BAD}, *viscA* C1A1^{Leu} T1$_{1/2}$ – modules 2-6 *fitAB*	This work
-14a	pCK_0824	ori p15A, cmR, *araC*- P_{BAD}, *xucA** C1A1^{Leu} – T1 modules 2-6 *fitAB*	This work
-14b	pCK_0825	ori p15A, cmR, *araC*- P_{BAD}, *xucA** C1A1^{Leu} T1$_{1/2}$ – modules 2-6 *fitAB*	This work
-15a	pCK_0826	ori p15A, cmR, *araC*- P_{BAD}, *xtpS* C1A1^{Leu} – T1 modules 2-6 *fitAB*	This work
-15b	pCK_0827	ori p15A, cmR, *araC*- P_{BAD}, *xtpS* C1A1^{Leu} T1$_{1/2}$ – modules 2-6 *fitAB*	This work
-16a	pCK_0828	ori p15A, cmR, *araC*- P_{BAD}, *xtpS* C1A1^{Leu}T1$_{1/2}$ – modules 2-6 *fitAB*	This work
-19	pCK_0680	ori p15A, cmR, *araC*- P_{BAD}, *ftrAB* 6 modular WT NRPS	This work
-17a	pCK_0868	ori CloDF13, specR, *araC*-P_{BAD} *mchA*-PKS and tacI	This work

-20b	pCK_0870	ori p15A, cmR, *araC- P_{BAD}*, *swrW* C1A1^{Ser} modules 2-6 *ftrAB*	This work
-19a	pCK_0873	ori p15A, cmR, *araC- P_{BAD}*, (*mchA*-PKS *mchB* C1A1MT^{Thr} - modules 2-6 *fitAB*	This work
-20b	pSB002	ori p15A, cmR, *araC- P_{BAD}*, *xabA* C1A1^{Pro}T1_C2A2^{Gly}T2$_{1/2}$ – modules 2-6 *fitAB*	This work
-21a	pLS_019	ori p15A, cm^R, araC-P_{BAD} I-*Ceu*I, I-*Sce*I gxps_A_1T_1C/E_2A_2_*xabA*_$T_3C_4A_4$_*gxps*_$T_4C/E_5A_5T_5$TE and *tacI-araE*	This work
-21b	pLS_191	ori p15A, cm^R, araC-P_{BAD} I-*Ceu*I, I-*Sce*I gxps_$A_1T_1C/E_2A_2T_2^{1/2}$_*xabA*_$T3^{1/2}C_4A_4T_4^{1/2}$_*gxps*_$T4^{1/2}C/E_5A_5T_5$TE and *tacI-araE*	This work
-22a	pLS_018	ori p15A, cm^R, araC-P_{BAD} I-*Ceu*I, I-*Sce*I gxps_A_1T_1C/E_2A_2_*xlds*_$T_2C_3A_3$_*gxps*_$T_4C/E_5A_5T_5$TE and *tacI-araE*	This work
-22b	pLS_017	ori p15A, cm^R, araC-P_{BAD} I-*Ceu*I, I-*Sce*I gxps_$A_1T_1C/E_2A_2T_2^{1/2}$_*xlds*_$T_2^{1/2}C_3A_3T_3^{1/2}$_*gxps*_$T_4^{1/2}C/E_5A_5T_5$TE and *tacI-araE*	This work
-23a	pLS_009	ori p15A, cm^R, araC-P_{BAD} I-*Ceu*I, I-*Sce*I gxps_A_1T_1C/E_2A_2_*cpnd*_$T_2C_3A_3$_*gxps*_$T_4C/E_5A_5T_5$TE and *tacI-araE*	This work
-23b	pLS_008	ori p15A, cm^R, araC-P_{BAD} I-*Ceu*I, I-*Sce*I gxps_$A_1T_1C/E_2A_2T2^{1/2}$_*cpnd*_$T_2^{1/2}C_3A_3T_3^{1/2}$_*gxps*_$T_4^{1/2}C/E_5A_5T_5$TE and *tacI-araE*	This work
-24a	pLS_003	ori p15A, cm^R, araC-P_{BAD} I-*Ceu*I, I-*Sce*I gxps_A_1T_1C/E_2A_2_*mchC$_A$*_$T_2C_3A_3$_*gxps*_$T_4C/E_5A_5T_5$TE and *tacI-araE*	This work
-24b	pLS_002	ori p15A, cm^R, araC-P_{BAD} I-*Ceu*I, I-*Sce*I gxps_$A_1T_1C/E_2A_2T2^{1/2}$_*mchC$_A$*_$T_2^{1/2}C_3A_3T_3^{1/2}$_*gxps*_$T_4^{1/2}C/E_5A_5T_5$TE and *tacI-araE*	This work
-25	pPI16_XUT	ori p15A, *cm^R*, *araC-P_{BAD}* *xldS*_C1A1T1$_{1/2}$-*xabA*_T1$_{1/2}$C1-*kolS*_A2T2C3-*gxpS*_A2T2$_{1/2}$-*xtvAB*_T2$_{1/2}$Red *tacI* and *araE*	This work
-26	pPI16	ori p15A, *cm^R*, *araC-P_{BAD}* *xldS*_C1A1T1$_{1/2}$-*xabA*_T1$_{1/2}$C1-*kolS*_A2T2C3-*gxpS*_A2T2$_{1/2}$-*xtvAB*_T2$_{1/2}$Red *tacI* and *araE*	This work
-27	pPI16_typeII	ori p15A, *cm^R*, *araC-P_{BAD}* *xldS*_C1A1T1$_{1/2}$-*xabA*_T1$_{1/2}$C1-*kolS*_A2T2C3-*gxpS*_A2T2$_{1/2}$-*xtvAB*_T2$_{1/2}$Red *tacI* and *araE*	This work
-28	pPI16_end	ori p15A, *cm^R*, *araC-P_{BAD}* *xldS*_C1A1T1$_{1/2}$-*xabA*_T1$_{1/2}$C1-*kolS*_A2T2C3-*gxpS*_A2T2$_{1/2}$-*xtvAB*_T2$_{1/2}$Red *tacI* and *araE*	This work

Table S4. Primer and templates used in this work to generate indicated plasmids. Sizes of the PCR products are depicted below the template.

Plasmids	Oligo-nucleotides	Sequence (5' to 3'), alternatively restriction enzymes	Template Product size in bp
pLP23	LP134	TGGGCTAACAGGAGGAATTCCATGCCTATGTCG TGCAATCG	*X. stockiae* gDNA 3.062
	LP135	GCTTGGTACTCATGCGTGACTACCGC	
	LP132	CAATCTGCGGTAGTCACGCATGAGTACCAAGC GCCACAAGGGGAAATTG	pJW76 5.347
	LP133	GAACATTCGGATCAAGTACCGTTAACGCGG	
	LP136	AACGGTACTTGATCCGAATGTTC	pJW76 5.545
	LP137	GGAATTCCTCCTGTTAGCCC	
pLP24	LP134	TGGGCTAACAGGAGGAATTCCATGCCTATGTCG TGCAATCG	*X. stockiae* gDNA 3.148
	LP139	AGAAACTGTCATGTCGGCCAACCTGTTCTAATC CTAATAAACTTTGC	
	LP138	GTTGGCCGACATGACAGTTTCTTTGCC	pJW76 5.251
	LP133	GAACATTCGGATCAAGTACCGTTAACGCGG	
	LP136	AACGGTACTTGATCCGAATGTTC	pJW76 5.545
	LP137	GGAATTCCTCCTGTTAGCCC	
pFP7	LP55	GAGGAATTCCATGCCTATGTCGTGCAATCG	*X. stockiae* gDNA 3.149
	LP60	CGCCCAAGGCAAAGAAATGGTCACGGCGACCA ACCTG	
	LP59	CCATTTCTTTGCCTTGGGCGGTCAC	pJW76 5.308
	LP44	GTAAATCACATACGCCAGATGTCGTGAGGTC	
	LP43	CGACATCTGGCGTATGTGATTTACACTTCTG	pJW76 5.487
	LP56	CGACATAGGCATGGAATTCCTCCTGTTAGC	
pFP8	LP55	GAGGAATTCCATGCCTATGTCGTGCAATCG	*X. stockiae* gDNA 3.157
	LP62	CGAGTGACCGCCCAATTCAAAGAAATGGTCAC	
	LP61	TTGAATTGGGCGGTCACTCGCTGTTGGC	pJW76 5.300
	LP44	GTAAATCACATACGCCAGATGTCGTGAGGTC	
	LP43	CGACATCTGGCGTATGTGATTTACACTTCTG	pJW76 5.487
	LP56	CGACATAGGCATGGAATTCCTCCTGTTAGC	
pFP9	LP55	GAGGAATTCCATGCCTATGTCGTGCAATCG	*X. stockiae* gDNA 3.171
	LP64	CTGACTGCCAGAAGAGAGTCACCACCC	
	LP63	GACTCTCTTCTGGCAGTCAGGATGATCGAACG	pJW76 5.286
	LP44	GTAAATCACATACGCCAGATGTCGTGAGGTC	
	LP43	CGACATCTGGCGTATGTGATTTACACTTCTG	pJW76 5.487
	LP56	CGACATAGGCATGGAATTCCTCCTGTTAGC	
pFP11	LP55	GAGGAATTCCATGCCTATGTCGTGCAATCG	*X. stockiae* gDNA 3.202
	LP66	CAATCCTATACGACGTATACGGGCAGTCATCTG	
	LP65	CCGTATACGTCGTATAGGATTGGGCCTGTC	pJW76 5.257
	LP44	GTAAATCACATACGCCAGATGTCGTGAGGTC	
	LP43	CGACATCTGGCGTATGTGATTTACACTTCTG	pJW76 5.487
	LP56	CGACATAGGCATGGAATTCCTCCTGTTAGC	
pLP31	LP134	TGGGCTAACAGGAGGAATTCCATGCCTATGTCG TGCAATCG	*X. stockiae* gDNA 3.297
	LP160	GCTAATTTCACGATGTTCAGTAATAACCTGAGC CAACTC	
	LP161	GTTATTACTGAACATCGTGAAATTAGCGTGCCT G	pJW76 5.110
	LP133	GAACATTCGGATCAAGTACCGTTAACGCGG	

	LP136	AACGGTACTTGATCCGAATGTTC	pJW76 5.545
	LP137	GGAATTCCTCCTGTTAGCCC	
pPI16	26	TTTTTGGGCTAACAGGAGGAATTCCATGAATAT GACACGTAACCATACATCC	*X. indica* gDNA 3.098
	29	GTGAGTGCCCGCCAAGCTCAAAGAAATGATCG TGGCGACCGACAC	
	12	TTCTTTGAGCTTGGCGGGC	*X. doucetiae* gDNA 1.536
	AL13-2	ATCCACCAGCAGTTGTTGTCG	
	40	GGAGCGACAACAACTGCTGGTGGATTGGAATG CAACCGCAACC	*P. luminescens* subsp. laumondii TT01 gDNA 3.203
	AT_492	GATAGGGGGTTTCTGTCGCGTTCCAAGTTTCCA ATAACAACTTGCGCTC	
	AT_226	TGGAACGCGACAGAAACC	*P. luminescens* subsp. laumondii TT01 gDNA 1.668
	9	ATTATCGTGTCGGCCGATTTGCTC	
	14	AAATCGGCCGACACGATAATTTTTTCAATATCG GAGGACATTCGC	*X. indica* gDNA 1.383
	6	TATACGAGCCGATGATTAATTGTCATTACTTATA TTCCGGTTCATATTTTTTGTCC	
	pACYC-2	TGACAATTAATCATCGGCTCG	pJW75 5.220
	pACYC-1	GGAATTCCTCCTGTTAGCC	
pPI16_XUT	26	TTTTTGGGCTAACAGGAGGAATTCCATGAATAT GACACGTAACCATACATCC	*X. indica* gDNA 3.098
	29	GTGAGTGCCCGCCAAGCTCAAAGAAATGATCG TGGCGACCGACAC	
	12	TTCTTTGAGCTTGGCGGGC	*X. doucetiae* gDNA 1.536
	AL13-2	ATCCACCAGCAGTTGTTGTCG	
	40	GGAGCGACAACAACTGCTGGTGGATTGGAATG CAACCGCAACC	*P. luminescens* subsp. laumondii TT01 gDNA 3.203
	AT_492	GATAGGGGGTTTCTGTCGCGTTCCAAGTTTCCA ATAACAACTTGCGCTC	
	AT_226	TGGAACGCGACAGAAACC	*P. luminescens* subsp. laumondii TT01 gDNA 1.578
	LP356	AATTTGGCGAGCAAAAGCATCC	
	LP357	AGAGGATGCTTTTGCTCGCCAAATTTCTGAGGA ACGTCTGACTTC	*X. indica* gDNA 1.478
	6	TATACGAGCCGATGATTAATTGTCATTACTTATA TTCCGGTTCATATTTTTTGTCC	
	pACYC-2	TGACAATTAATCATCGGCTCG	pJW75 5.220
	pACYC-1	GGAATTCCTCCTGTTAGCC	
pPI16_type II	26	TTTTTGGGCTAACAGGAGGAATTCCATGAATAT GACACGTAACCATACATCC	*X. indica* gDNA 3.098
	29	GTGAGTGCCCGCCAAGCTCAAAGAAATGATCG TGGCGACCGACAC	
	12	TTCTTTGAGCTTGGCGGGC	*X. doucetiae* gDNA 1.536
	AL13-2	ATCCACCAGCAGTTGTTGTCG	

	40	GGAGCGACAACAACTGCTGGTGGATTGGAATG CAACCGCAACC	*P. luminescens* subsp. laumondii TT01 gDNA 3.203
	AT_492	GATAGGGGGTTTCTGTCGCGTTCCAAGTTTCCA ATAACAACTTGCGCTC	
	AT_226	TGGAACGCGACAGAAACC	*P. luminescens* subsp. laumondii TT01 gDNA 1.680
	LP358	CAAGGCAAAAAAATTATCGTGTCGGC	
	LP359	CCGACACGATAATTTTTTTGCCTTGGGAGGACA TTCGCTATTAGC	*X. indica* gDNA 1.376
	6	TATACGAGCCGATGATTAATTGTCATTACTTATA TTCCGGTTCATATTTTTTGTCC	
	pACYC-2	TGACAATTAATCATCGGCTCG	pJW75 5.220
	pACYC-1	GGAATTCCTCCTGTTAGCC	
pPI16_end	26	TTTTTGGGCTAACAGGAGGAATTCCATGAATAT GACACGTAACCATACATCC	*X. indica* gDNA 3.098
	29	GTGAGTGCCCGCCAAGCTCAAAGAAATGATCG TGGCGACCGACAC	
	12	TTCTTTGAGCTTGGCGGGC	*X. doucetiae* gDNA 1.536
	AL13-2	ATCCACCAGCAGTTGTTGTCG	
	40	GGAGCGACAACAACTGCTGGTGGATTGGAATG CAACCGCAACC	*P. luminescens* subsp. laumondii TT01 gDNA 3.203
	AT_492	GATAGGGGGTTTCTGTCGCGTTCCAAGTTTCCA ATAACAACTTGCGCTC	
	AT_226	TGGAACGCGACAGAAACC	*P. luminescens* subsp. laumondii TT01 gDNA 1.803
	LP360	TGCGCAGATTTTCTCGGTAAATGTCGCC	
	LP361	GACATTTACCGAGAAAATCTGCGCATATCTGAA TAATAATCAAAAAAACAATAACGAAATG	*X. indica* gDNA 1.250
	6	TATACGAGCCGATGATTAATTGTCATTACTTATA TTCCGGTTCATATTTTTTGTCC	
	pACYC-2	TGACAATTAATCATCGGCTCG	pJW75 5.220
	pACYC-1	GGAATTCCTCCTGTTAGCC	
pCK_0678	ck002 ck0467 ck0436b ck0468 ck0465 ck0468	CATGGAATTCCTCCTGTTAG CATCAGGATATGTTAATTAACCTAGGCTGCTGC CAC AGGAATTCCATGACAAAATCTGAATATTTAGTAA GTTCA GAATTGTCAGAAACCTACCAAGCTTTGCG CCTAGGTTAATTAACATATCCTGATGGGCTTTG GCTCCTG TTCCCGCAAAGCTTGGTAGGTTTCTGAC	pCK_0401 3.672 *X. mauleonii* gDNA 3.773 *X. mauleonii* gDNA 6.992
pCK_0679	 ck0459 ck0460 ck0471 ck0472	MluI/SnaBI CAAAGCGGGACCAAAGCCATG TGAGACCTTTTTTTGGTCTCGGAATTCCTCCTGT TAG CCGAGACCAAAAAAAGGTCTCACCCCTTGAATA CAAGGCGTTGC CCCGTTCGCTGGGATATTCTGG	pCK_0678 12.499 pCK_0401 230 pCK_0678 365

pCK_0680 NRPS-19		NcoI/PacI	pCK_0678 14.247
	ck0469b	GGTGGCAGCAGCCTAGGTTAATTAACTGGCTTT ATTAAGAT-	*X. mauleonii* gDNA
	ck0470	ACCTCAAGAAAACCCCAGCCCCTGATAGGTATG TTTG	12.632
pCK_0681		MluI/AscI	pCK_0680 12.905
	ck0594	GGCACCACCGATATACAGTTCACC	pCK_0680
	ck0463b	AGGAATTCCATGACAAAATCTGAATATTTAGTAA GTTCA	2.520 pCK_0401
	ck0459	CAAAGCGGGACCAAAGCCATG	230
	ck0460	TGAGACCTTTTTTTGGTCTCGGAATTCCTCCTGT TAG	
pCK_0682	ck0455	CTGTGATATCAGCCAATTAATTAACCTAGGCTG CTGCCAC	pCK_0401 3.681
	ck0456	GATCTCATGGAATTCCTCCTGTTAGCCCA	
	ck0451	TTTGGGCTAACAGGAGGAATTCCATGAGATCAT TTGAG-GATTCACTGA	*X. innexi* gDNA 10.179
	ck0452	GGGTCTTTAGACCACCCGATTGC	
	ck0453	GCGCAATCGGGTGGTCTAAAGAC	*X. innexi* gDNA
	ck0454	CTAGGTTAATTAATTGGCTGATATCACAGTGCT GTAATGG	3.904
pCK_0683 NRPS-8		BglII/AvrII	pCK_0682 17.584
	ck0457	GAACCAAACAGGGTTATCGTCAGTGC	*X. innexi* gDNA
	ck0522	TGCTCAGCGGTGGCAGCAGCCTAGGTTAATTTA CGCCAATACCTTTTCCTGAC	8.441
pCK_0684		AvrII/AscI	pCK_0682 12.549
	ck0454	CTAGGTTAATTAATTGGCTGATATCACAGTGCT GTAATGG	pCK_0682 3693
	ck0460	TGAGACCTTTTTTTGGTCTCGGAATTCCTCCTGT TAG	
	ck0461b	CGAGACCAAAAAAAGGTCTCAGCCCCTTATCCG CAGGATAAAC	pCK_0682 174
	ck0462	TGTCATCAGATGATGCGCCAGTTGG	
pCK_0685		BglII/AvrII	pCK_0684 16.242
	ck0457	GAACCAAACAGGGTTATCGTCAGTGC	*X. innexi* gDNA
	ck0523	TATTGCTCAGCGGTGGCAGCAGCCTAGGTTAAT TTACGCCAATACCTTTTCCTGAC	8.444
pCK_0760 NRPS-9a		BsaI/AatII	pCK_0685 20.443
	ck0618	TATGTTGCCCCCCGTAACGCA	pCK_0683
	ck0592	AATATAAGCAGCCATATCGCTGAGCG	2.658
	ck0475	TTTTTTTGGGCTAACAGGAGGAATTCAATGAGA ACATCTGAAAGCTCGTTG	*X. bovienii* gDNA 3.003
	ck0635	TGCGTTACGGGGGGCAACATAACCGTCCCGGT TTCCCCA	
pCK_0761 NRPS-9b		BsaI/AatII	pCK_0685 20.443

	ck0617 ck0592 ck0475 ck0636	AATTCCCTGAGCGCCATTAAGCTG AATATAAGCAGCCATATCGCTGAGCG TTTTTTTGGGCTAACAGGAGGAATTCAATGAGA ACATCTGAAAGCTCGTTG GCTTAATGGCGCTCAGGGAATTTCCCCCGATCC GGAAAAAGTTA	pCK_0683 2.550 *X. bovienii* gDNA 3.112
pCK_0762 NRPS-10a	 ck0618 ck0592 ck0477 ck0637	BsaI/AatII TATGTTGCCCCCCGTAACGCA AATATAAGCAGCCATATCGCTGAGCG TTTTTTTGGGCTAACAGGAGGAATTCAATGAGA ATACCTGAAGGTTCGT TGCGTTACGGGGGGCAACATAACTGTCCCGGT TTTCCCATACG	pCK_0685 20.443 pCK_0683 2.658 *X. doucetiae* gDNA 2.997
pCK_0763 NRPS-10b	 ck0617 ck0592 ck0477 ck0638	BsaI/AatII AATTCCCTGAGCGCCATTAAGCTG AATATAAGCAGCCATATCGCTGAGCG TTTTTTTGGGCTAACAGGAGGAATTCAATGAGA ATACCTGAAGGTTCGT GCTTAATGGCGCTCAGGGAATTGCCACCGATA CGGAAAAAATTATCC	pCK_0685 20.443 pCK_0683 2.550 *X. doucetiae* gDNA 3.106
pCK_0768 NRPS-11a	 ck0618 ck0592 ck0487 ck0648	BsaI/AatII TATGTTGCCCCCCGTAACGCA AATATAAGCAGCCATATCGCTGAGCG TTTTTTTGGGCTAACAGGAGGAATTCAATGAGA AAAGCTGAGGATCATTTGAA TGCGTTACGGGGGGCAACATAACTGTCTCTGTT GCCGAAAGC	pCK_0685 20.443 pCK_0683 2.658 X. sp. KK7.4 gDNA 2.943
pCK_0769 NRPS-11b	 ck0617 ck0592 ck0487 ck0649	BsaI/AatII AATTCCCTGAGCGCCATTAAGCTG AATATAAGCAGCCATATCGCTGAGCG TTTTTTTGGGCTAACAGGAGGAATTCAATGAGA AAAGCTGAGGATCATTTGAA GCTTAATGGCGCTCAGGGAATTGCCGCCGATA CGGAAGAAATTATC	pCK_0685 20.443 pCK_0683 2.550 X. sp. KK7.4 gDNA 3.052
pCK_0820 NRPS-12a	 ck0618 ck0592 ck0708 ck0717	BsaI/AatII TATGTTGCCCCCCGTAACGCA AATATAAGCAGCCATATCGCTGAGCG TTTTTTTGGGCTAACAGGAGGAATTCAATGAAT CACCCTGAAAATATGAAAC TGCGTTACGGGGGGCAACATATTCTTGTGTGAT TACTGCTGAATG	pCK_0685 20.443 pCK_0683 2.658 *X. indica* gDNA 3.030
pCK_0822 NRPS-13a	 ck0618 ck0592 ck0711 ck0719	BsaI/AatII TATGTTGCCCCCCGTAACGCA AATATAAGCAGCCATATCGCTGAGCG TTTTTTTGGGCTAACAGGAGGAATTCAATGAAC AAACAAACTGATGTGAAGAG	pCK_0685 20.443 pCK_0683 2.658 Serratia sp. SCBI gDNA 4011

		TGCGTTACGGGGGGCAACATAGTTTTCACGCATGGCGGC	
pCK_0823 NRPS-13b		BsaI/AatII	pCK_0685 20.443
	ck0617	AATTCCCTGAGCGCCATTAAGCTG	pCK_0683
	ck0592	AATATAAGCAGCCATATCGCTGAGCG	2.550
	ck0711	TTTTTTTGGGCTAACAGGAGGAATTCAATGAACAAACAAACTGATGTGAAGAG	Serratia sp. SCBI gDNA
	ck0720	GCTTAATGGCGCTCAGGGAATTACCGCCCAACTCGAAGAAG	4120
pCK_0824 NRPS-14a		BsaI/AatII	pCK_0685 20.443
	ck0618	TATGTTGCCCCCCGTAACGCA	pCK_0683
	ck0592	AATATAAGCAGCCATATCGCTGAGCG	2.658
	ck0714	TTTTTTTGGGCTAACAGGAGGAATTCAATGAAGCATTCCACCCGCC	*P. lurida* gDNA
	ck0721	TGCGTTACGGGGGGCAACATACAGGCGAGTGACGAAGGC	2.877
pCK_0825 NRPS-14b		BsaI/AatII	pCK_0685 20.443
	ck0617	AATTCCCTGAGCGCCATTAAGCTG	pCK_0683
	ck0592	AATATAAGCAGCCATATCGCTGAGCG	2.550
	ck0714	TTTTTTTGGGCTAACAGGAGGAATTCAATGAAGCATTCCACCCGCC	*P. lurida* gDNA
	ck0722	GCTTAATGGCGCTCAGGGAATTCCCGCCGAGTTCAAAGAAG	2.986
pCK_0826 NRPS-15a		BsaI/AatII	pCK_0685 20.443
	ck0618	TATGTTGCCCCCCGTAACGCA	pCK_0683
	ck0592	AATATAAGCAGCCATATCGCTGAGCG	2.658
	ck0723	TTTTTTTGGGCTAACAGGAGGAATTCAATGGATAACATTCTGGCCTCG	*X. bovienii* gDNA
	ck0729	TGCGTTACGGGGGGCAACATAAACATAGCGGCTCTGTTTAAAATC	2.877
pCK_0827 NRPS-15b		BsaI/AatII	pCK_0685 20.443
	ck0617	AATTCCCTGAGCGCCATTAAGCTG	pCK_0683
	ck0592	AATATAAGCAGCCATATCGCTGAGCG	2.550
	ck0723	TTTTTTTGGGCTAACAGGAGGAATTCAATGGATAACATTCTGGCCTCG	*X. bovienii* gDNA
	ck0730	GCTTAATGGCGCTCAGGGAATTGCCCCCCAGATGAAAAAAGT	2.986
pCK_0828 NRPS-16		BsaI/AatII	pCK_0685 20.443
	ck0618	TATGTTGCCCCCCGTAACGCA	pCK_0683
	ck0592	AATATAAGCAGCCATATCGCTGAGCG	2.658
	ck0726	TTTTTTTGGGCTAACAGGAGGAATTCAATGAGCGAACATACTTATTCTTTAACC	*B. subtilis* 168 gDNA
	ck0731	TGCGTTACGGGGGGCAACATAGTAGGTCTCCGCATCTGC	2.925
pCK_0868	ck0828	TTAATTAACCTAGGCTGCTGCCACC	pCK_0406
	ck0829	CATTGAATTCCTCCTGTTAGCCCAAAAAAACG	3.173
	ck0785b	TTTTTTTGGGCTAACAGGAGGAATTCAATGAGCGCAGTGTCCAATATTGA	*M. xanthus* gDNA
	ck0867	ACTTCCGCTTCGGGAAGGACAATCT	3.281

	ck0866 ck0868	AGATTGTCCTTCCCGAAGCGGAAGT TGGCAGCAGCCTAGGTTAATTAATGGTGTACTC ATGCTGTCTCCCTCT	*M. xanthus* gDNA 3.261
pCK_0870 NRPS-20b		BsaI/AatII	pCK_0681 21.482
	ck0787	GGCGGCAATTCCCTGATGG	pCK_0680
	ck0788	GCATTGAAGAATTTTTCTTGTGCAGC	2135
	ck0820	TTTTTTTGGGCTAACAGGAGGAATTCAATGTCC GCTTATTCCCTGACGA	*S. marcescens* *gDNA*
	ck0822	TAGCCATCAGGGAATTGCCGCCCAGCGCGAAG AA	3.055
pCK_0873		BsaI/AatII	pCK_0685 20.451
	ck0870	TTGGGCTAACAGGAGGAATTCAATGAGTACACC AGCTGACAACATGAA	*M. xanthus* gDNA 4.375
	ck0798	TTCCTGTGCGTTACGGGGGGCAACGTAGGCCG TCTCCAGG	pCK_0683
	ck0790	GTTGCCCCCCGTAACGCA	2.665
	ck0592	AATATAAGCAGCCATATCGCTGAGCG	
pSB002 NRPS-18b		BsaI/AatII	pCK_0685 20.443
	ck0617	AATTCCCTGAGCGCCATTAAGCTG	pCK_0683
	ck0592	AATATAAGCAGCCATATCGCTGAGCG	2.550
	SB001	TTTTTTTGGGCTAACAGGAGGAATTCCATGTCT ATGTCATGT-CACCGTATTAACAACG	*X. szentirmaii* gDNA
	SB003	GCTTAATGGCGCTCAGGGAATTCCCGCCCAGC TCAAAGAAATG	6.490
pCK_0881	ck0828	TTAATTAACCTAGGCTGCTGCCACC	pCK_0401
	ck0921	CATTGAATTCCTCCTGTTAGCCCAAA	3.669
	ck0857	CGAGACCAAAGAAGAAGGTCTCAGCTGCACCG CAAGGAGAAACCGAAAC	*P. luminescens* subsp. laumondii
	ck0886	TTGCTCAGCGGTGGCAGCAGCCTAGGTTAATTA ATTACAGCGCCTCCGCTTCACAATTCATTG	TT01 gDNA 4.365
	ck0873	TTTGGGCTAACAGGAGGAATTCAATGAAAGATA GCATGGCTAAAAAGGAA	*P. luminescens* subsp. laumondii
	ck0874	TGAGACCTTCTTCTTTGGTCTCGATAAATTTGGC GAGCAAAAGCATC	TT01 gDNA 4.993
pCK_0882	ck0828	TTAATTAACCTAGGCTGCTGCCACC	pCK_0401
	ck0921	CATTGAATTCCTCCTGTTAGCCCAAA	3.669
	ck0860	CGAGACCAAAGAAGAAGGTCTCAGGTGGCCAT TCGTTGCTTGCGG	*P. luminescens* subsp. laumondii
	ck0886	TTGCTCAGCGGTGGCAGCAGCCTAGGTTAATTA ATTACAGCGCCTCCGCTTCACAATTCATTG	TT01 gDNA 4.266
	ck0873	TTTGGGCTAACAGGAGGAATTCAATGAAAGATA GCATGGCTAAAAAGGAA	*P. luminescens* subsp. laumondii
	ck0875	TGAGACCTTCTTCTTTGGTCTCGCAAGGCAAAA AAATTATCGTGTCGG	TT01 gDNA 5.092
pLS_002		BsaI	pCK_0882 12.921
	ls06	GCCGACACGATAATTTTTTTGCCTTGGGCGGGC ACTCGCTGCTCGCGAT	*M. xanthus* gDNA 3.194
	ls07	TACCGCAAGCAACGAATGGCCCCCCAAGTCGA AGAAGTTGTCCTCCGCG	
pLS_003		BsaI	pCK_0881

			12.921
	ls08	GCTTTTGCTCGCCAAATTTATGAGCCGCCTCGCACGCCTA	*M. xanthus* gDNA 3.189
	ls09	TTCGGTTTCTCCTTGCGGTGCAGCGAAGCGCGTCTCGCTCGCG	
pLS_008		BsaI	pCK_0882 12.921
	ls24	CGACACGATAATTTTTTTGCCTTGGGCGGCCACTCCTTGCTGGC	*C. crocatus* gDNA 3.200
	ls25	ACCGCAAGCAACGAATGGCCCCCCAGCGCGAAGAAGTCGTCCTGC	
pLS_009		BsaI	pCK_0881 12.921
	ls26b	GGATGCTTTTGCTCGCCAAATTTATGTCACGCCCCGCACGCC	*C. crocatus* gDNA 3.205
	ls27b	GGTTTCGGTTTCTCCTTGCGGTGCAGCGAACTCGAAAGCTCCCTCGGCA	
pLS_017		BsaI	pCK_0882 12.921
	ls52	CCGACACGATAATTTTTTTGCCTTGGGTGGCCATTCATTACTCGCTG	*X. indica* gDNA 3.241
	ls53	TACCGCAAGCAACGAATGGCCACCGAGTTCGAAGAAGTGGTCATAACG	
pLS_018		BsaI	pCK_0881 12.921
	ls68	GCTTTTGCTCGCCAAATTTATGAAGCGCCCATTGGCAAATTGGAA	*X. indica* gDNA 3.241
	ls55	CGGTTTCTCCTTGCGGTGCAGCATAGCCACGTGTAACAACCGCTG	
pLS_019		BsaI	pCK_0882 12.921
	ls60	GAGGATGCTTTTGCTCGCCAAATTTATCAAGCGCCGGAAAGCCCAATGGA	*X. mauleonii* gDNA 3.288
	ls61	GGTTTCGGTTTCTCCTTGCGGTGCAGCATATTGACTCAATACAAACGCGGATGGC	
pLS_0191	ls71_1	GGTGGCCATTCGTTGCTTGCG	pCK_0882 6.395
	ls74_1	CAGGTGCTACATTTGAAGAGATAAATTGC	
	ls73	CTCTTCAAATGTAGCACCTGAAGTCAGC	pCK_0882 6.546
	ls72_1	CAAGGCAAAAAAATTATCGTGTCGGCC	
	ls62	CGGCCGACACGATAATTTTTTTGCCTTGGGCGGCCATTCATTGCTTG	*X. mauleonii* gDNA 3.288
	ls63	CGTACCGCAAGCAACGAATGGCCACCCAATTCAAAGAAATGATCATGGCGAC	

Table S5. Detected compounds in this work.

Peptide	MS detected $[M+H]^+$	MS calculated $[M+H]^+$	Molecular ion formula	Δppm	Reference
1	444.3061	444.3068	$C_{22}H_{42}N_3O_6$	1.5	synthetic
1	444.3062	444.3068	$C_{22}H_{42}N_3O_6$	1.3	
2	430.2911	430.2912	$C_{21}H_{40}N_3O_6$	0.1	
3	416.2750	416.2755	$C_{20}H_{38}N_3O_6$	1.3	
4, **5**	767.3932	767.3974	$C_{39}H_{55}N_6O_{10}$	5.5	isolated NP
6	783.3912	783.3923	$C_{39}H_{54}N_6O_{11}$	1.4	
7	811.4217	811.4236	$C_{41}H_{58}N_6O_{11}$	2.4	
8	839.4531	839.4549	$C_{43}H_{62}N_6O_{11}$	2.2	
9	783.3912	783.3923	$C_{39}H_{54}N_6O_{11}$	0.9	
10	811.4219	811.4236	$C_{41}H_{58}N_6O_{11}$	2.1	
11	839.4531	839.4549	$C_{43}H_{62}N_6O_{11}$	2.2	
12	782.4071	782.4083	$C_{39}H_{55}N_7O_{10}$	1.6	
13	810.4375	810.4397	$C_{41}H_{59}N_7O_{10}$	2.6	
14	838.4680	838.4710	$C_{43}H_{63}N_7O_{10}$	3.5	
15	753.3808	753.3818	$C_{38}H_{52}N_6O_{10}$	1.3	
16	869.4631	869.4655	$C_{44}H_{64}N_6O_{12}$	2.8	
17	867.4833	867.4862	$C_{45}H_{66}N_6O_{11}$	3.4	
18	895.5143	895.5175	$C_{47}H_{70}N_6O_{11}$	3.6	
19	725.3855	725.3869	$C_{37}H_{52}N_6O_9$	1.9	
20	993.5499	993.5543	$C_{52}H_{76}N_6O_{13}$	4.4	
21	995.5662	995.5700	$C_{52}H_{78}N_6O_{13}$	3.8	
22	977.5557	977.5594	$C_{52}H_{76}N_6O_{12}$	3.8	
23	979.5715	979.5751	$C_{52}H_{78}N_6O_{12}$	3.6	
24	955.4986	977.5019	$C_{54}H_{68}N_6O_{11}$	3.3	
25	836.4167	836.4888	$C_{42}H_{57}N_7O_{11}$	2.6	
26	799.4429	799.4461	$C_{38}H_{58}N_{10}O_9$	4.0	Isolated NP
27	813.4579	813.4618	$C_{39}H_{60}N_{10}O_9$	4.7	
28	913.5475	913.5506	$C_{45}H_{72}N_{10}O_{10}$	3.4	
29	941.5780	941.5819	$C_{47}H_{76}N_{10}O_{10}$	4.1	
30	931.5573	931.5611	$C_{45}H_{74}N_{10}O_{11}$	4.1	
31	945.5728	945.5768	$C_{46}H_{76}N_{10}O_{11}$	4.2	
32	959.5892	959.5924	$C_{47}H_{78}N_{10}O_{11}$	3.4	
33	973.6033	973.6080	$C_{48}H_{80}N_{10}O_{11}$	4.9	
34	457.3378	457.3384	$C_{23}H_{44}N_4O_5$	1.3	synthetic
35	471.3534	471.3541	$C_{24}H_{46}N_4O_5$	1.4	
36	431.2857	431.2864	$C_{20}H_{39}N_4O_6$	1.6	synthetic
37	445.3010	445.3021	$C_{21}H_{41}N_4O_6$	1.7	
38	415.2910	415.2915	$C_{20}H_{39}N_4O_5$	1.2	synthetic
39	429.3064	429.3071	$C_{21}H_{41}N_4O_5$	1.8	
40	511.3845	511.3854	$C_{27}H_{51}N_4O_5$	1.7	
41	525.3998	525.4010	$C_{28}H_{53}N_4O_5$	2.3	
42	539.4159	539.4167	$C_{29}H_{55}N_4O_5$	1.5	
43	458.3218	458.3225	$C_{23}H_{44}N_3O_6$	1.5	

Table S6. ^{1}H (500 MHz) and ^{13}C (125 MHz) NMR data of compound **1** in DMSO-d_6 (δ in ppm). COSY (bold) and key HMBC (arrows) are shown.

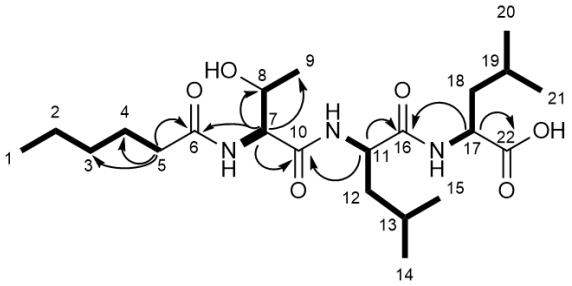

Position	δ_C, type[a]	δ_H, mult. (*J* in Hz)
1	13.86, CH_3	0.88-0.79, ov
2	21.90, CH_2	1.31-1.81, m
3	30.85, CH_2	1.31-1.81, m
4	25.00, CH_2	1.64-1.42, m
5	35.10, CH_2	2.17, m
6	172.54, C	-
7	57.85, CH	4.26, dd (12.0, 6.0)
7NH	-	7.70, d (8.32)
8	66.44, CH	3.95, m
9	19.39, CH_3	1.01, d (6.34)
10	169.76, C	-
11	50.90, CH	4.35, dd(15.0, 8.4)
11NH	-	7.81, d (8.53)
12	41.01, CH_2	1.64-1.42, ov
13	24.27 – 24.03, CH	1.64-1.42, ov
14	-	0.88-0.79, ov
15	-	0.88-0.79, ov
16	171.82, C	-
17	50.10, CH	4.20, ddd (10.0, 8.3, 4.8)f
17NH	-	8.03, d (8.19)
18	40.04, CH_2	1.64-1.42, ov
19	24.27 – 24.03, CH	1.64-1.42, ov
20	-	0.88-0.79, ov
21	-	0.88-0.79, ov
22	173.92, C	-

Table S7. ^{1}H (500 MHz) and ^{13}C (125 MHz) NMR spectroscopic data of compounds **4** and **5** in DMSO-d_6 (δ in ppm and J in Hz).

no.	**4**		**5**	
	δ_C, type	δ_H (mult., J)	δ_C, type	δ_H (mult., J)
1	169.4		169.4	
2		6.69 (d, 5.7)		7.06 (d, 5.7)
3	37.1	3.46 (td, 13.0, 5.6)	36.9	3.46 (td, 12.8, 5.8)
		3.31 (m)		3.34 (m)
4	34.3	2.52 (m)	34.4	2.54 (m)
		2.23 (m)		2.22 (m)
5	173.3		173.6	
6		8.50 (d, 4.4)		8.38 (d, 5.1)
7	57.4	4.25 (m)	57.4	4.30 (m)
8	35.3	2.61 (dd, 14.4, 4.8)	35.3	2.64 (m)
		2.34 (dd, 14.4, 3.7)		2.37 (dd, 14.0, 2.2)
9	127.8		128.0	
10	130.2	7.04 (d, 8.3)	130.1	7.07 (d, 8.3)
11	115.6	6.71 (d, 8.3)	115.6	6.73 (d, 8.3)
12	156.6		156.6	
13	115.6	6.71 (d, 8.3)	115.6	6.73 (d, 8.3)
14	130.2	7.04 (d, 8.3)	130.1	7.07 (d, 8.3)
15	174.6		174.6	
16		8.76 (d, 8.7)		8.97 (d, 8.4)
17	54.4	4.81 (m)	55.0	4.62 (m)
18	34.9	3.17 (dd, 14.2, 3.2)	35.0	3.24 (dd, 14.0, 3.2)
		2.65 (m)		2.64 (overlap)
19	128.4		128.5	
20	130.3	7.02 (d, 8.3)	130.3	7.06 (d, 8.4)
21	115.1	6.58 (d, 8.3)	115.2	6.60 (d, 8.4)
22	156.1		156.2	
23	115.1	6.58 (d, 8.3)	115.2	6.60 (d, 8.4)
24	130.3	7.02 (d, 8.3)	130.3	7.06 (d, 8.4)
25	171.8		171.7	
26		7.40 (d, 8.1)		7.36 (d, 7.9)
27	51.9	4.17 (ddd, 12.0, 8.1, 4.2)	51.9	4.17 (ddd, 11.9, 8.0, 4.2)
28	39.2	1.82 (m)	39.3	1.81 (m)
		1.40 (m)		1.42 (m)
29	24.6	1.74 (m)	24.6	1.78 (m)
30	21.1	0.83 (d, 6.5)	21.1	0.84 (d, 6.4)
31	23.4	0.88 (d, 6.6)	23.8	0.88 (d, 5.2)
32	171.7		171.7	
33	72.0	5.11 (qd, 6.2, 1.8)	72.1	5.12 (qd, 6.1, 1.7)
34	16.0	1.02 (d, 6.2)	16.0	1.04 (d, 6.1)
35	56.2	4.46 (dd, 10.2, 1.8)	56.4	4.44 (m)
36		7.97 (d, 10.2)		7.88 (d, 10.1)
37	173.1		173.9	
38	56.9	4.33 (dd, 10.5, 8.6)	51.6	4.42 (m)
39	35.2	1.86 (overlap)	39.8	1.54 (m)
40	24.7	1.44 (overlap)	24.6	1.60 (m)
		1.20 (m)		
41	10.2	0.74 (t, 7.4)	21.1	0.62 (d, 6.4)
42	15.8	0.91 (d, 6.8)	23.4	0.90 (d, 5.9)
43		8.00 (d, 8.6)		8.01 (d, 7.9)
44	169.5		169.5	
45	22.8	1.83 (s)	22.8	1.81 (s)

Table S8. ^{1}H (500 MHz) and ^{13}C (125 MHz) NMR spectroscopic data fof compounds **7** and **10** in DMSO-d_6 (δ in ppm and J in Hz).

no.	**7**		**10**	
	δ_C, type	δ_H (mult., J)	δ_C, type	δ_H (mult., J)
1	170.3		169.0	
2		7.03 (m)		6.93 (m)
3	35.1	3.39 (m)	36.7	3.50 (m)
		3.21 (m)		3.20 (m)
4	34.4	2.37 (m)	34.1	2.50 (m)
		2.19 (m)		2.26 (m)
5	172.2		173.0	
6		8.20 (d, 6.6)		8.38 (d, 4.6)
7	56.4	4.22 (m)	57.2	4.28 (m)
8	36.1	2.54 (m)	35.5	2.65 (m)
				2.42 (dd, 14.2, 3.8)
9	128.2		127.8	
10	130.4	6.94 (d, 8.4)	130.2	7.08 (d, 8.4)
11	115.4	6.65 (d, 8.4)	115.6	6.72 (d, 8.4)
12	156.4		156.6	
13	115.4	6.65 (d, 8.4)	115.6	6.72 (d, 8.4)
14	130.4	6.94 (d, 8.4)	130.2	7.08 (d, 8.4)
15	172.2		174.8	
16		8.29 (d, 8.9)		8.89 (d, 8.4)
17	55.1	4.32 (m)	55.0	4.49 (m)
18	36.0	3.02 (dd, 13.9, 3.8)	35.5	3.11 (dd, 14.0, 3.0)
		2.68 (dd, 13.9, 10.4)		2.65 (m)
19	128.6		128.5	
20	130.4	6.97 (d, 8.5)	130.4	7.04 (d, 8.4)
21	115.4	6.65 (d, 8.5)	115.3	6.62 (d, 8.4)
22	156.3		156.3	
23	115.4	6.65 (d, 8.5)	115.3	6.62 (d, 8.4)
24	130.4	6.97 (d, 8.5)	130.4	7.04 (d, 8.4)
25	171.8		171.6	
26		7.57 (d, 7.9)		7.40 (d, 7.9)
27	51.5	4.32 (overlap)	51.9	4.13 (m)
28	39.6	1.67 (m)	39.4	1.78 (m)
		1.51 (m)		1.41 (m)
29	24.5	1.67 (overlap)	24.5	1.73 (m)
30	22.0	0.86 (d, 6.3)	21.2	0.84 (d, 7.0)
31	22.3	0.90 (d, 6.3)	23.3	0.88 (d, 6.5)
32	171.5		171.6	
33	71.4	5.21 (qd, 6.3, 3.5)	71.5	5.20 (qd, 6.4, 2.1)
34	16.9	1.06 (d, 6.3)	16.1	1.04 (d, 6.4)
35	54.9	4.70 (dd, 9.3, 3.5)	56.2	4.50 (dd, 9.8, 2.1)
36		7.78 (d, 9.3)		7.69 (d, 9.8)
37	173.2		171.6	
38	35.5	2.19 (overlap)	57.9	4.48 (dd, 8.6, 3.0)
39	25.5	1.51 (overlap)		7.63 (d, 8.6)
40	31.4	1.21 (m)	172.9	
41	22.3	1.25 (m)	35.1	2.08 (m)
42	14.3	0.84 (t, 7.0)	25.4	1.47 (m)
43	169.8		31.3	1.20 (m)
44		7.93 (d, 7.6)	22.4	1.26 (m)
45	59.6	3.93 (dd, 7.6, 3.8)	14.4	0.84 (t, 7.0)
46	65.8	4.09 (m)	67.0	4.23 (m)
47	20.7	1.00 (d, 6.4)	20.1	1.07 (d, 6.3)

Table S9. ^{1}H (500 MHz) and ^{13}C (125 MHz) NMR spectroscopic data for compound **26** in DMSO-d_6 (δ in ppm and J in Hz).

no.	**26**	
	δ_C, type	δ_H (mult., J)
1	157.7	
2		8.05 (t, 5.0)
3	40.8	3.04 (m)
4	25.6	1.54 (m)
5	28.1	1.74 (m)
6	53.7	4.01 (m)
7	171.0	
9	69.9	5.00 (m)
10	15.0	1.10 (d, 6.5)
11	54.5	4.48 (dd, 8.4, 4.4)
12		8.03 (d, 8.4)
13	169.7	
14	22.8	1.90 (s)
15	167.6	
16		8.75 (d, 9.2)
17	55.6	4.62 (m)
18	29.8	3.16 (dd, 14.4, 8.0)
		2.99 (dd, 14.4, 6.7)
19	109.9	
20	124.1	7.12 (d, 2.0)
21		10.87 (d, 2.0)
22	136.5	
23	111.7	7.32 (d, 8.1)
24	121.3	7.05 (m)
25	118.8	6.96 (m)
26	118.6	7.54 (d, 7.9)
27	127.8	
28	172.0	
29		8.56 (d, 4.7)
30	61.0	4.19 (dd, 7.7, 4.7)
31	66.0	3.91 (m)
32	20.1	1.08 (d, 6.3)
33	173.6	
34		8.73 (d, 5.7)
35	60.9	3.88 (dd, 5.7, 4.7)
36	29.1	2.18 (m)
37	17.8	0.90 (d, 6.9)
38	19.4	0.95 (d, 7.0)
39	171.4	
40		6.83 (d, 8.0)
41	56.7	4.19 (dd, 8.0, 4.9)
42	35.5	1.87 (m)
43	26.3	1.19 (m)
		1.14 (m)
44	11.9	0.77 (t, 7.4)
45	15.0	0.75 (d, 7.0)
46	171.9	
47		7.43 (d, 5.8)

Table S10. ^{1}H (500 MHz) and ^{13}C (125 MHz) NMR data of compound **41** in DMSO-d_6 (δ in ppm). COSY (bold) and key HMBC (arrows) are shown.

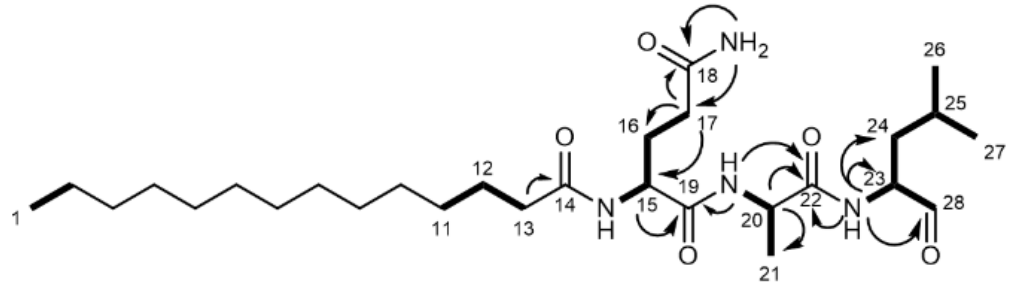

Position	δ_C, type[a]	δ_H, mult. (*J* in Hz)
1	-	0.91 – 0.80, ov
11	-	1.30 – 1.15, ov
12	25.19, CH_2	1.55 – 1.38, ov
13	35.15, CH_2	2.15 – 2.03, ov
14	172.74, C	-
15	52.33, CH	4.21 - 4.14, m
15NH	-	8.05 – 7.92, m
16	28.66, CH_2	1.91 – 1.66, m
17	31.53, CH_2	2.15 – 2.03, m
17NH	-	7.24 (s)
17NH	-	6.74 (s)
18	173.80, C	-
19	171.21, C	-
20	48.05, CH	4.33 – 4.21, m
20NH	-	8.05 – 7.92, m
21	18.19, CH_3	1.30 – 1.15, ov
22	172.56, C	-
23	56.54, CH	4.14 – 4.05, m
23NH	-	8.23 – 8.17, m
24	36.33, CH_2	1.55 – 1.38, ov
25	24.00, CH	2.15 – 2.03, ov
26	-	0.91 – 0.80, ov
27	-	0.91 – 0.80, ov
28	201.05, CH	9.39 – 9.35, m

Table S11. Crystallographic data collection and refinement statistics of yCP:41.

	yCPC14QAL
Crystal parameters	
Space group	$P2_1$
Cell constants	a = 135.0 Å
	b = 300.9 Å
	c = 144.0 Å
	β = 112.8 °
CPs / AU[a]	1
Data collection	
Beam line	X06SA, SLS
Wavelength (Å)	1.0
Resolution range (Å)[b]	50–3.25 (3-35–3.25)
No. observations	481076
No. unique reflections[c]	157953
Completeness (%)[b]	95.1 (93.7)
R_{merge} (%)[b, d]	10.5 (65.4)
I/□ (I)[b]	11.1 (2.4)
Refinement (REFMAC5)	
Resolution range (Å)	30-3.25
No. refl. working set	149904
No. refl. test set	7890
No. non hydrogen	49565
No. of ligand atoms	148
Solvent (H_2O, ions, MES)	95
R_{work}/R_{free} (%)[e]	17.5 / 21.2
r.m.s.d. bond (Å) / angle (°)[f]	0.003 / 1.2
Average B-factor (Å^2)	91.3
Ramachandran Plot (%)[g]	97.6 / 2.2 / 0.2
PDB accession code	xxxx

[a] Asymmetric unit
[b] The values in parentheses for resolution range, completeness, R_{merge} and I/σ (I) correspond to the highest resolution shell
[c] Data reduction was carried out from a single crystal. Friedel pairs were treated as identical reflections
[d] $R_{merge}(I) = \Sigma_{hkl}\Sigma_j \mid I(hkl)_j - \langle I(hkl)\rangle \mid / \Sigma_{hkl}\, \Sigma_j\, I(hkl)_j$, where $I(hkl)_j$ is the j^{th} measurement of the intensity of reflection hkl and $\langle I(hkl)\rangle$ is the average intensity
[e] $R = \Sigma_{hkl} \mid |F_{obs}| - |F_{calc}| \mid / \Sigma_{hkl} |F_{obs}|$, where R_{free} is calculated without a sigma cut off for a randomly chosen 5% of reflections, which were not used for structure refinement, and R_{work} is calculated for the remaining reflections
[f] Deviations from ideal bond lengths/angles
[g] Percentage of residues in favored / allowed / outlier region

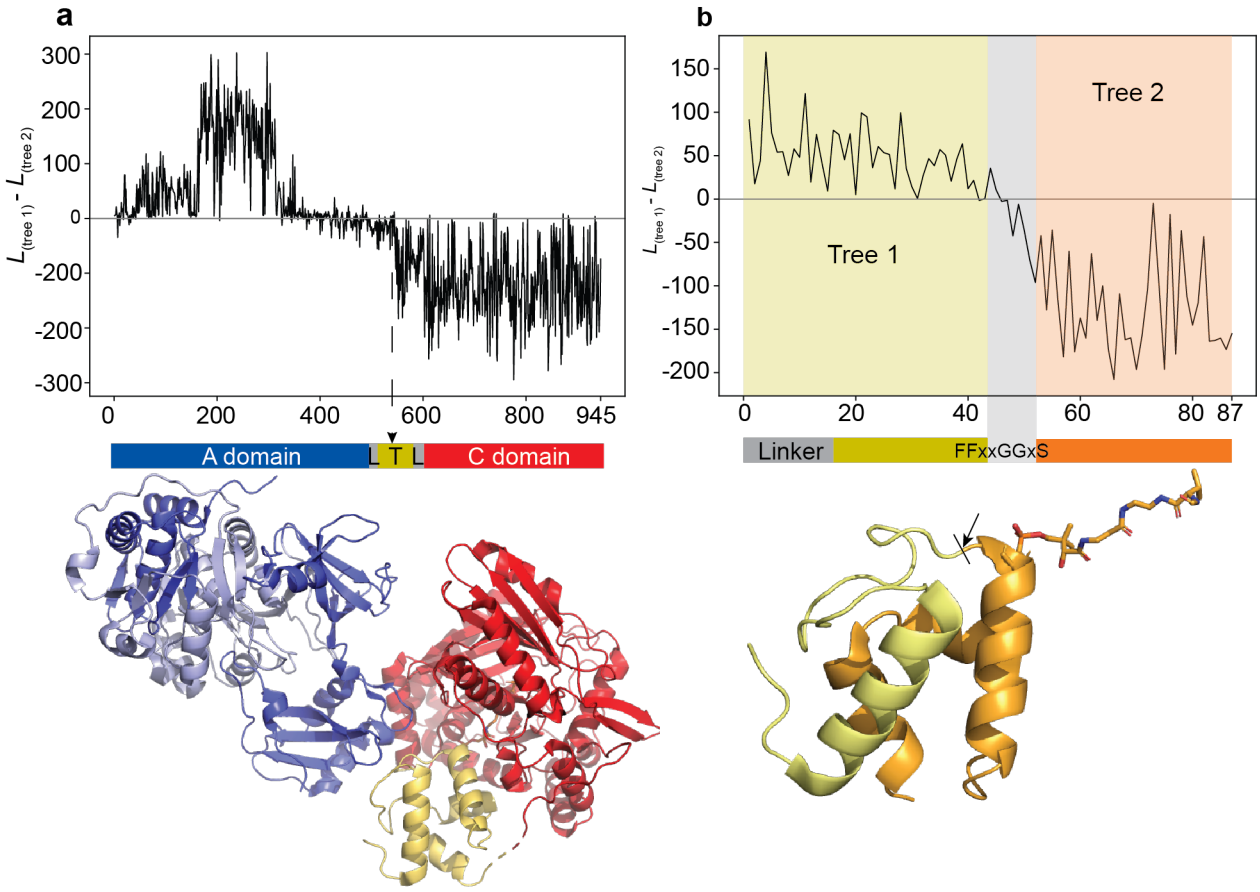

Fig. S1. Evolutionary analysis of ATC tridomains and T domains of representative NRPS. (**a**) Likelihood difference plot of two phylogenetic trees of ATC tridomains (also called XUs) that together best describe the alignment using a phylogenetic hidden Markov model. Positive numbers indicate that sites are better describe by tree 1, negative numbers indicate sites that are better described by tree two. Protein structure of XU is shown below. A domain is colored in blue, T-domain in yellow and C domain in red. (**b**) Likelihood difference plot as in **a**, but for an alignment of T domain plus A-T linker. Partitions detected by the hidden Markov model are indicated in different colors according to tree number. Recombination breakpoint is annotated in grey and lies around two conserved glycines. Protein structure of A-T-Linker and T domain is shown below. The first part of the T domain is colored in yellow and the second part in orange. An arrow points to the fusion site used for engineering.

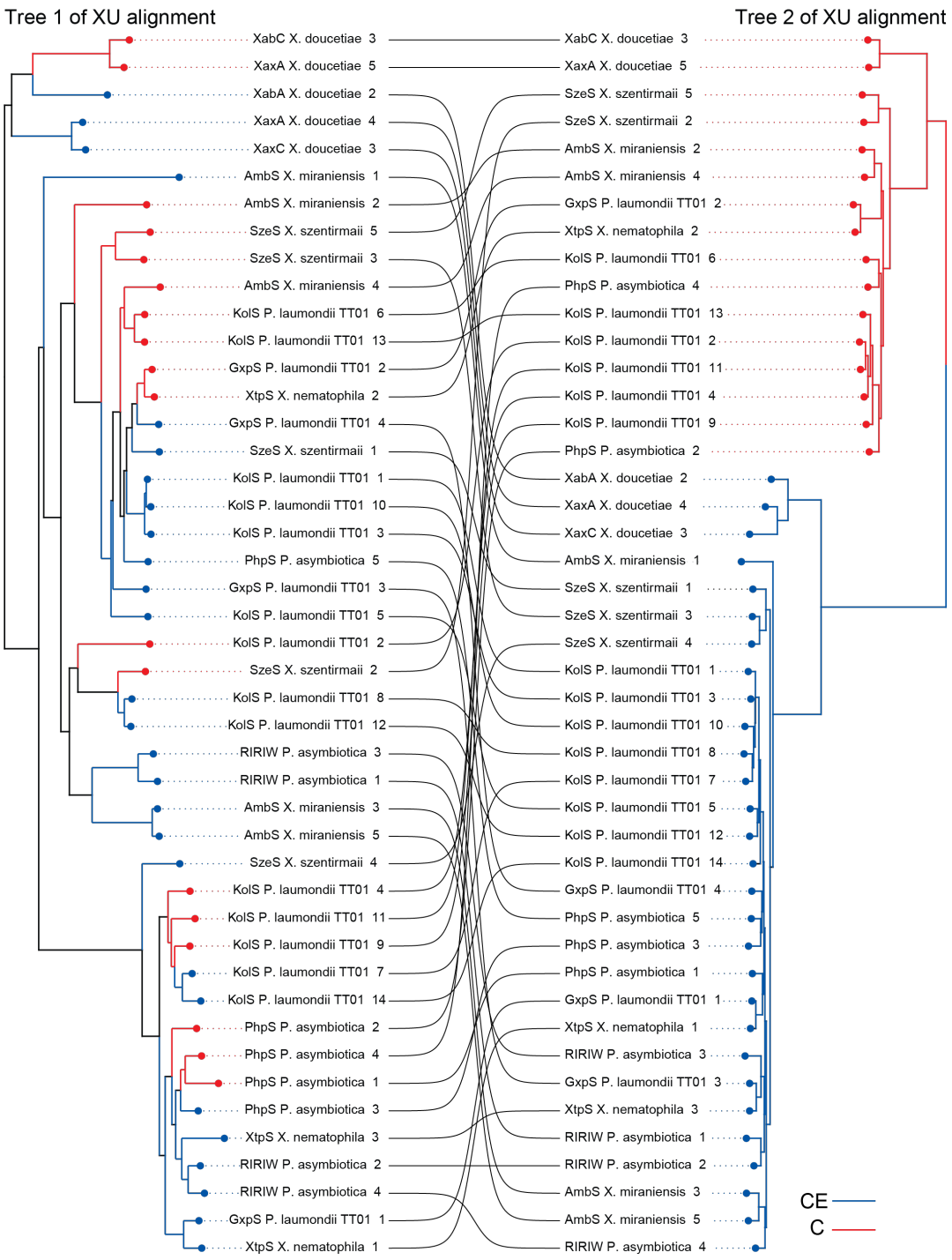

Fig S2. Comparison of Tree 1 and Tree 2 from the XU alignment. Taxon names indicate abbreviation of NRPSs, followed by bacterial species and then numbers of the XU within that NRPS. Lines connect the same NRPS and XU between the two trees. Red branches label XUs that contain $^{L}C_{L}$ domains and blue branches label XUs with dual C/E domains.

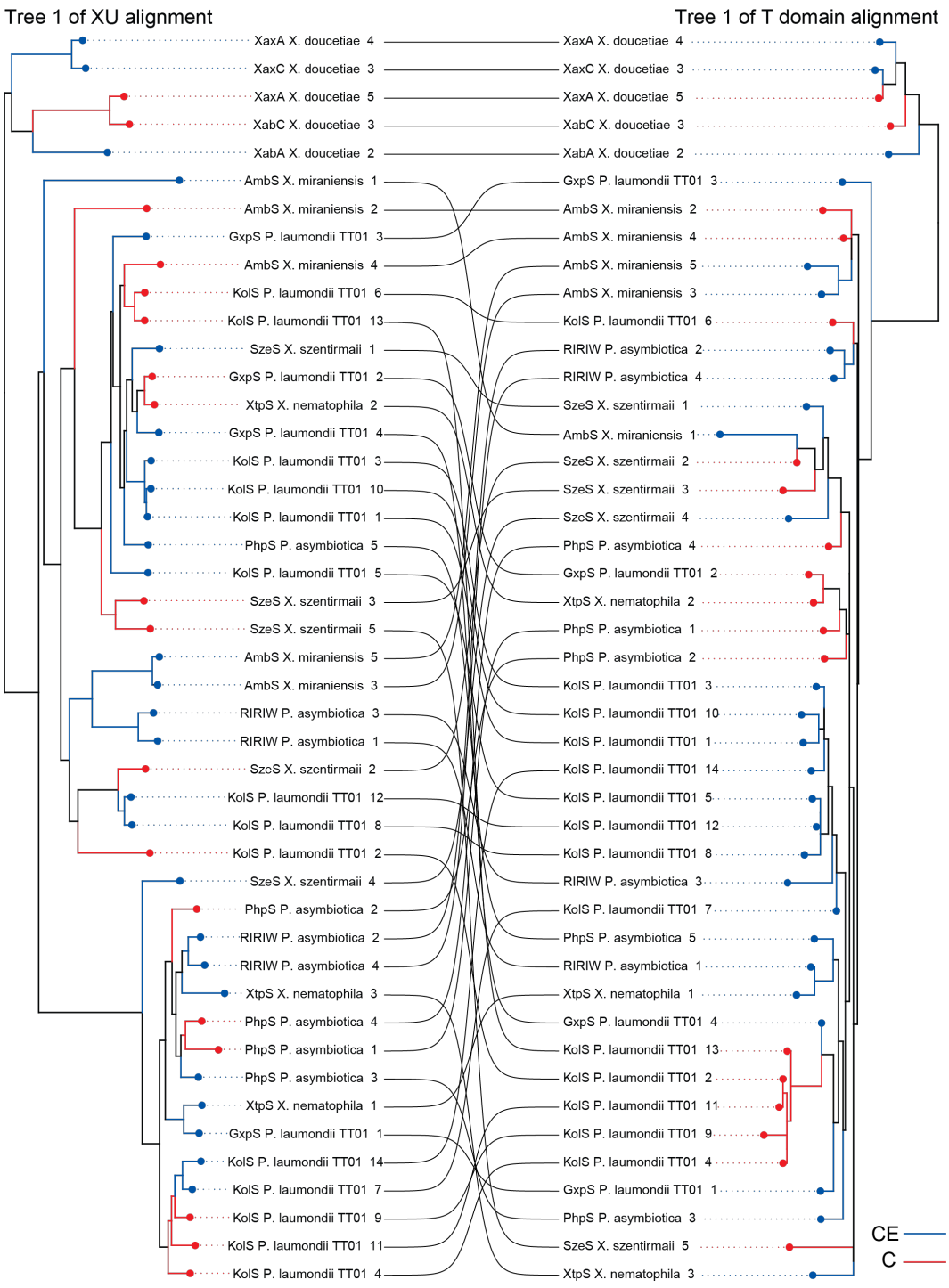

Fig. S3. Comparison of Tree 1 from XU domain alignment and Tree 1 from T domain alignment. Taxon names indicate abbreviation of NRPS, followed by bacterial species and then numbers of the XU within that NRPS. Lines connect the same NRPS and XU between the two trees. Red branches label $^{L}C_{L}$ domains and blue branches label dual C/E domains.

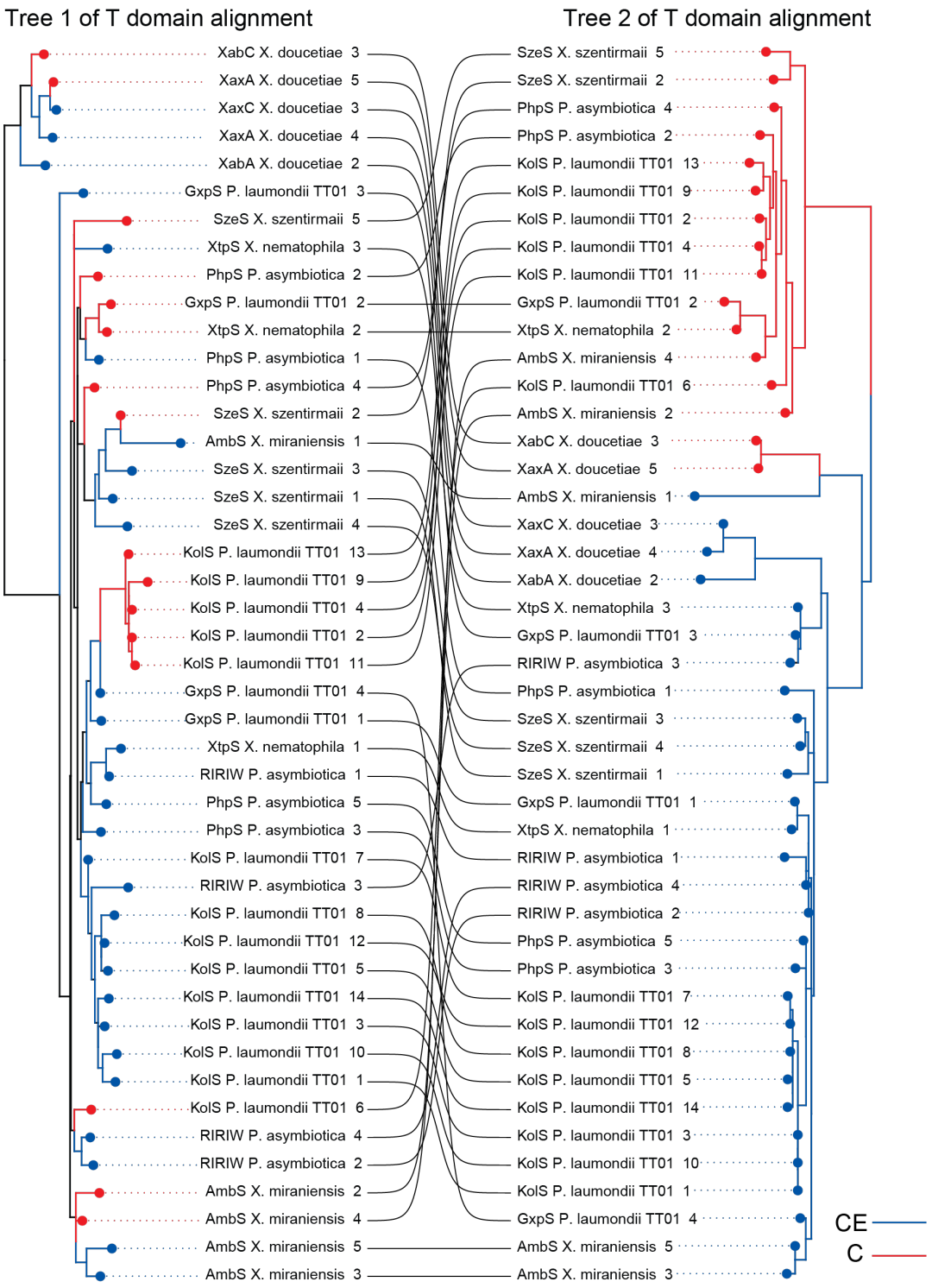

Fig S4. Comparison of Tree 1 from T domain alignment and Tree 2 from T domain alignment. Taxon names indicate abbreviation of NRPS, followed by bacterial species and then numbers of the XU within that NRPS. Lines connect the same NRPS and XU between the two trees. Red branches label $^{L}C_{L}$ domains and blue branches label dual C/E domains.

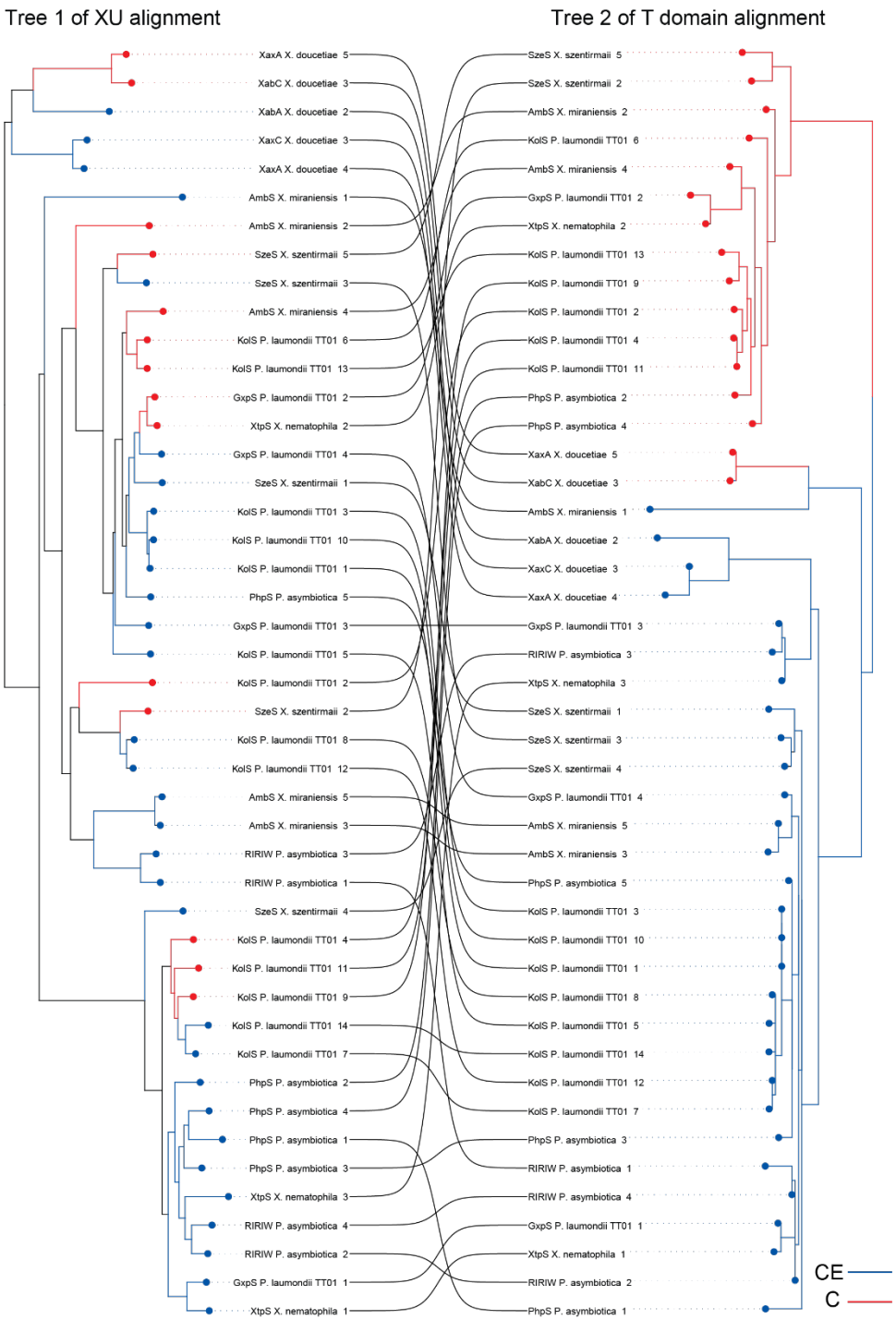

Fig. S5. Comparison of Tree 1 from XU domain alignment and Tree 2 from T domain alignment. Taxon names indicate abbreviation of NRPS, followed by bacterial species and then numbers of the XU within that NRPS. Lines connect the same NRPS and XU between the two trees. Red branches label $^{L}C_{L}$ domains and blue branches label dual C/E domains.

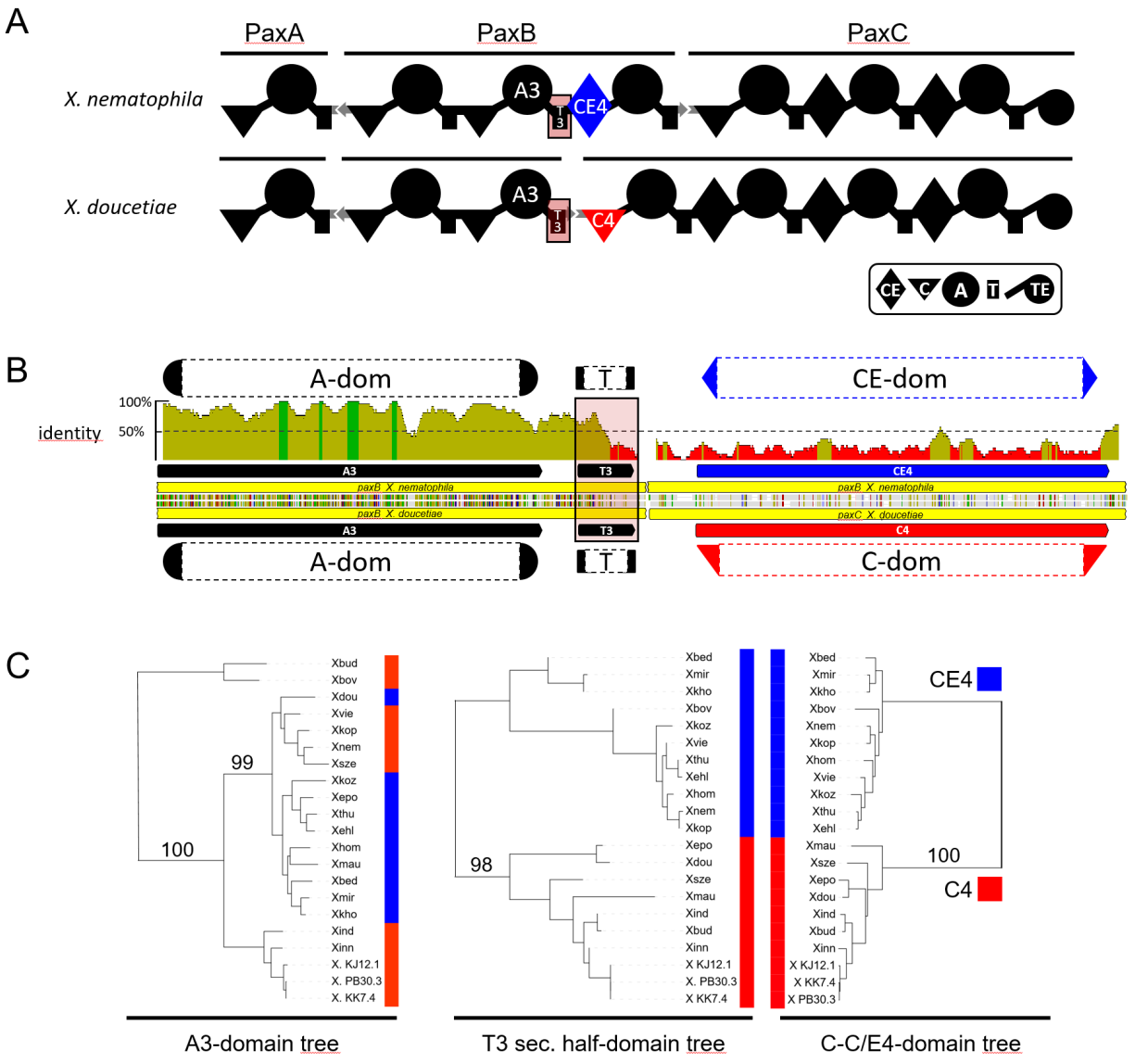

Figure S6. Phylogenetic analysis of T-domains in relation to preceding A-domain and following C/CE-domain. In (**A**) a schematic representation of the PAX producing NRPS[24,25] with the T3-domain under scrutiny highlighted (reddish square). The following CE4-domain is shown in blue and the C4-domain in red. In (**B**) a dual alignment of the A3-T3-CE4/C4 domains from *X. nematophila compared* to *X. doucetiae* can be seen. The amino acid alignment in the middle is shown with agreements in colour, genes as yellow bars and the domains indicated in the colour used in (**A**). The mean pairwise identity over all pairs in the column are calculated for a sliding window size 20 amino acids (green 100% identity, greenish-brown at least 30% under 100%, red below 30%). The drop of pairwise identity from high value between the A-domain region to the low identity between C- and CE-domains occurs in the middle of the T-domain. In (**C**) a phylogenetic tree of A3-, T3- second half (corresponds to T-fusion point IV in figure 2) and C4/CE4-domains is presented. The phylogenetic tree was calculated for the A3-domain, T3-domain second half and the following C/CE-domains separately. To this end multiple alignments of the protein sequences were generated using Clustal Omega 1.2.2.[26] with the refinement iterations number set at 10 while evaluating

the full distance matrix for the initial guide tree as well as for the refinement iteration guide tree. Only bootstrap values at critical junctions are indicated. The colours blue (CE) and red (C) refer to the condensation domains of the A3-T3-C4/CE4 unit. Abbreviations of the indicated PAX NRPS organisms: Xbud, *X. budapestensis*; Xbed, *X. beddingii*; Xbov, *X. bovienii*; Xdou, *X. doucetiae*; Xehl, *X. ehlersii*; X eap, *X. eapokensis*; Xhom, *X. hominickii*; Xind, *X. indica*; Xkho, *X. khoisanae*; Xkop, *X. koppenhoeferi*; Xkoz, *X. kozodoii*; Xmau, *X. mauleonii*; Xmir, *X. miraniensis*; Xnem, *X. nematophila*; Xsze, *X. szentirmaii*; Xthu, *X. thuongxuanensis* str. 30TX1, Xvie, *X. vietnamensis, X. sp.* KJ12.1, X KK7.4, *X.* sp. KK7.4, *X.* sp. PB30.3, X PB30.3). PaxABC sequences were identified using the PaxABC peptide sequences of *X. nematophila* and *X. doucetiae* as query. Domain annotation was implemented by use of AntiSMASH 6.0[27].

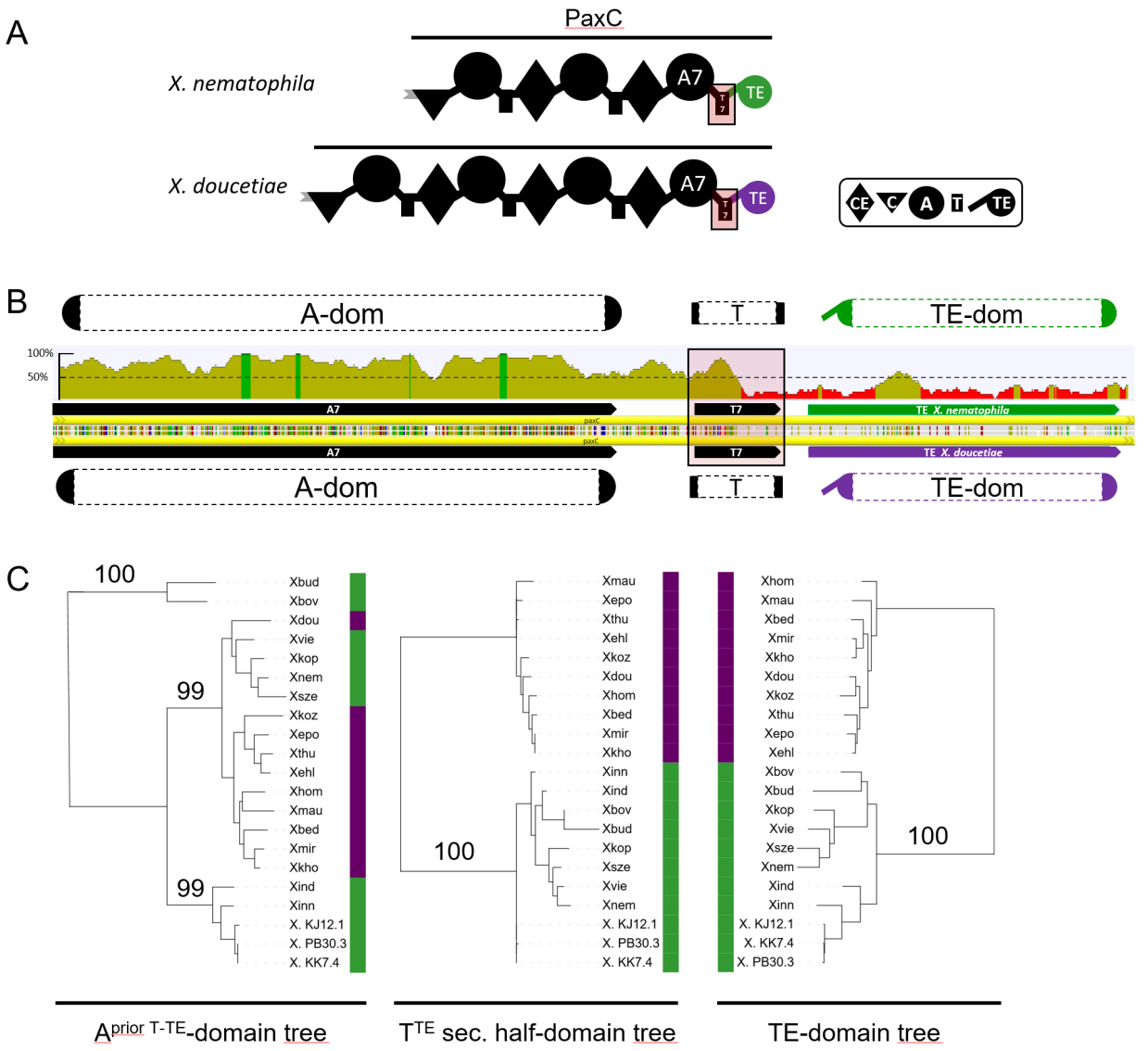

Figure S7. Phylogenetic analysis of T-domains in relation to preceding A-domain and the following TE-domain of the PAX-NRPS. The PAX biosynthesis in *Xenorhabdus* contains one of two types TE-domains being equally distributed in the *in silico* accessible biosynthesis. In (**A**) the final NRPS multienzymes are depicted with the *X. nematophila* TE-type in green and the *X. doucetiae* TE-type in purple. (**B**) A dual alignment of the A7-T7-TE unit from *X. nematophila* and *X. doucetiae* visualises the low identity between the two TE-types and that the drop of the sequence identity occurs in the middle of the T-domain. The phylogenetic tree in (**C**) was derived as described in Figure S6. The colour bars in all three phylogenetic trees refer to the TE in the A-T-TE unit. The *Xenorhabdus* species abbreviations are as in Figure S6.

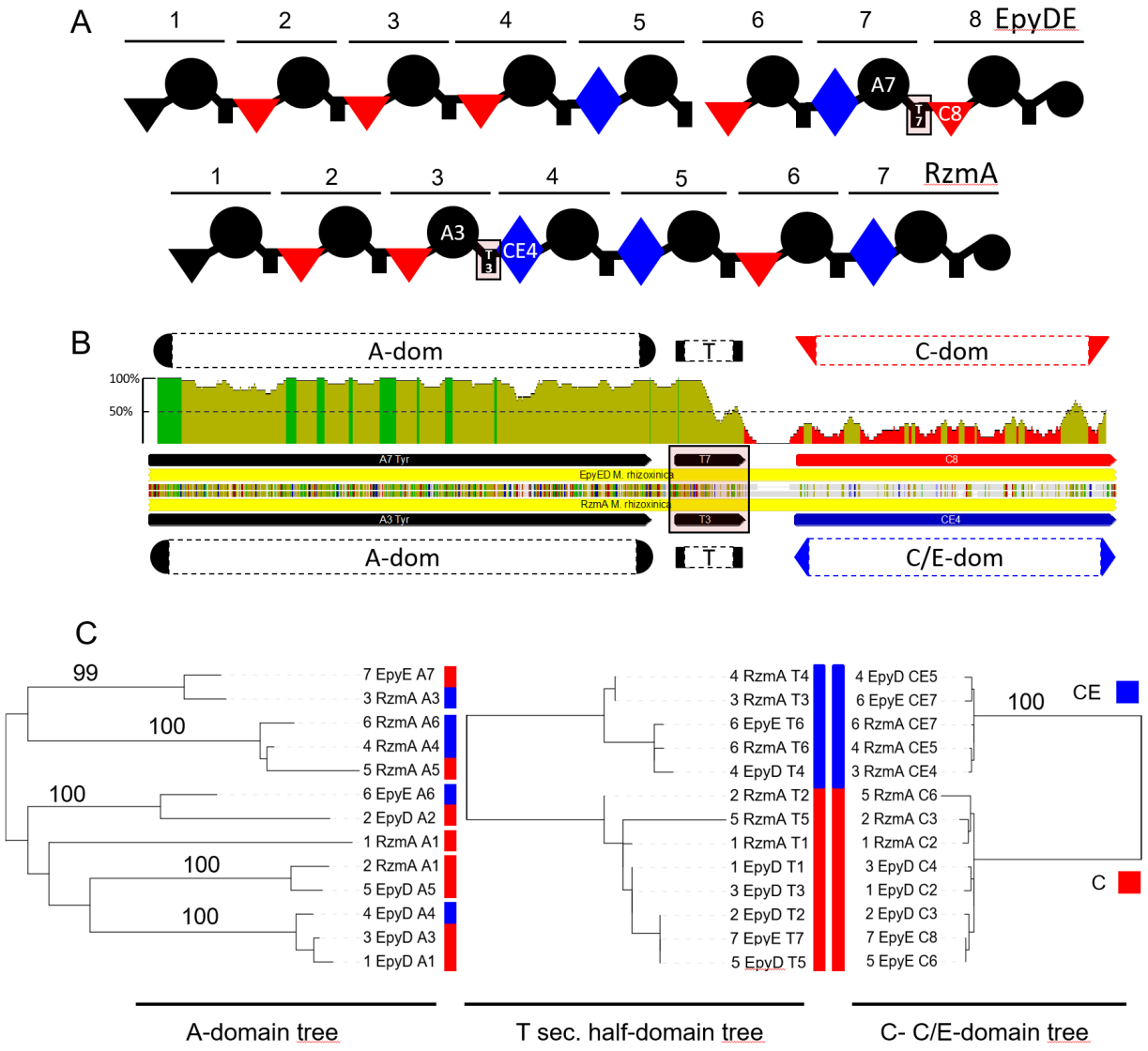

Figure S8. Phylogenetic analysis of T-domains in relation to preceding A-domain and following C/CE-domain of RzmA and EpyDE. (**A**) Schematic representation of the endopyrrole A producing NRPS EpyDE[28] and the rhizomide A producing NRPS RzmA[29] from *Mycetohabitans rhizoxinica* (DSM 19002). In (**B**) the EpyDE A7-T7-C8 unit and the RzmA A3-T3-CE4 unit are shown in a dual alignment. The phylogenetic trees of the A-domains, the T-domain second half and the C/CE-domains of RzmA and EpyDE were generated separately as described in Figure S6 using the same colour code (**C**).

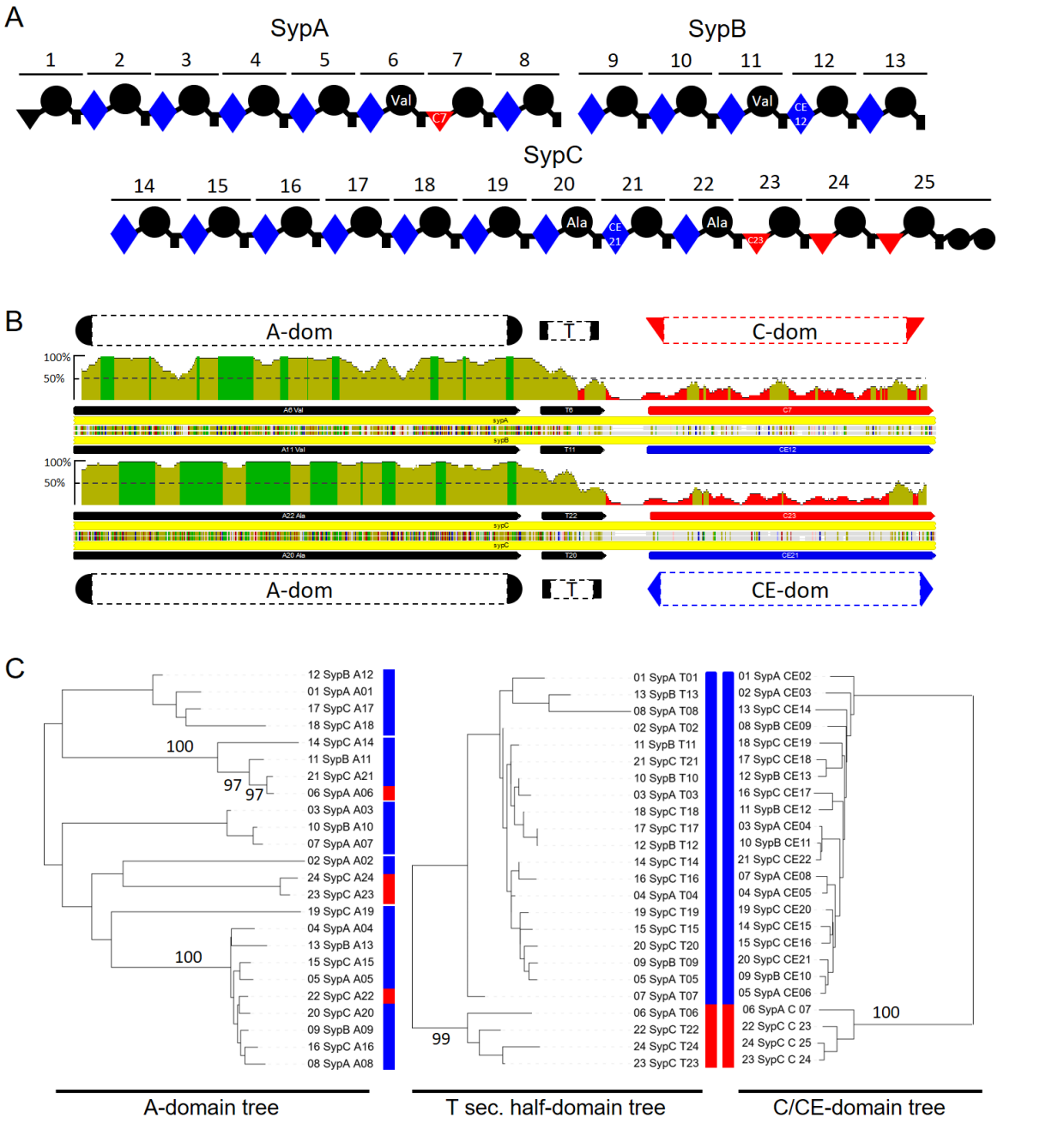

Figure S9. Phylogenetic analysis of T-domains in relation to preceding A-domain and following C/CE-domain of the syringopeptin SP-25a NRPS synthesis (SypABC; ALU60730.1, ALU60731.1, ALU60732.1) of *Pseudomonas syringae pv. lapsa* (DSM 50274) (**A**). The indicated A-domain substrate specificity was derived from published SP-25a[30] in conjunction with AntiSMASH 6.0 predictions[27]. In (**B**) two dual alignments of the SypA A7-T7-C8 to the SypB A11-T11-CE12 (top) and the SypC A20-T20-CE21 unit to the A22-T22-C23 (bottom) are shown. The phylogenetic trees of the A-domains, the T-domain second half and the C/CE-domains of SypABC were generated separately as described in Figure S6 using the same colour code (**C**).

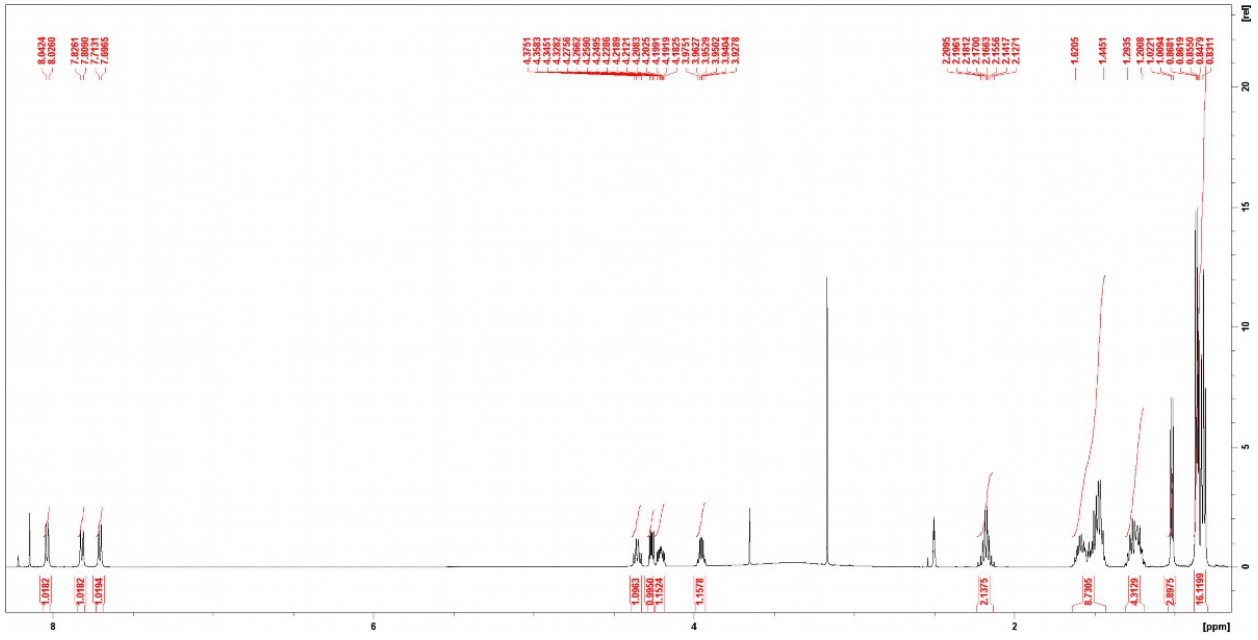

Figure S10. ^{1}H NMR (500 MHz, DMSO-d_6) spectrum compound **1**.

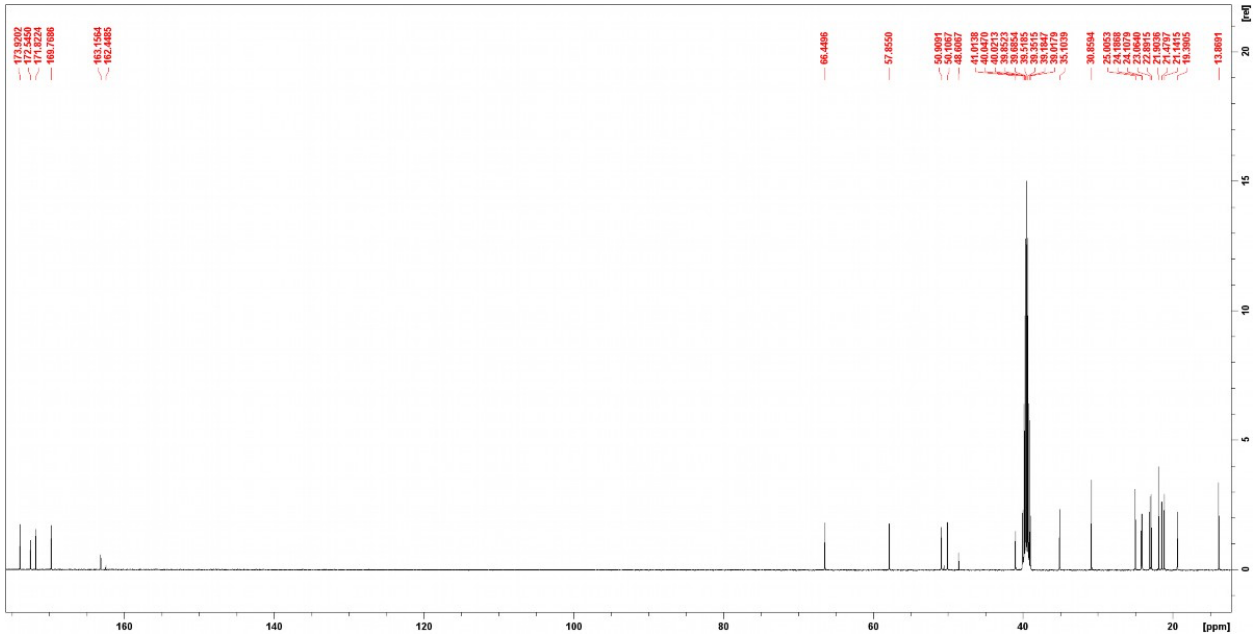

Figure S11. ^{13}C NMR (125 MHz, DMSO-d_6) spectrum of compound **1**.

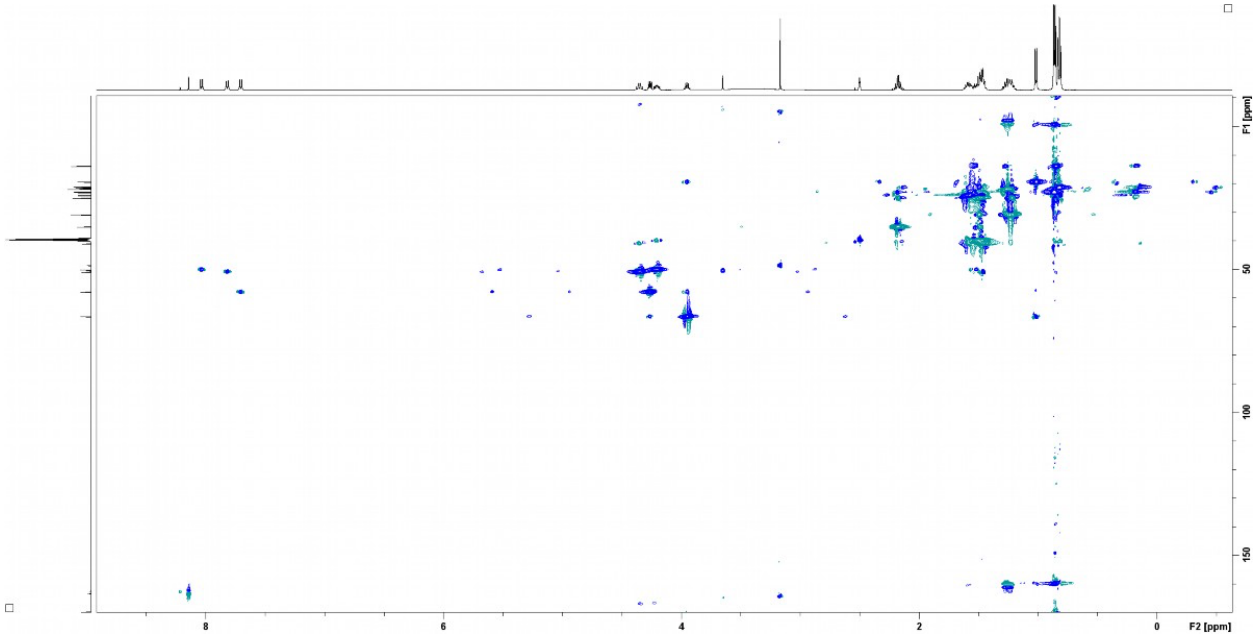

Figure S12. HSQC (DMSO-d_6) spectrum compound **1**.

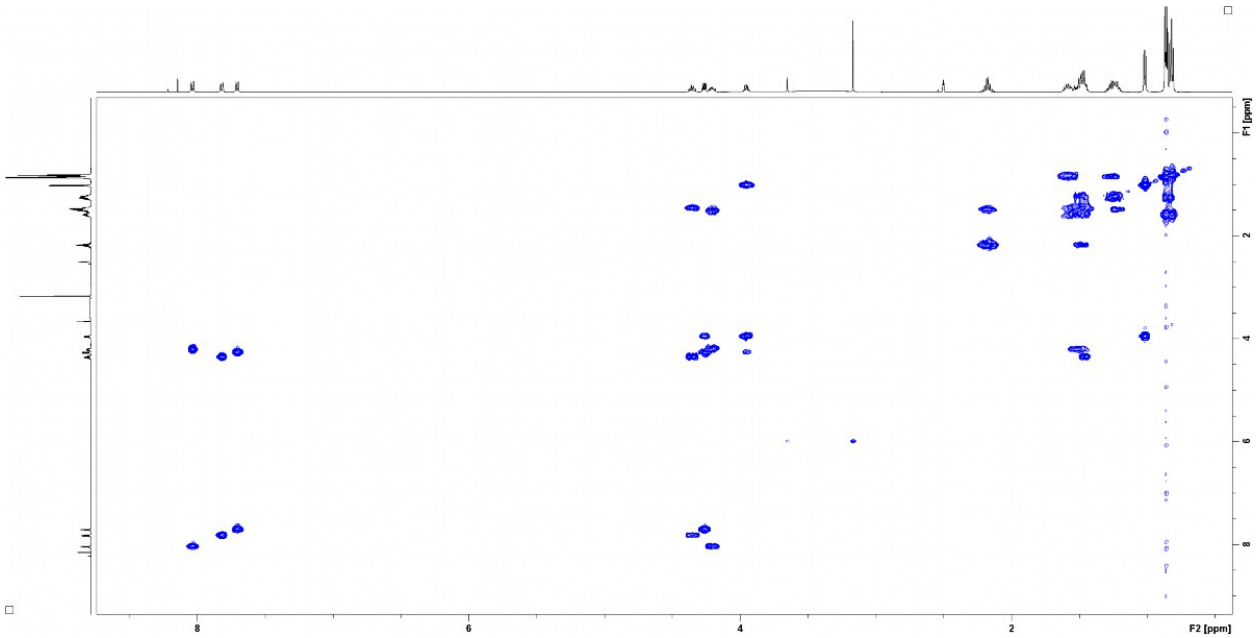

Figure S13. ^{1}H-^{1}H COSY (DMSO-d_6) spectrum of compound **1**.

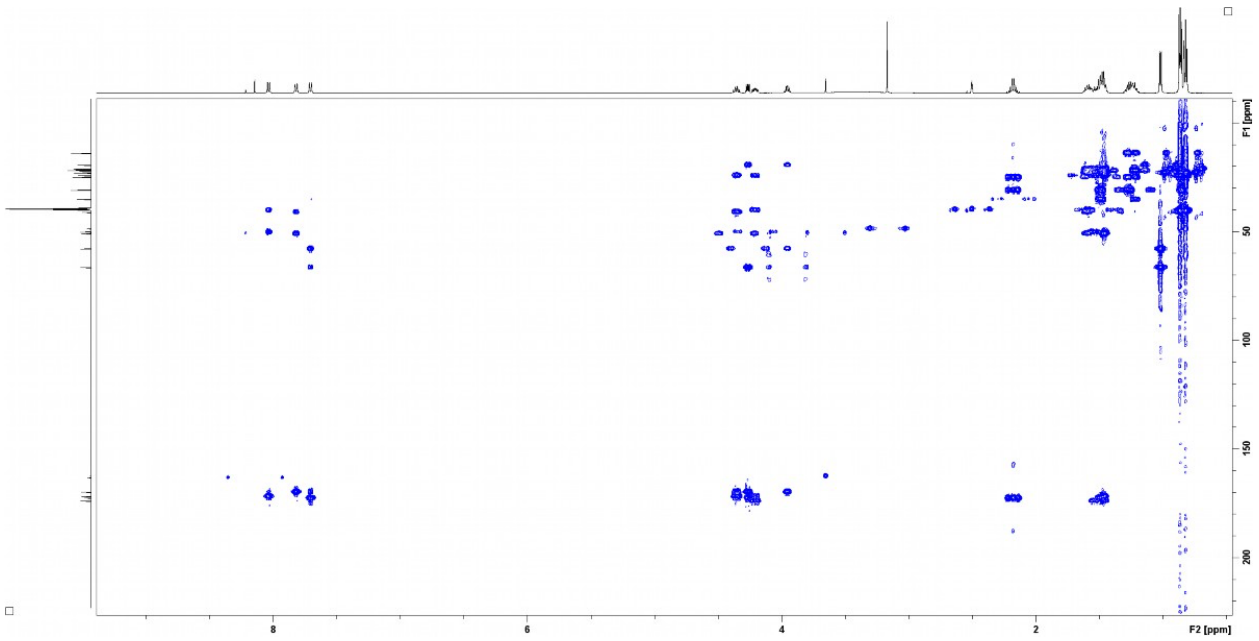

Figure S14. HMBC (DMSO-d_6) spectrum of compound **1**.

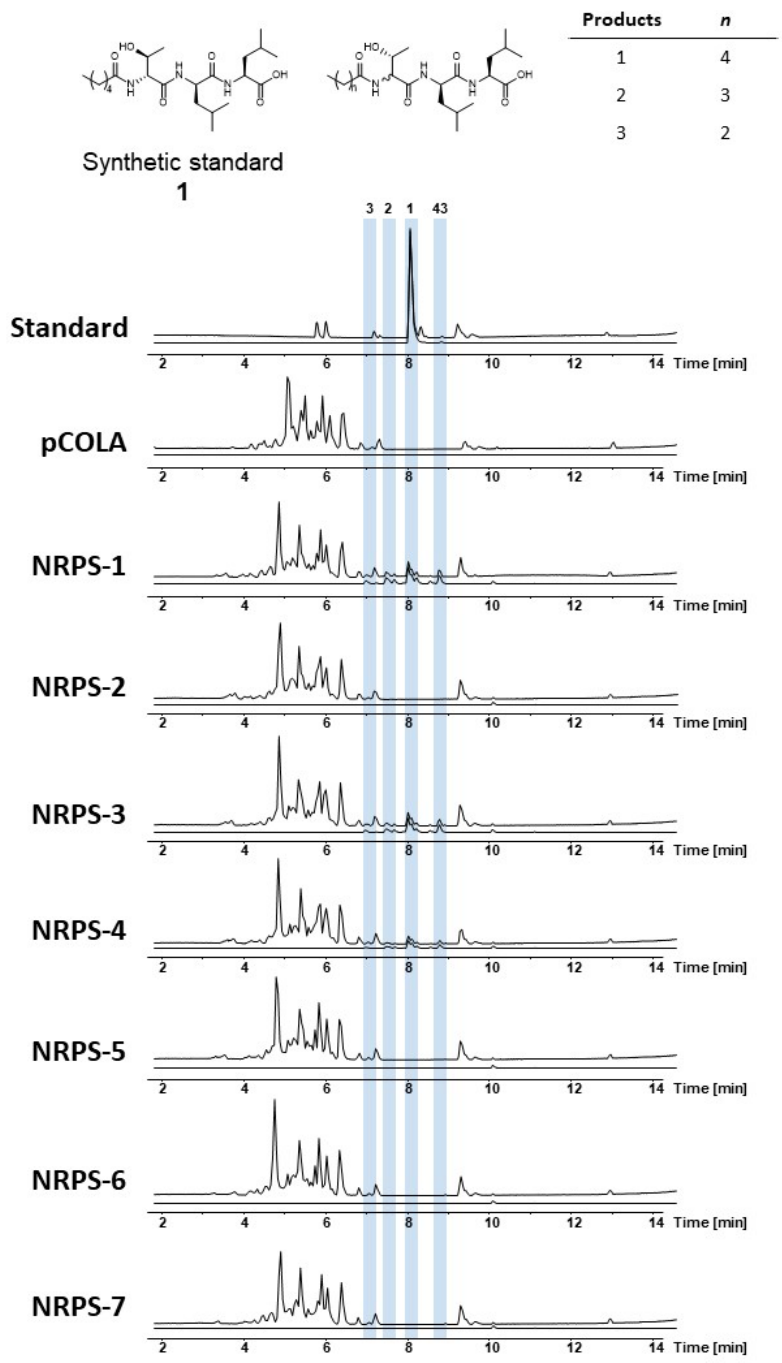

Figure S15. HPLC/MS data refers to Figure 2 (NRPS-1 to -7) of compound **1**, **2**, **3** and **43** produced in *E. coli* DH10B::*mtaA*. Base Peak Chromatogram (BPC, top) and Extracted Ion Chromatogram (EIC, below) of **1** (*m/z* $[M+H]^+$ = 444.30), **2** (*m/z* $[M+H]^+$ = 430.29), **3** (*m/z* $[M+H]^+$ = 416.27) and **43** (*m/z* $[M+H]^+$ = 458.32). Chromatograms were compared to an empty vector control and a synthetic standard of compound **1** (*m/z* $[M+H]^+$ = 444.30).

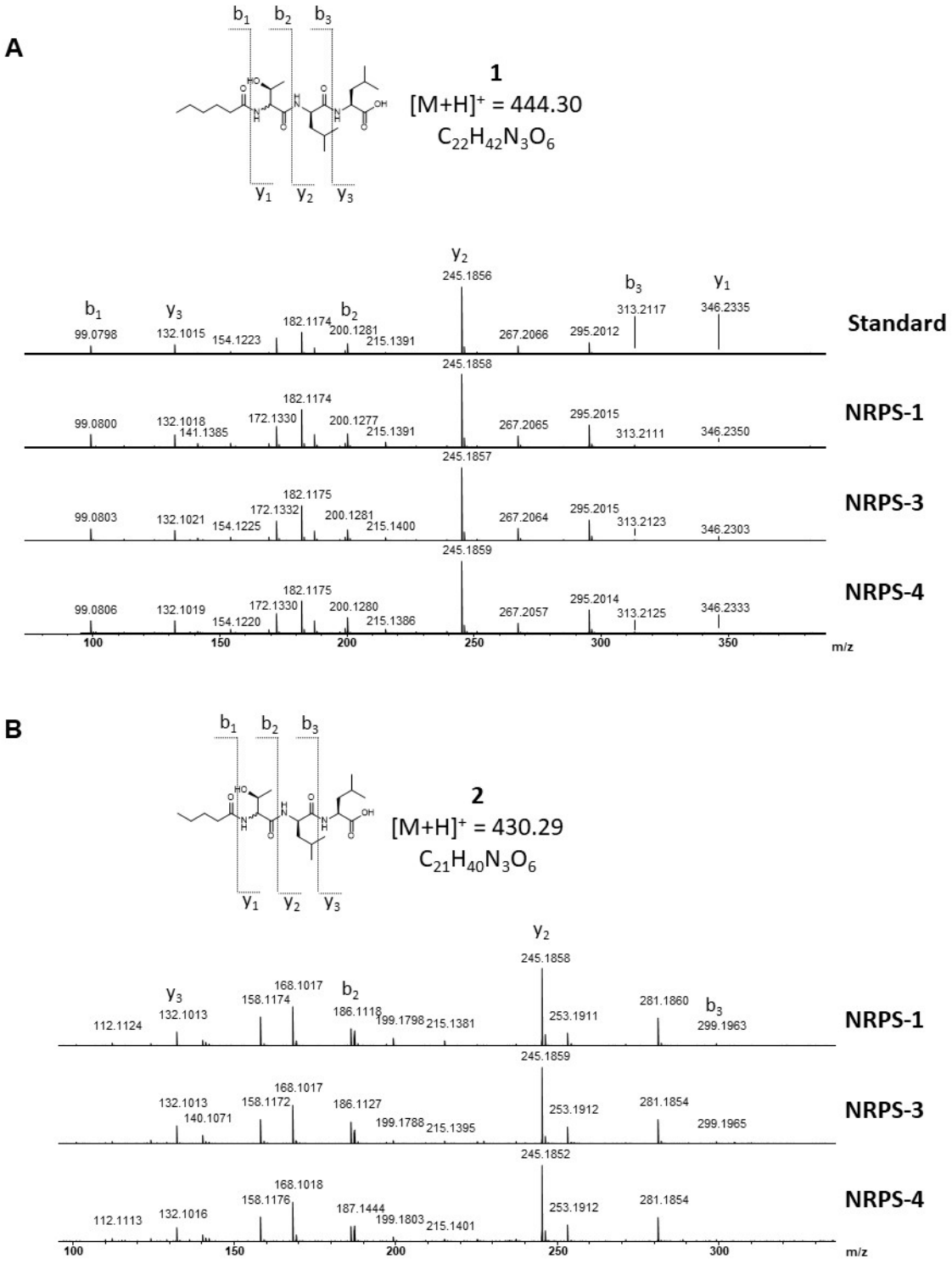

Figure S16. HPLC/MS data refers to Figure 2 (NRPS-1, -3 and -4) of compound **1** (**A**) and **2** (**B**) produced in *E. coli* DH10B::*mtaA*. Comparison of MS^2 spectra. Compound **1** fragmentation was compared to a synthetic **1**.

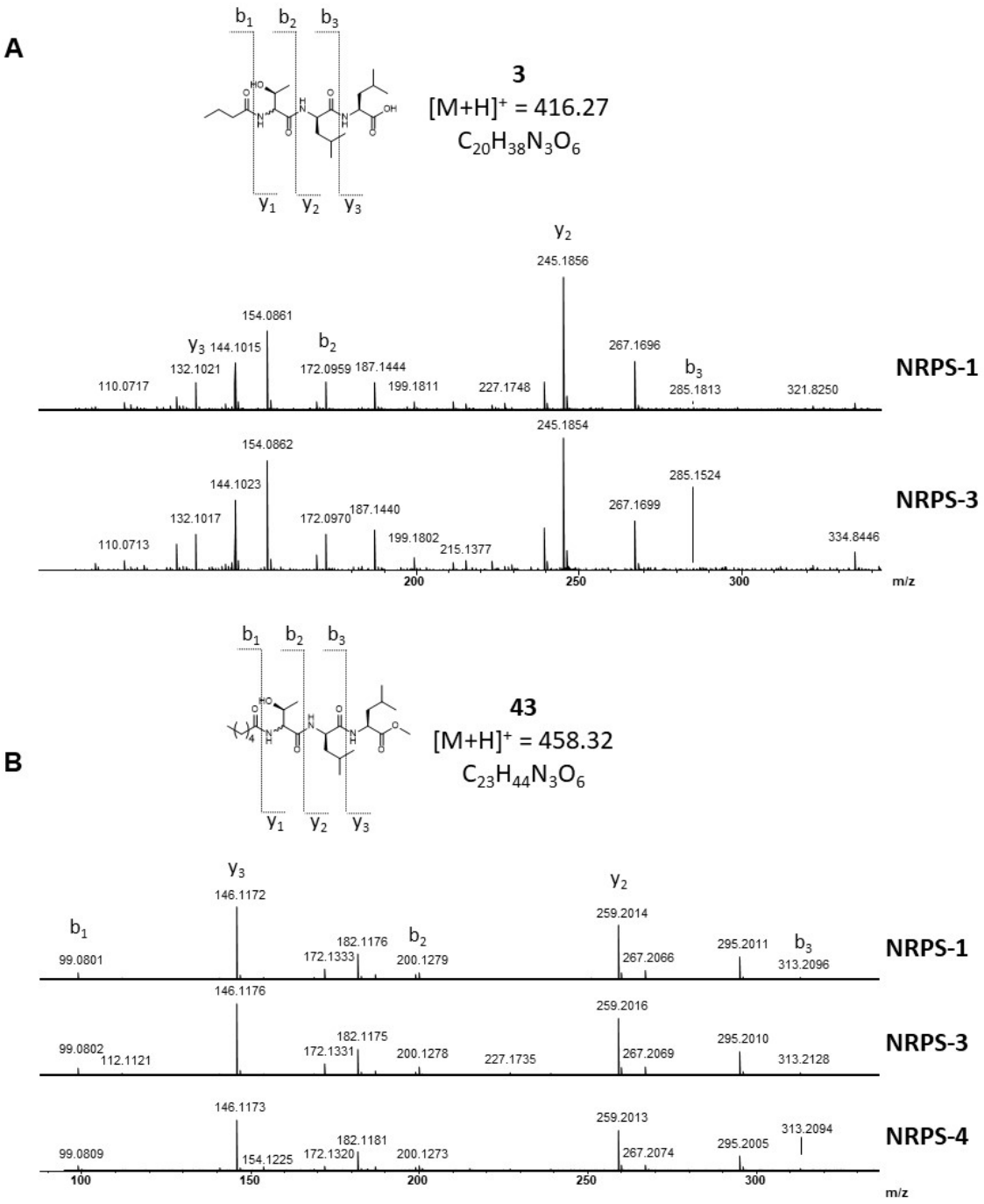

Figure S17. HPLC/MS data refers to Figure 2 (NRPS-1, -3 and -4) of compound **3** (**A**) and **43** (**B**) produced in *E. coli* DH10B::*mtaA*. Comparison of MS^2 spectra.

A

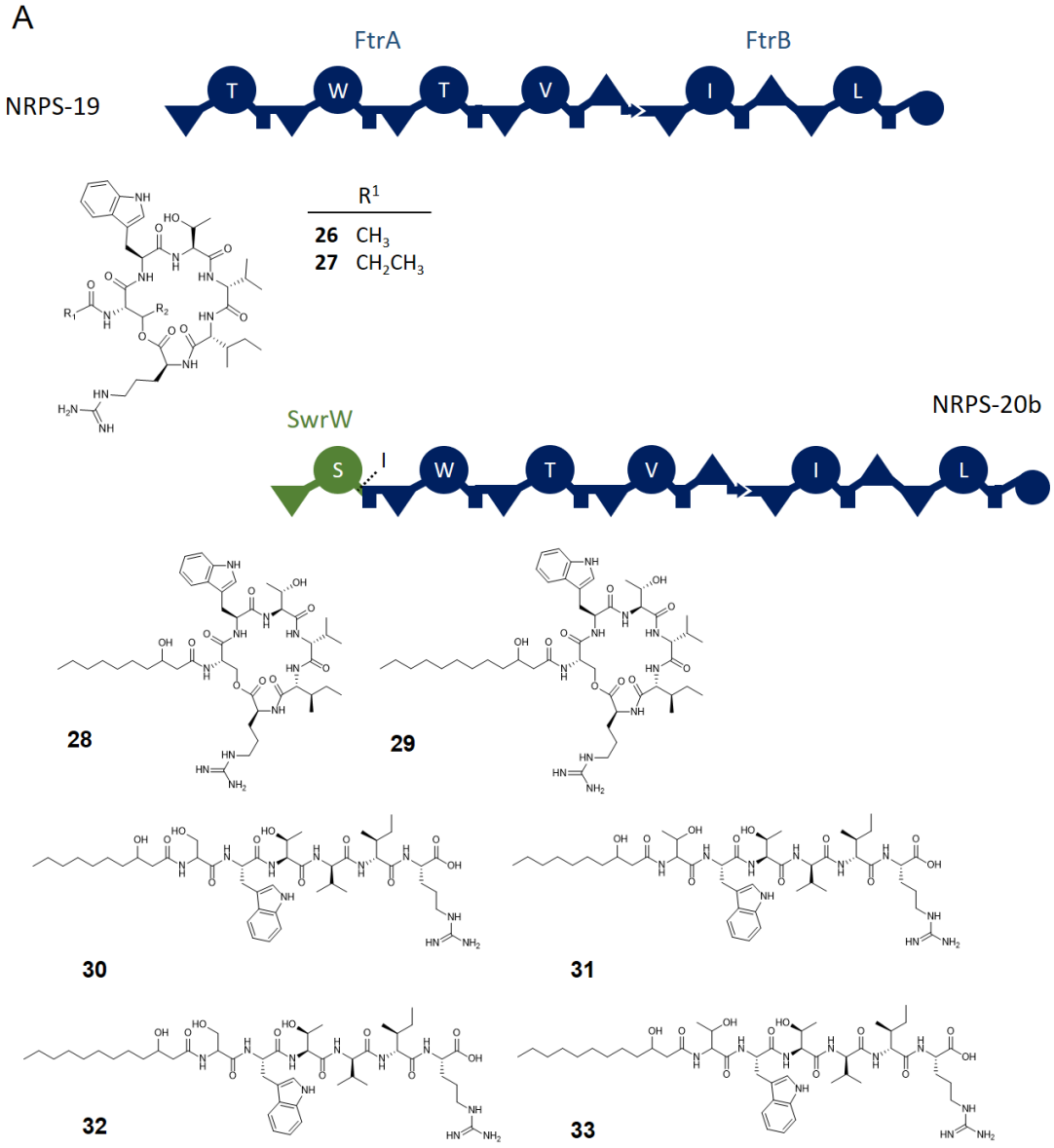

B

NRPS	Peptide	Peptide	Organism	Donor BGC	Fusion site	Production (mg l^{-1})	% of NRPS-8
-19	**26, 27**	C2-TWTviR	*X. mauleonii*	*ftrAB*	WT	56.0 ±3.5	100
-20b	**28 , 29**	C10-βOH-SWTviR	*S. marcescens*	*swrW*	IV	2.5 ±0.2	4

Figure S18. (**A**) Domain architecture of Fatttvir (**FA** **T**hr **T**yr **T**hr **V**al **I**le a**R**g) producing FtrAB (NRPS-19) and NRPS-20b with their peptide product structures **26-33** shown below. Structure elucidation of **26** is shown at Figures S19 – S21 and S44 - S49. (**B**) For quantification the signal intensities for **28** and **29** were summarized and compared to the summarized amount of **26** and **27** in the WT.

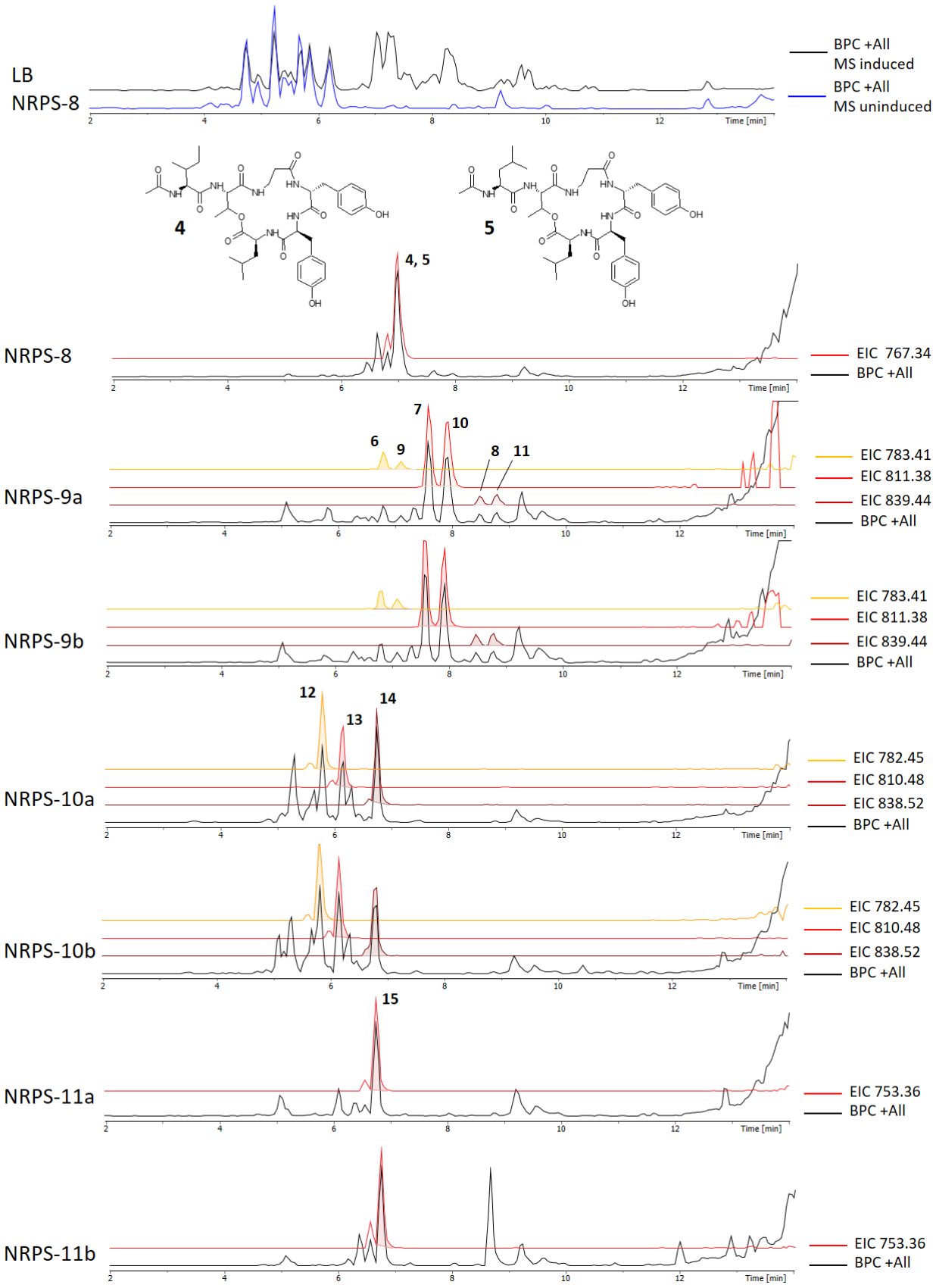
LB
NRPS-8
BPC +All
MS induced
BPC +All
MS uninduced
Time [min]
4
5
4, 5
NRPS-8
EIC 767.34
BPC +All
6
9
7
10
8
11
NRPS-9a
EIC 783.41
EIC 811.38
EIC 839.44
BPC +All
NRPS-9b
12
13
14
NRPS-10a
EIC 782.45
EIC 810.48
EIC 838.52
BPC +All
NRPS-10b
15
NRPS-11a
EIC 753.36
BPC +All
NRPS-11b

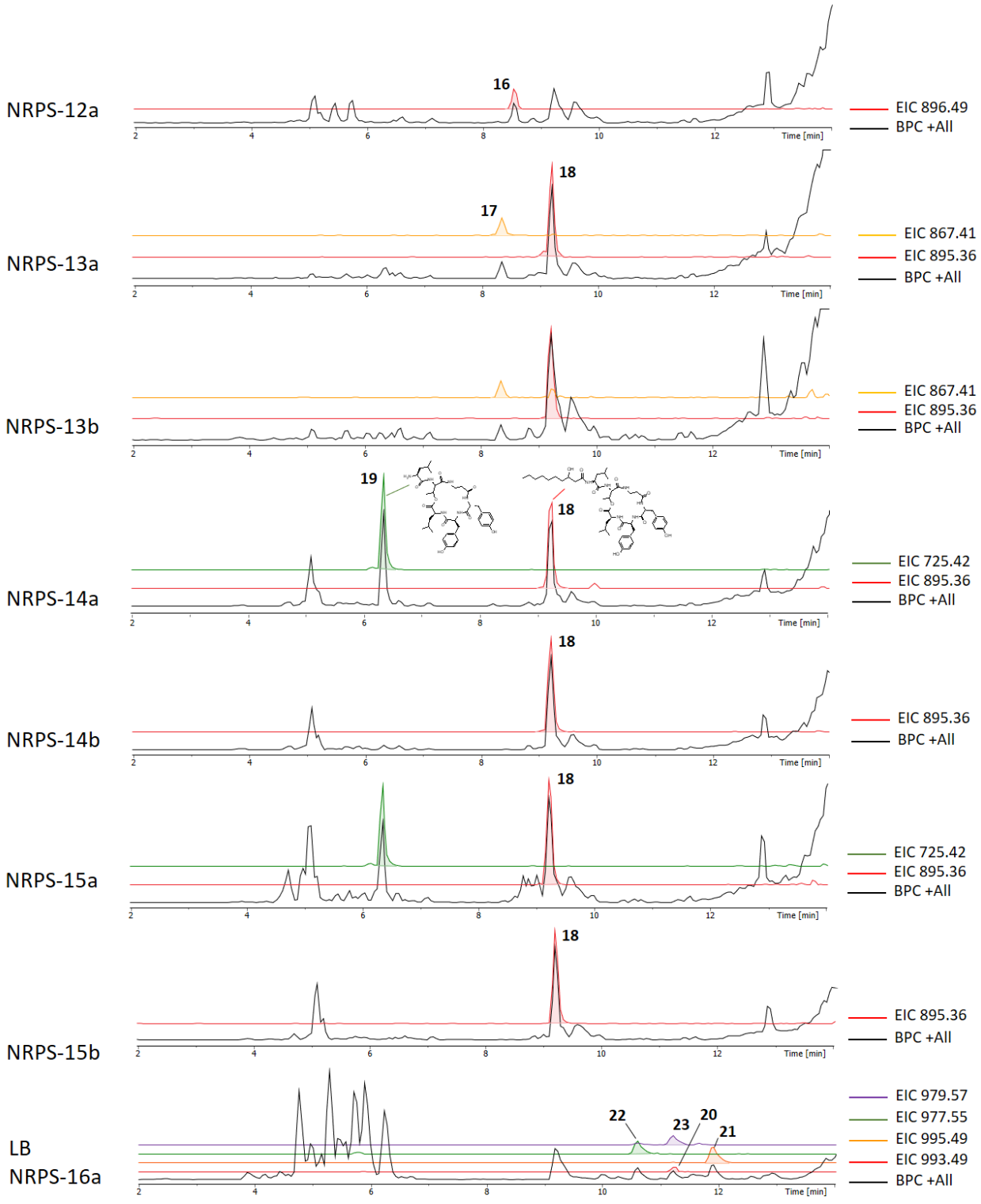
NRPS-12a
16
EIC 896.49
BPC +All
NRPS-13a
17
18
EIC 867.41
EIC 895.36
BPC +All
NRPS-13b
EIC 867.41
EIC 895.36
BPC +All
NRPS-14a
19
18
EIC 725.42
EIC 895.36
BPC +All
NRPS-14b
18
EIC 895.36
BPC +All
NRPS-15a
18
EIC 725.42
EIC 895.36
BPC +All
NRPS-15b
18
EIC 895.36
BPC +All
LB
NRPS-16a
22
23
20
21
EIC 979.57
EIC 977.55
EIC 995.49
EIC 993.49
BPC +All
Time [min]

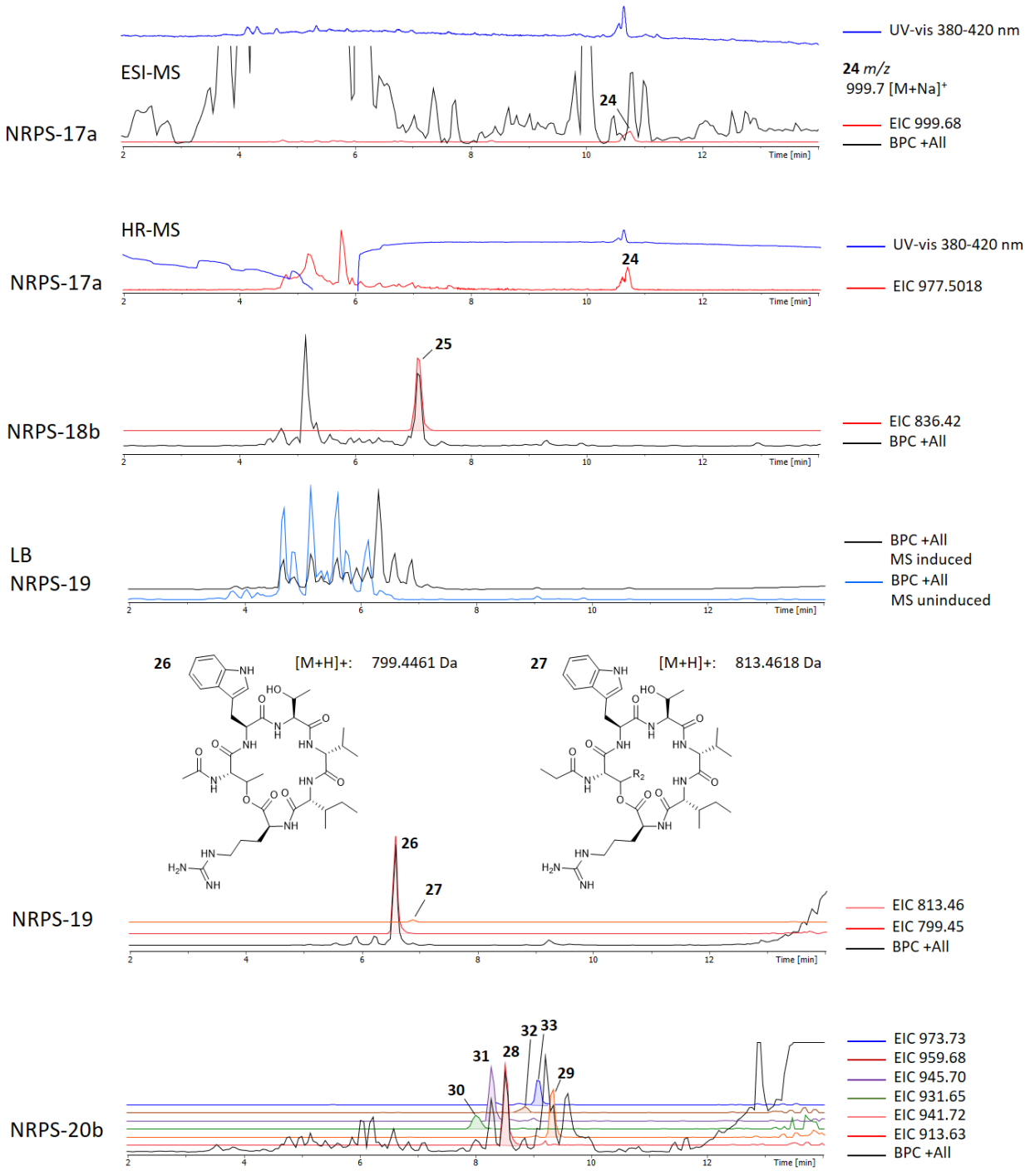

Figure S19. Chromatograms and structures of **4**, **5**, **26** and **27** and their NRPS-engineering derivatives.

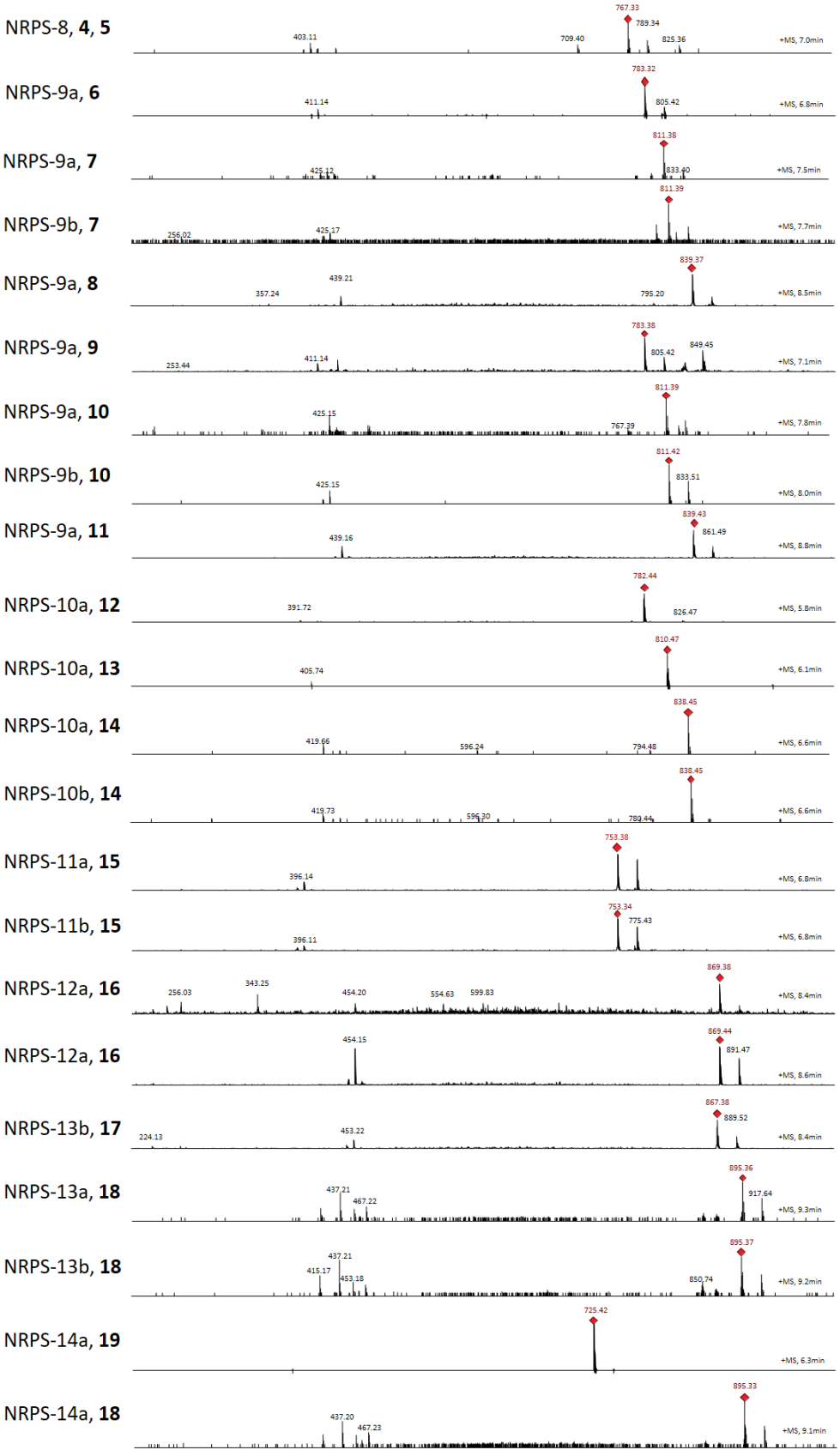
NRPS-8, 4, 5
767.33
789.34
403.11
709.40
825.36
+MS, 7.0min
NRPS-9a, 6
783.32
411.14
805.42
+MS, 6.8min
NRPS-9a, 7
811.38
425.12
833.40
+MS, 7.5min
NRPS-9b, 7
811.39
256.02
425.17
+MS, 7.7min
NRPS-9a, 8
839.37
439.21
357.24
795.20
+MS, 8.5min
NRPS-9a, 9
783.38
805.42
849.45
411.14
253.44
+MS, 7.1min
NRPS-9a, 10
811.39
425.15
767.39
+MS, 7.8min
NRPS-9b, 10
811.42
833.51
425.15
+MS, 8.0min
NRPS-9a, 11
839.43
861.49
439.16
+MS, 8.8min
NRPS-10a, 12
782.44
391.72
826.47
+MS, 5.8min
NRPS-10a, 13
810.47
405.74
+MS, 6.1min
NRPS-10a, 14
838.45
419.66
596.24
794.48
+MS, 6.6min
NRPS-10b, 14
838.45
419.73
596.30
+MS, 6.6min
NRPS-11a, 15
753.38
396.14
+MS, 6.8min
NRPS-11b, 15
753.34
775.43
396.11
+MS, 6.8min
NRPS-12a, 16
869.38
256.03
343.25
454.20
554.63
599.83
+MS, 8.4min
NRPS-12a, 16
454.15
869.44
891.47
+MS, 8.6min
NRPS-13b, 17
867.38
889.52
224.13
453.22
+MS, 8.4min
NRPS-13a, 18
895.36
917.64
437.21
467.22
+MS, 9.3min
NRPS-13b, 18
895.37
437.21
415.17
453.18
850.74
+MS, 9.2min
NRPS-14a, 19
725.42
+MS, 6.3min
NRPS-14a, 18
895.33
437.20
467.23
+MS, 9.1min

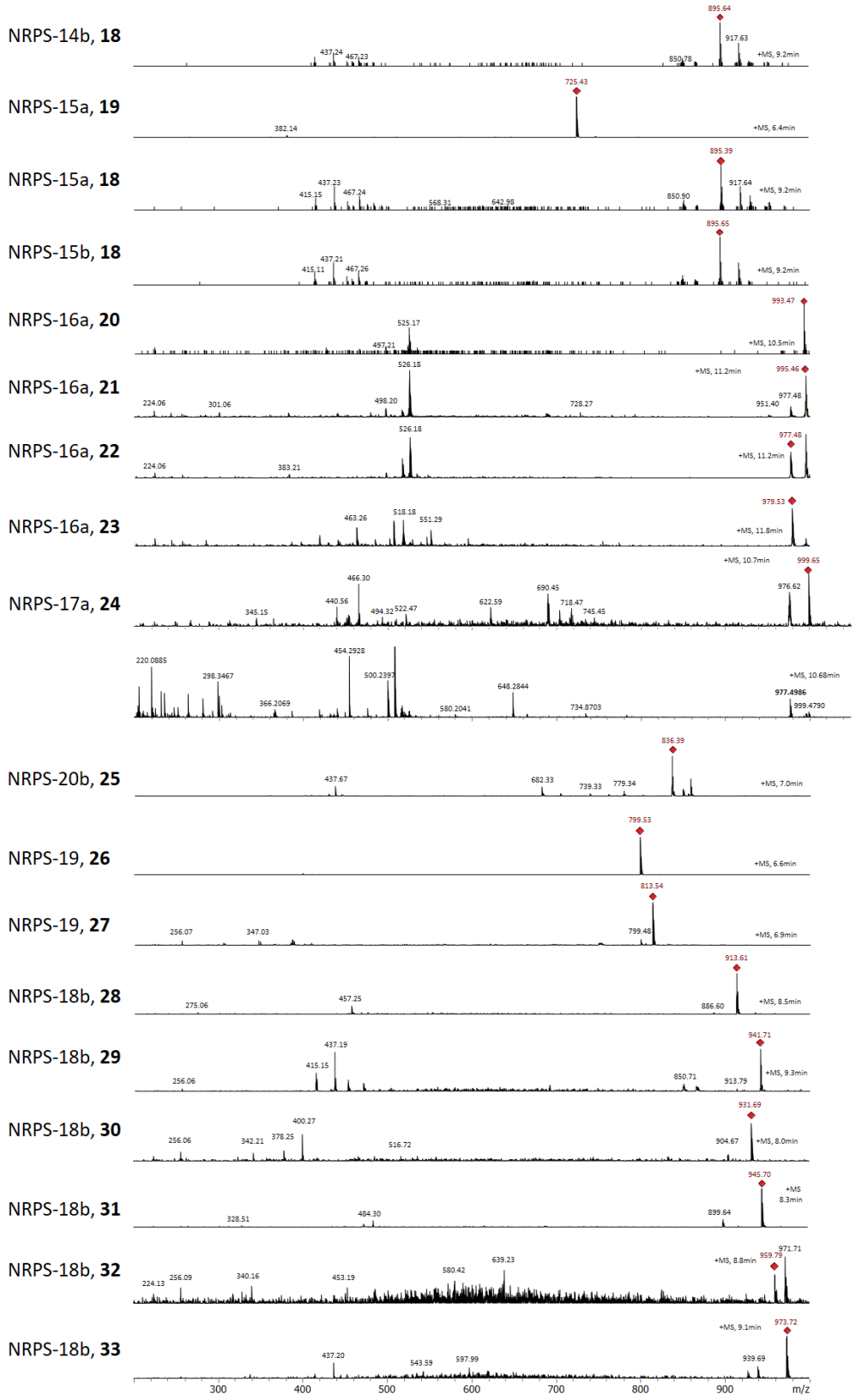

Figure S20. MS-spectra of peptides **4**-**33** of NRPS-8 to -20 corresponding to the extracted ion chromatograms in **Fig. S19**.

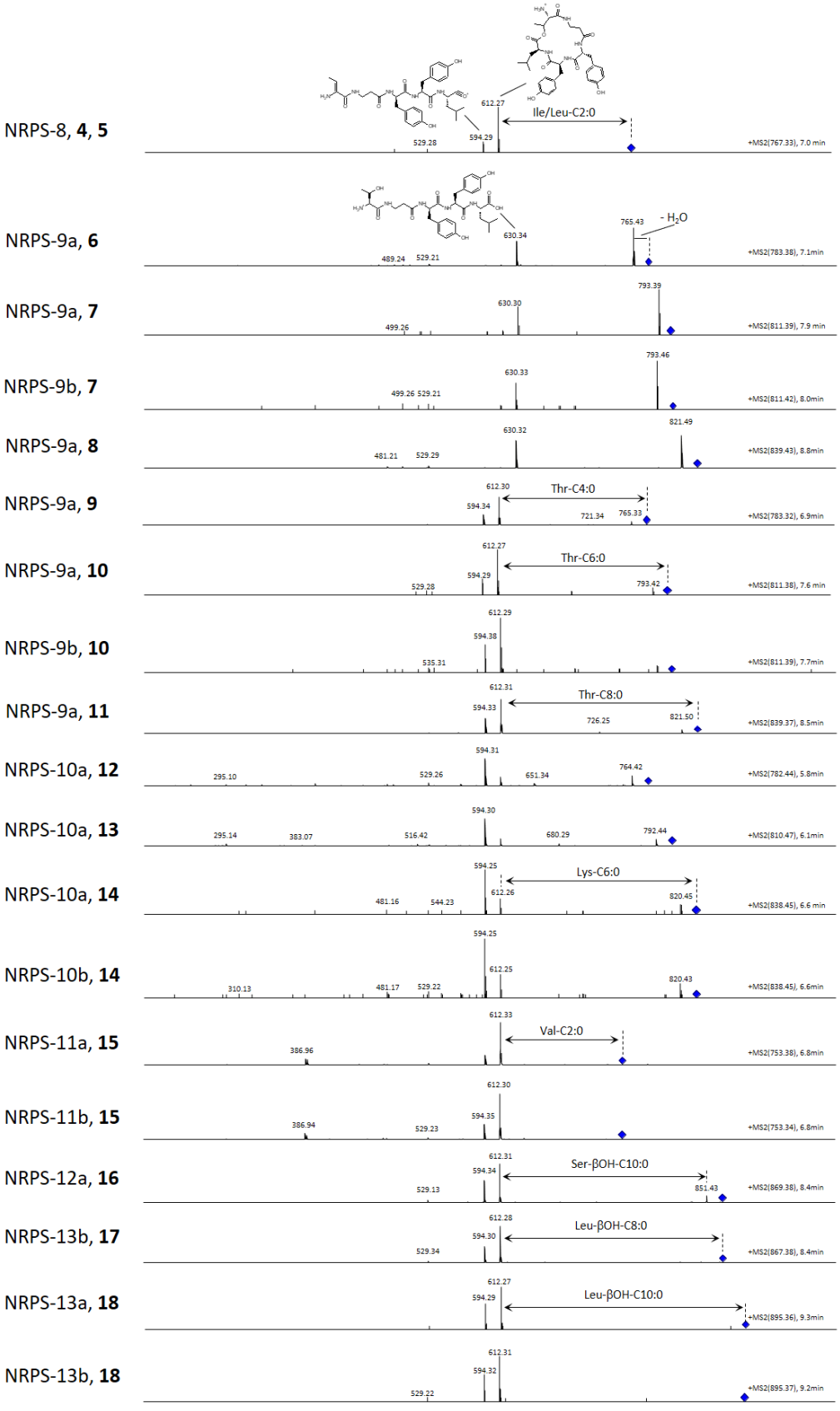
NRPS-8, 4, 5
612.27
Ile/Leu-C2:0
594.29
529.28
+MS2(767.33), 7.0 min
NRPS-9a, 6
765.43
- H2O
630.34
489.24
529.21
+MS2(783.38), 7.1min
NRPS-9a, 7
793.39
630.30
499.26
+MS2(811.39), 7.9 min
NRPS-9b, 7
793.46
630.33
499.26 529.21
+MS2(811.42), 8.0min
NRPS-9a, 8
821.49
630.32
481.21
529.29
+MS2(839.43), 8.8min
NRPS-9a, 9
612.30
Thr-C4:0
594.34
721.34
765.33
+MS2(783.32), 6.9min
NRPS-9a, 10
612.27
Thr-C6:0
594.29
529.28
793.42
+MS2(811.38), 7.6 min
NRPS-9b, 10
612.29
594.38
535.31
+MS2(811.39), 7.7min
NRPS-9a, 11
612.31
Thr-C8:0
594.33
726.25
821.50
+MS2(839.37), 8.5min
NRPS-10a, 12
594.31
295.10
529.26
651.34
764.42
+MS2(782.44), 5.8min
NRPS-10a, 13
594.30
295.14
383.07
516.42
680.29
792.44
+MS2(810.47), 6.1min
NRPS-10a, 14
594.25
Lys-C6:0
612.26
481.16
544.23
820.45
+MS2(838.45), 6.6 min
NRPS-10b, 14
594.25
612.25
310.13
481.17
529.22
820.43
+MS2(838.45), 6.6min
NRPS-11a, 15
612.33
Val-C2:0
386.96
+MS2(753.38), 6.8min
NRPS-11b, 15
612.30
594.35
386.94
529.23
+MS2(753.34), 6.8min
NRPS-12a, 16
612.31
Ser-βOH-C10:0
594.34
529.13
851.43
+MS2(869.38), 8.4min
NRPS-13b, 17
612.28
Leu-βOH-C8:0
594.30
529.34
+MS2(867.38), 8.4min
NRPS-13a, 18
612.27
Leu-βOH-C10:0
594.29
+MS2(895.36), 9.3min
NRPS-13b, 18
612.31
594.32
529.22
+MS2(895.37), 9.2min

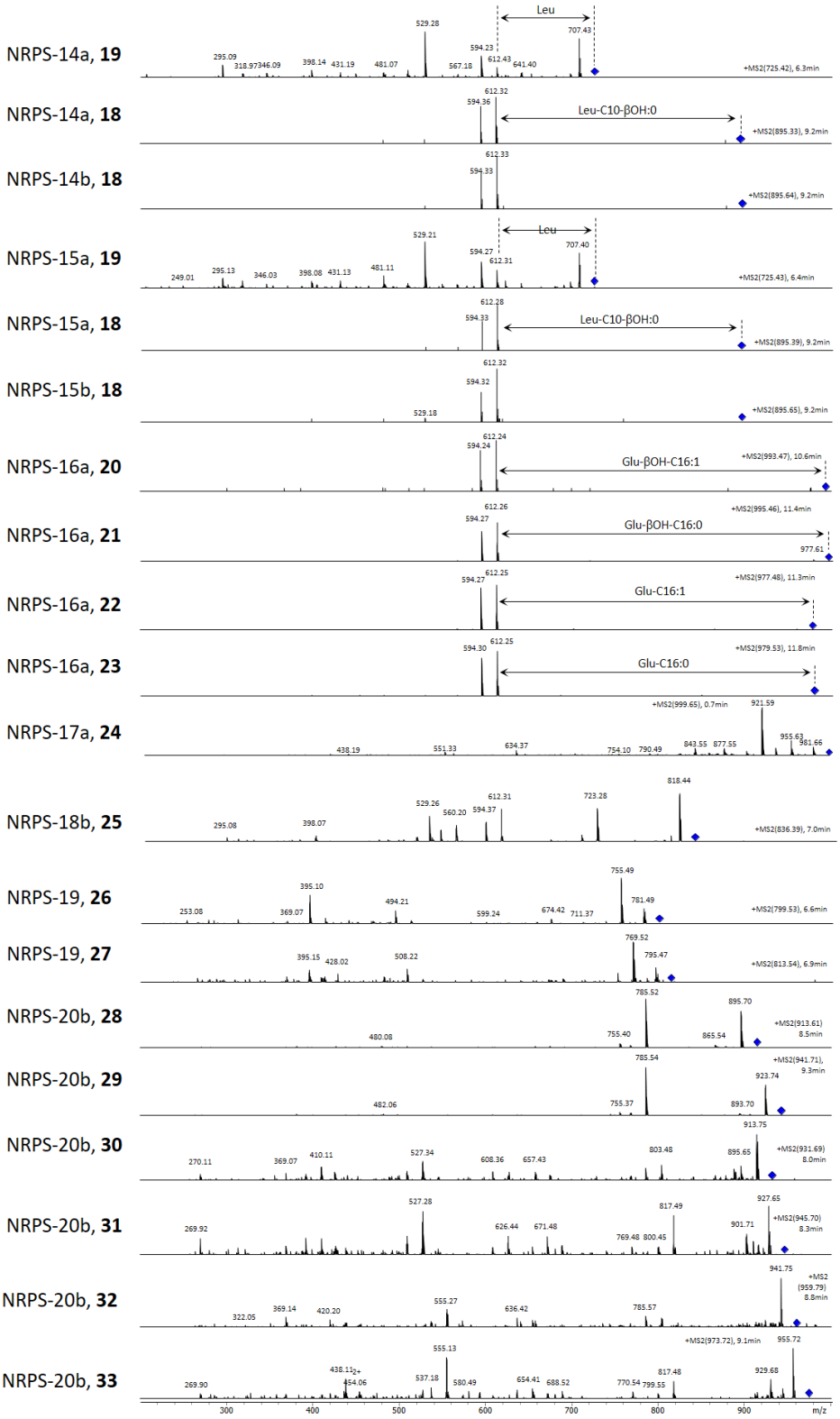

Figure S21. MS^2 spectra of peptides **4-33** of NRPS-8 to -20 corresponding to the signals in **Fig. S20**.

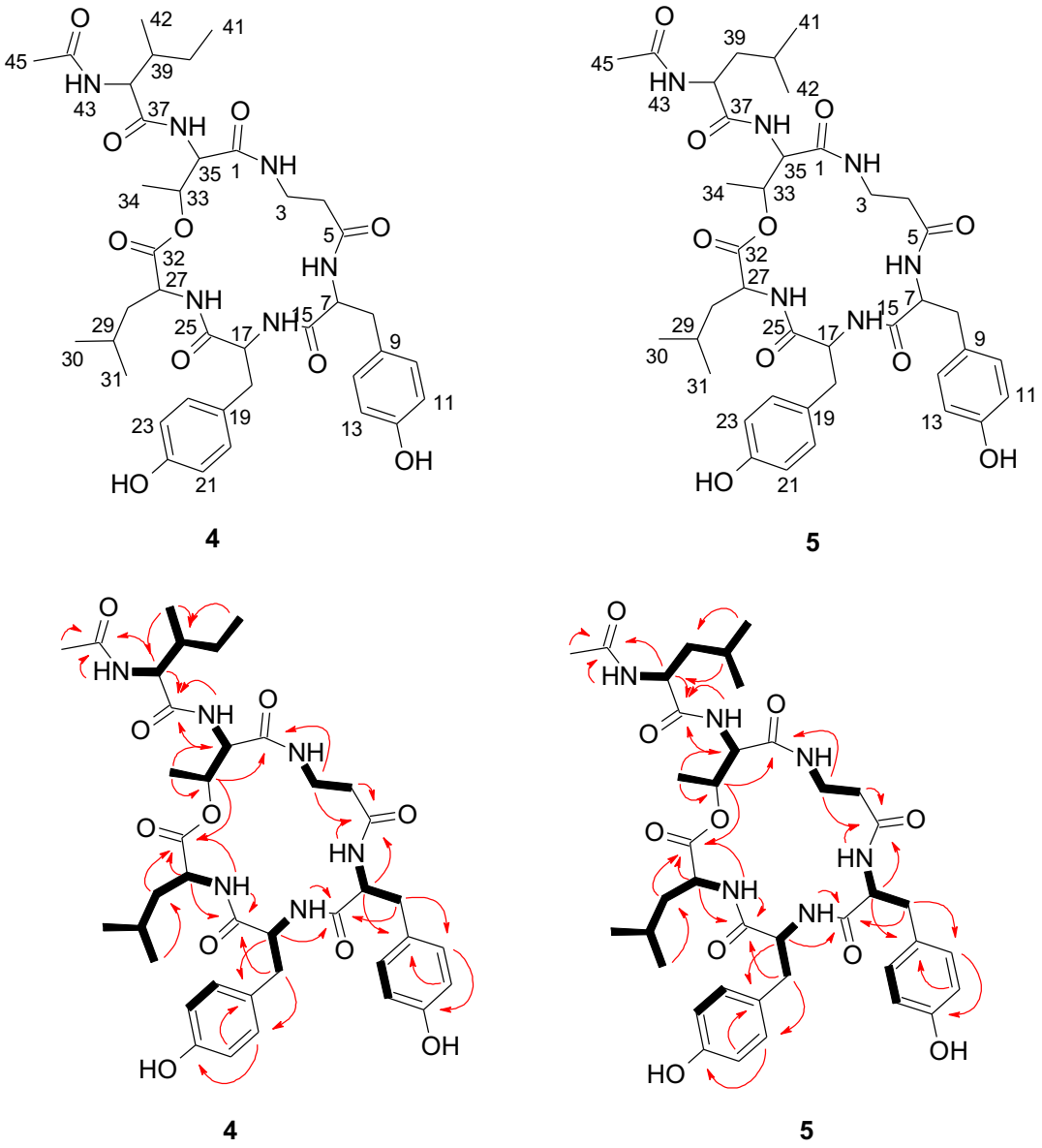

Figure S22. Key HMBC and ^{1}H-^{1}H COSY correlations of compounds **4** and **5**.

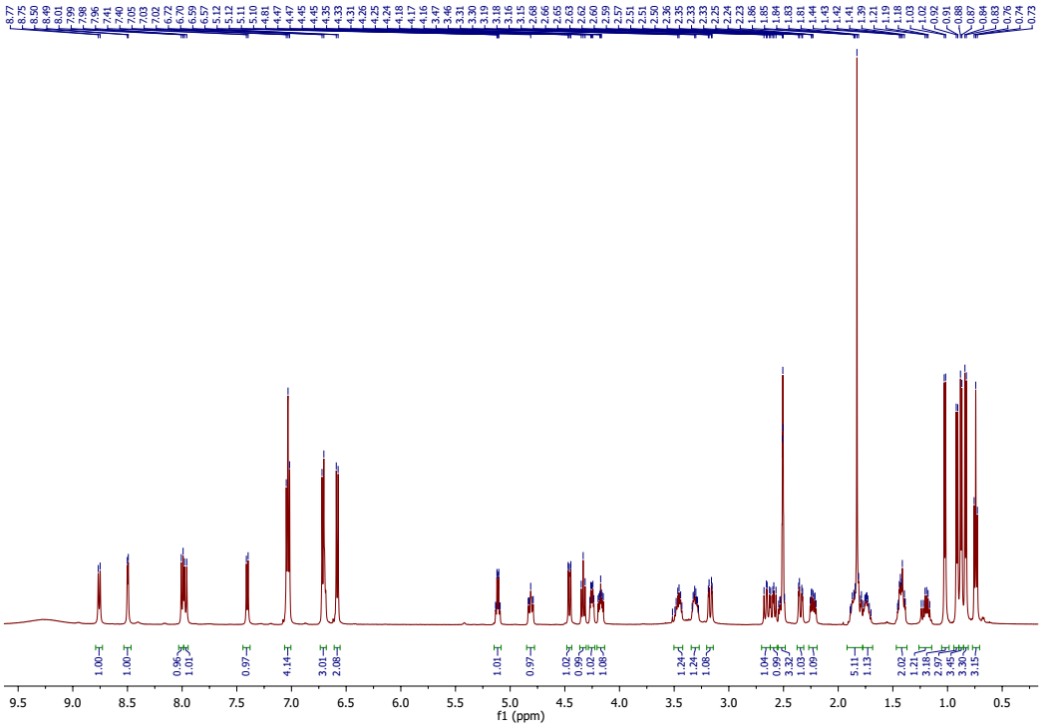

Figure S23. ^{1}H NMR spectrum of compound **4**.

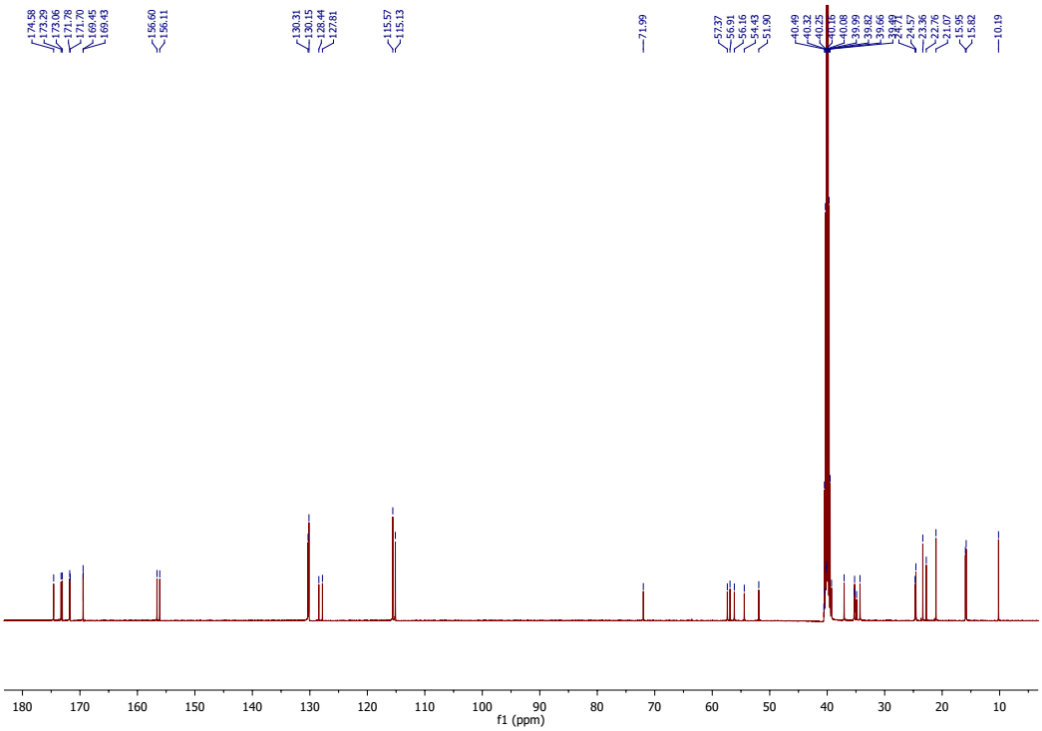

Figure S24. ^{13}C NMR spectrum of compound **4.**

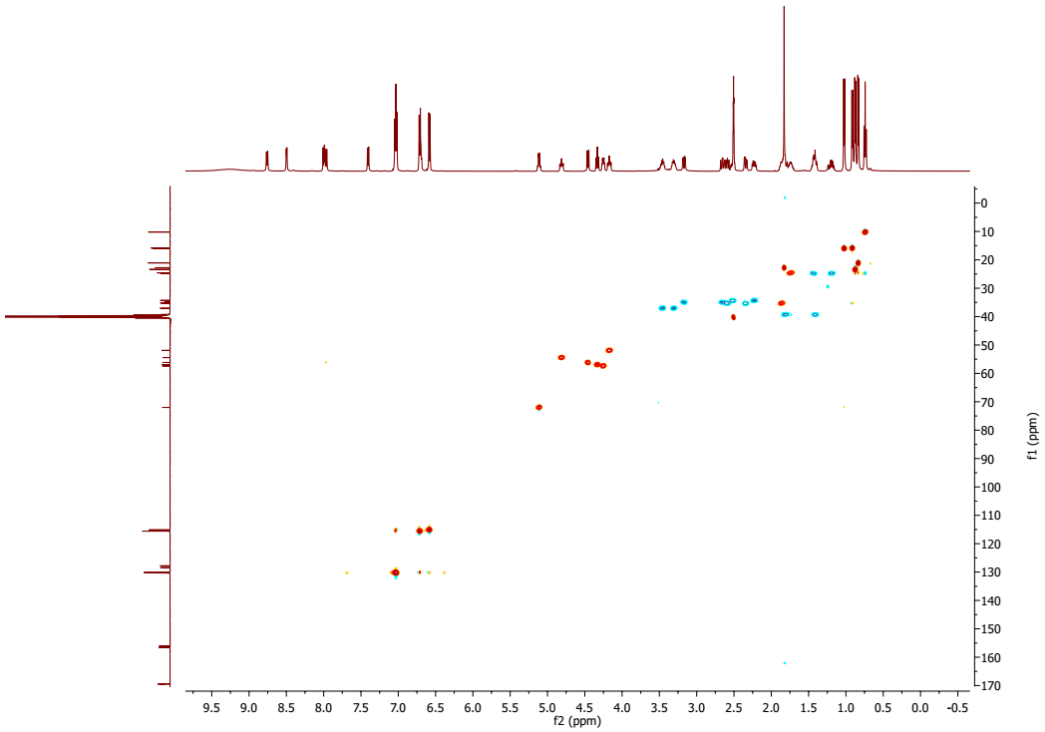

Figure S25. HSQC spectrum of compound **4**.

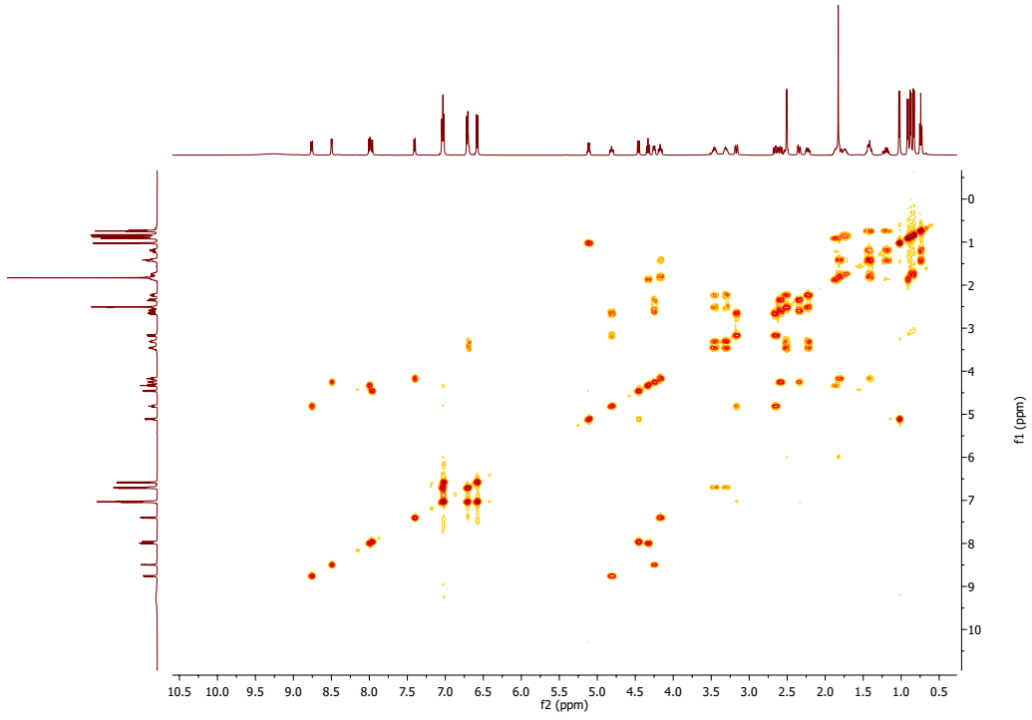

Figure S26. ^{1}H-^{1}H COSY spectrum of compound **4**.

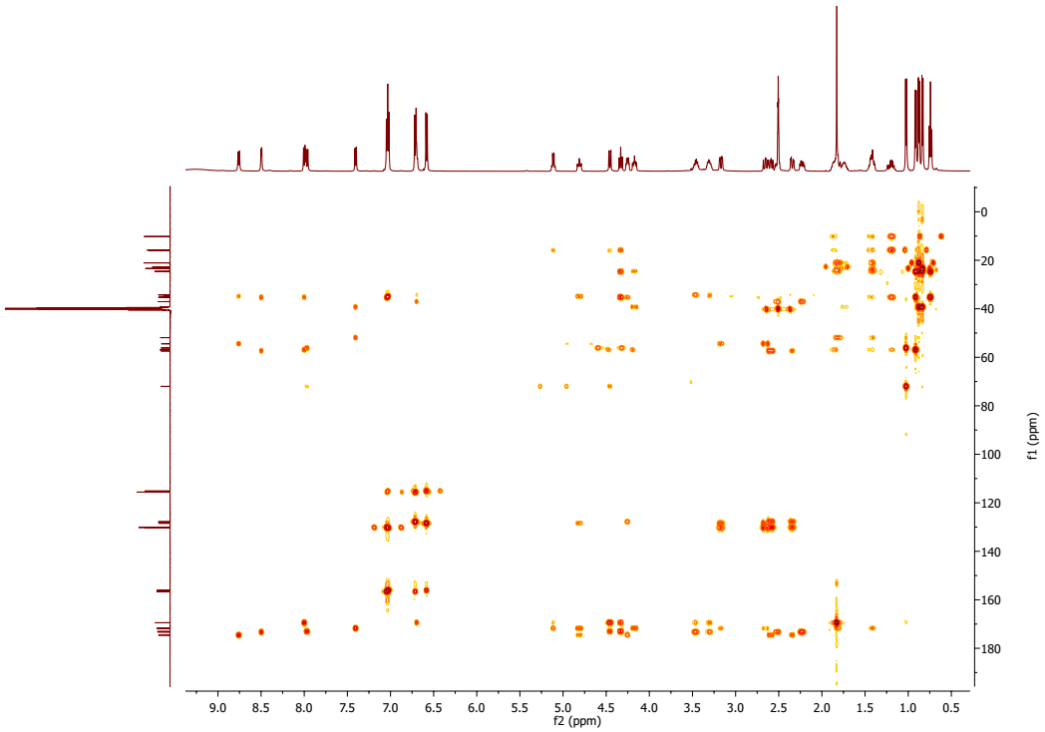

Figure S27. HMBC spectrum of compound **4**.

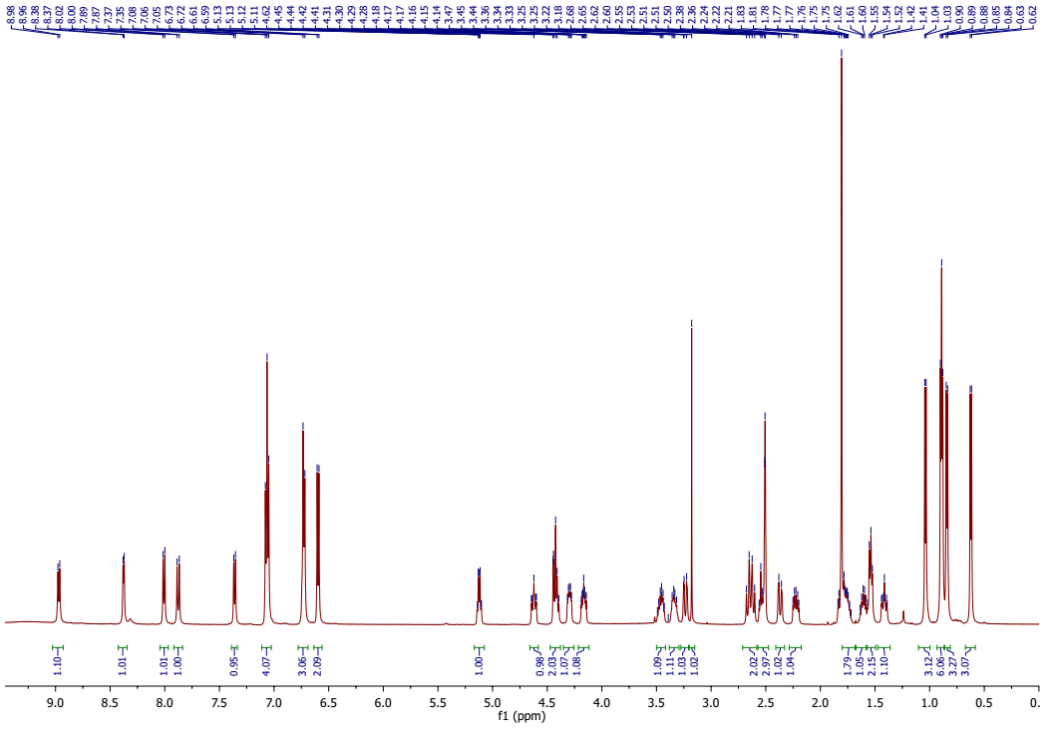

Figure S28. ^{1}H NMR spectrum of compound **5**.

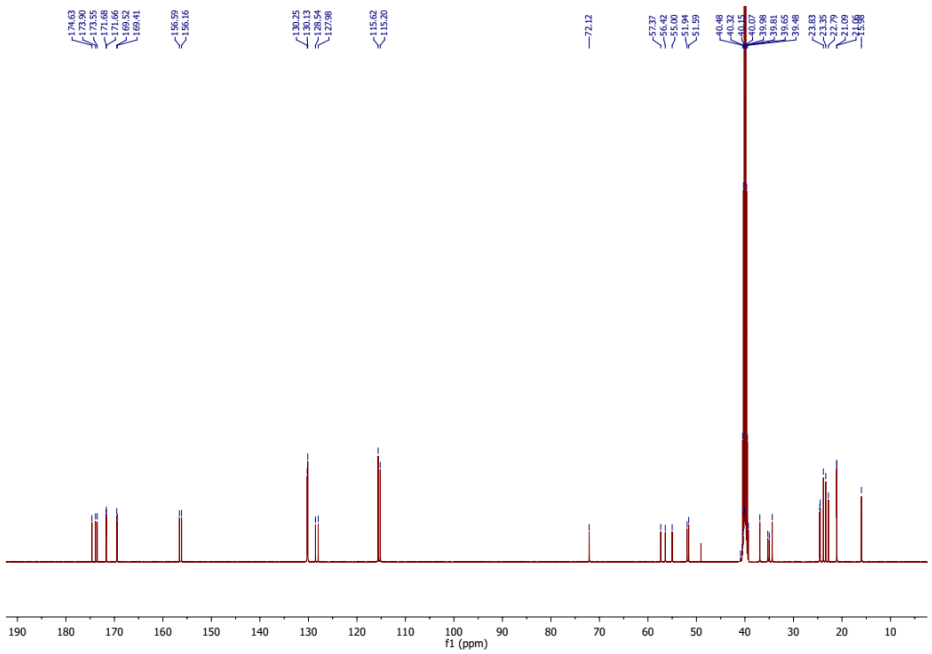

Figure S29. ^{13}C NMR spectrum of compound **5**.

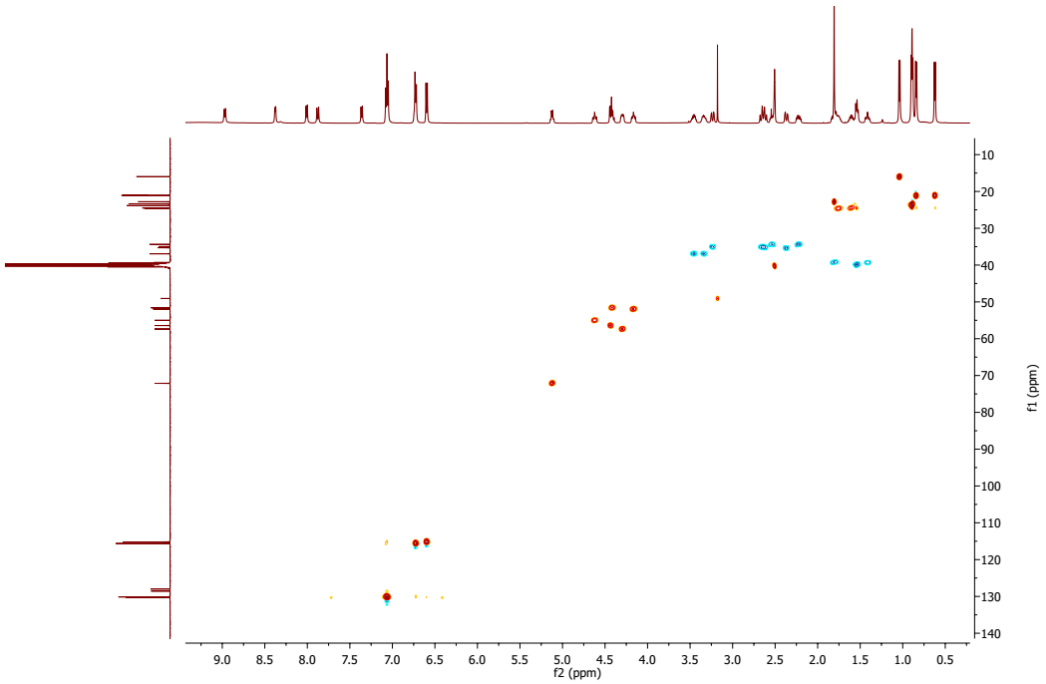

Figure S30. HSQC spectrum of compound **5**.

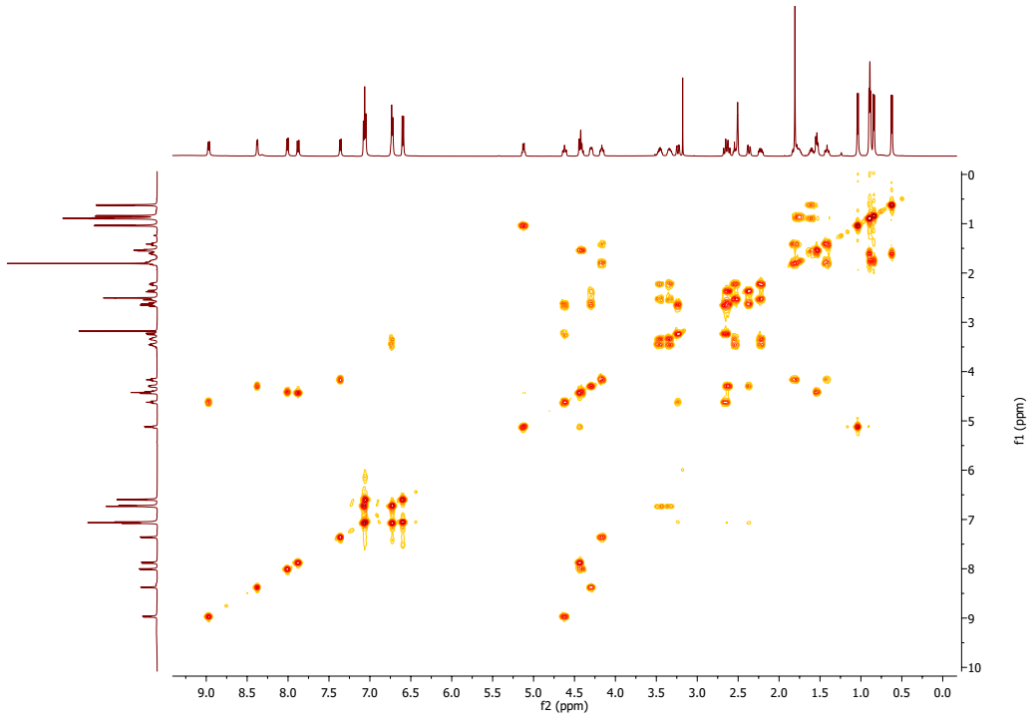

Figure S31. ^{1}H-^{1}H COSY spectrum of compound **5**.

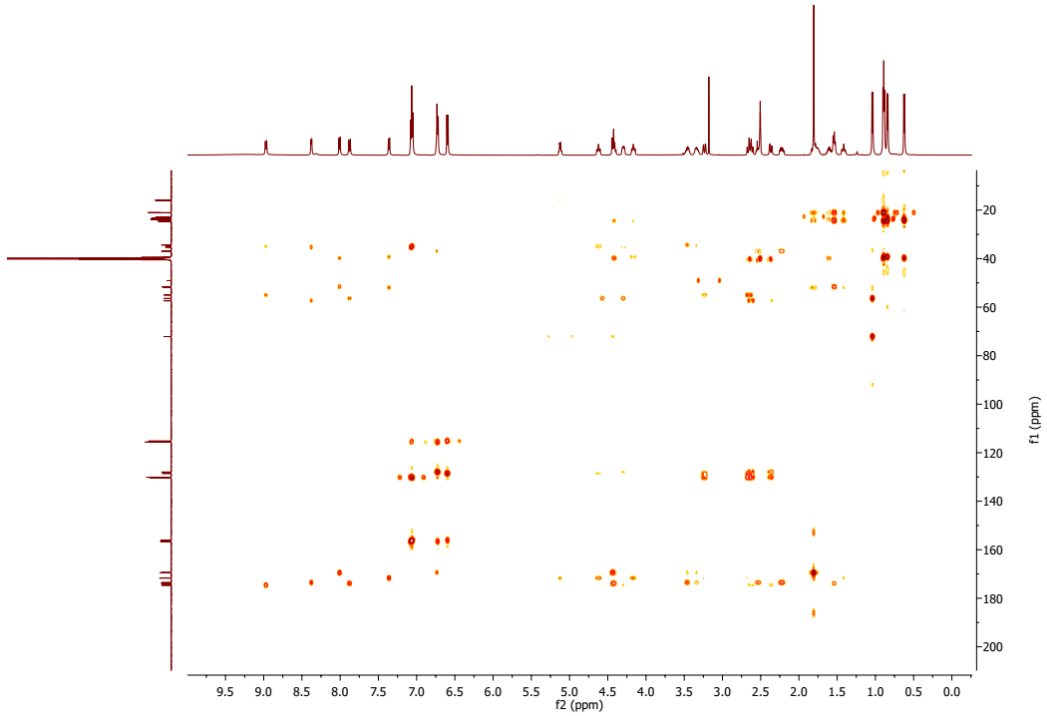

Figure S32. HMBC spectrum of compound **5**.

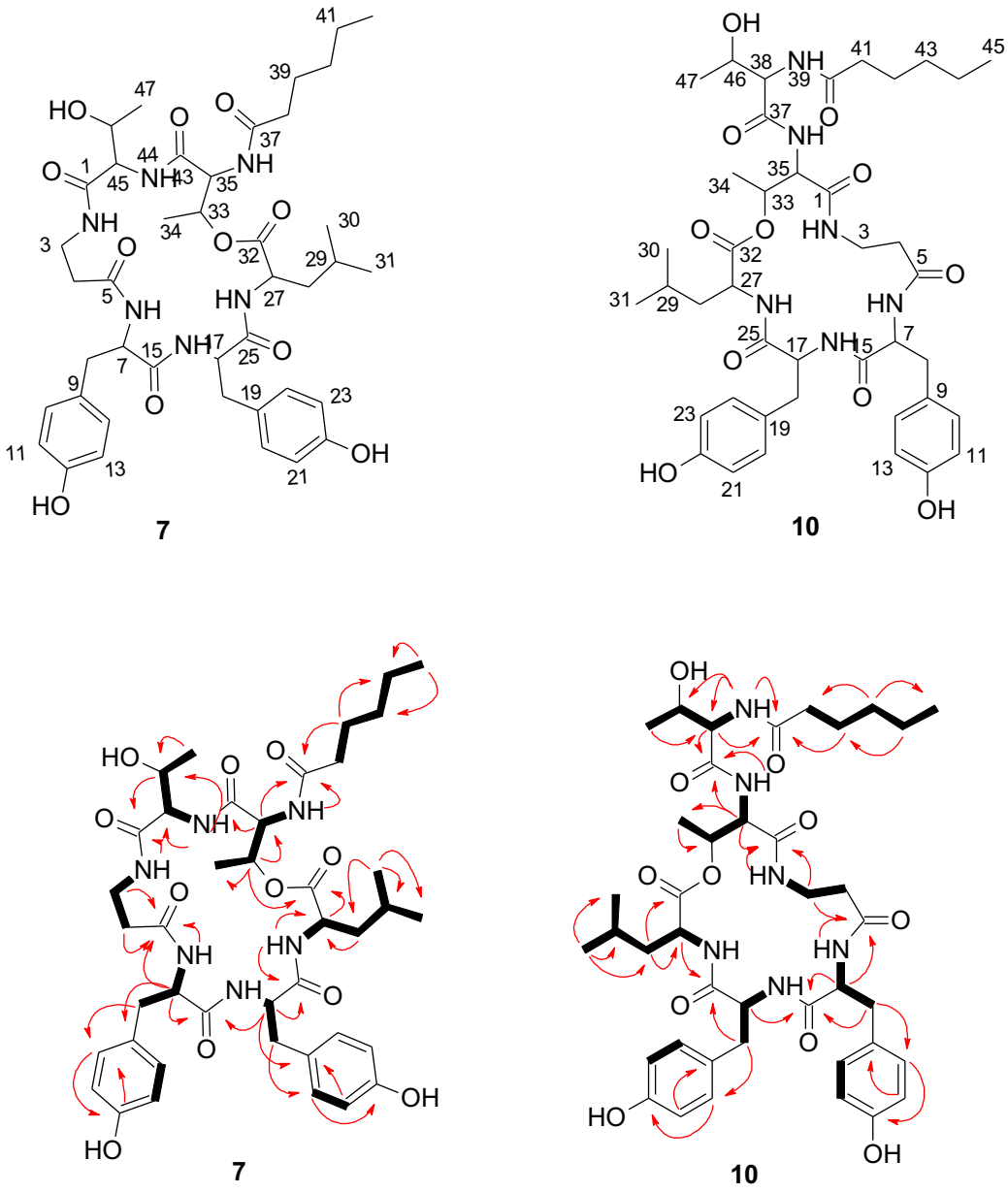

Figure S33. Key HMBC and ^{1}H-^{1}H COSY correlations of compounds **7** and **10**.

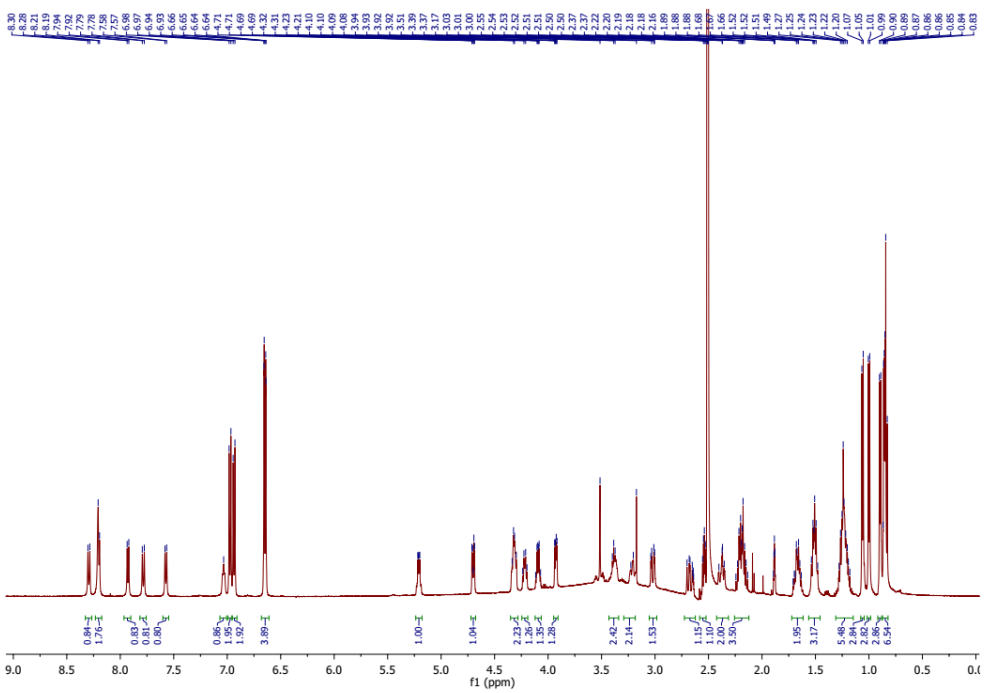

Figure S34. ^{1}H NMR spectrum of compound **7.**

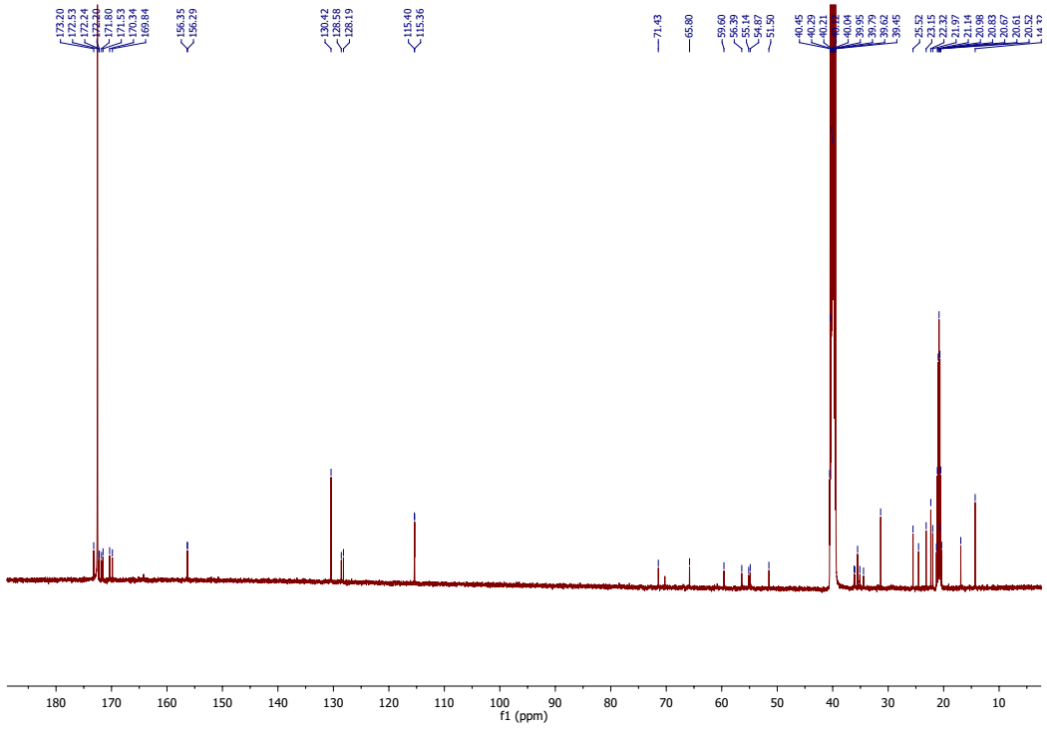

Figure S35. ^{13}C NMR spectrum of compound **7**.

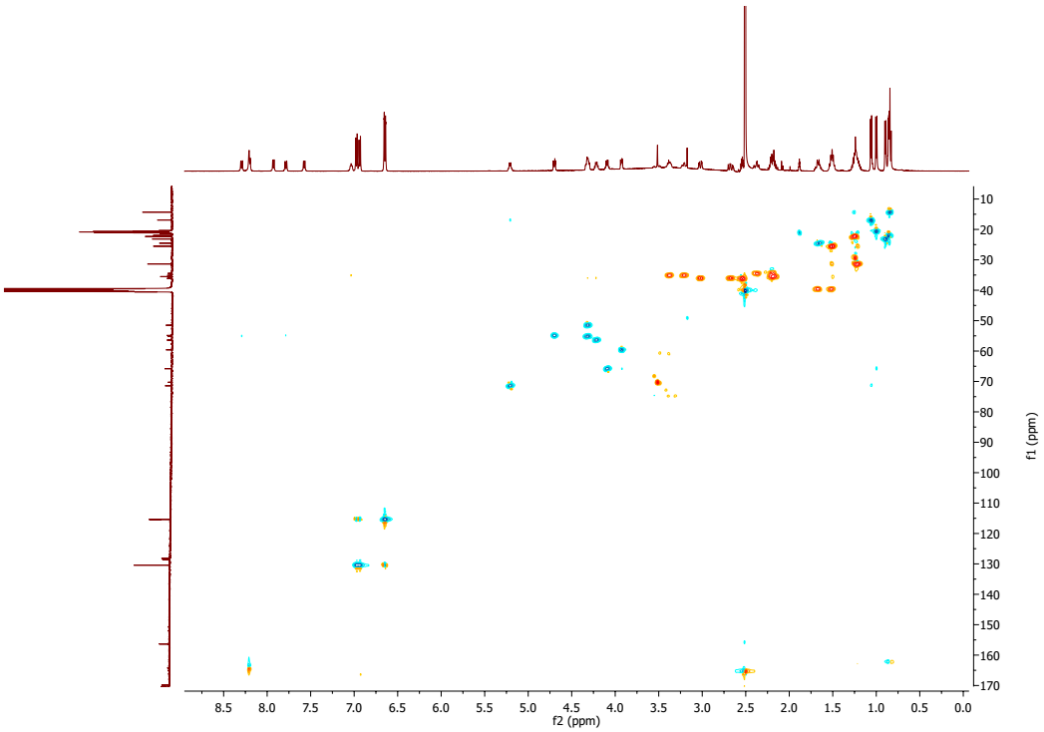

Figure S36. HSQC spectrum of compound **7**.

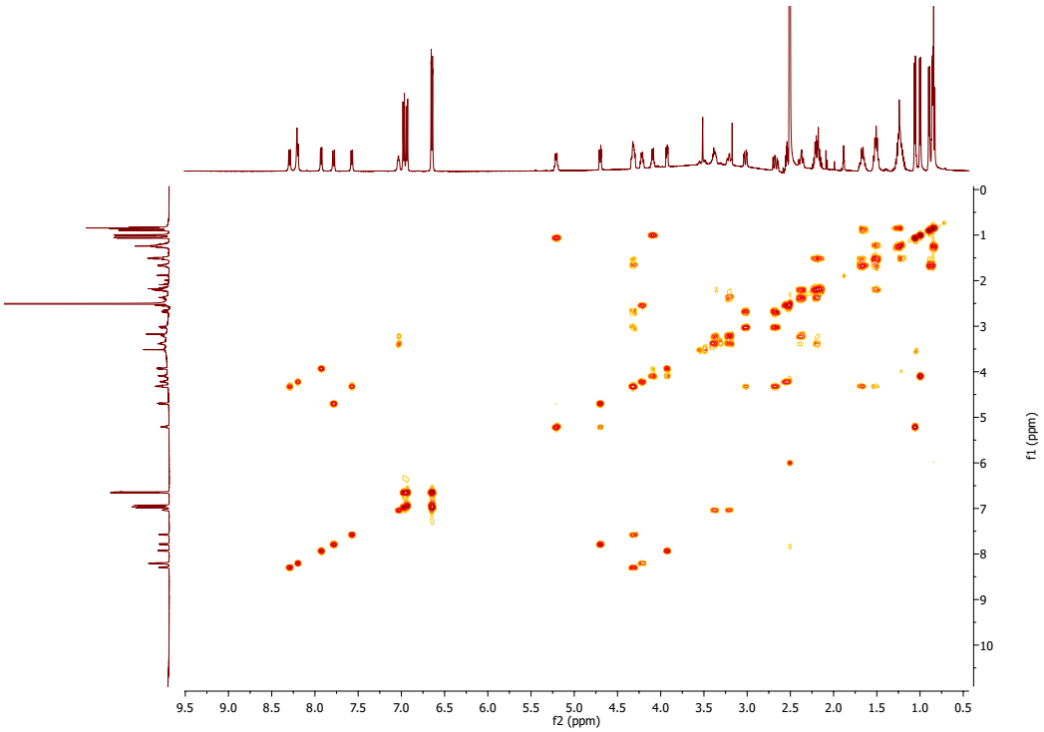

Figure S37. ^{1}H-^{1}H COSY spectrum of compound **7**.

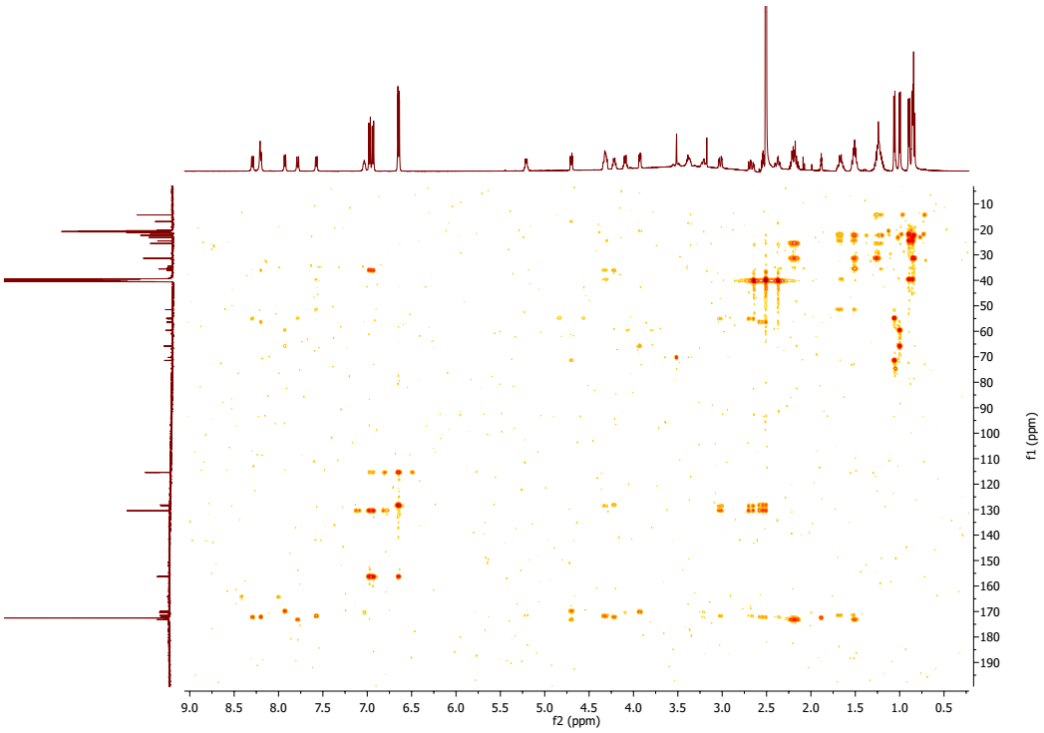

Figure S38. HMBC spectrum of compound **7**.

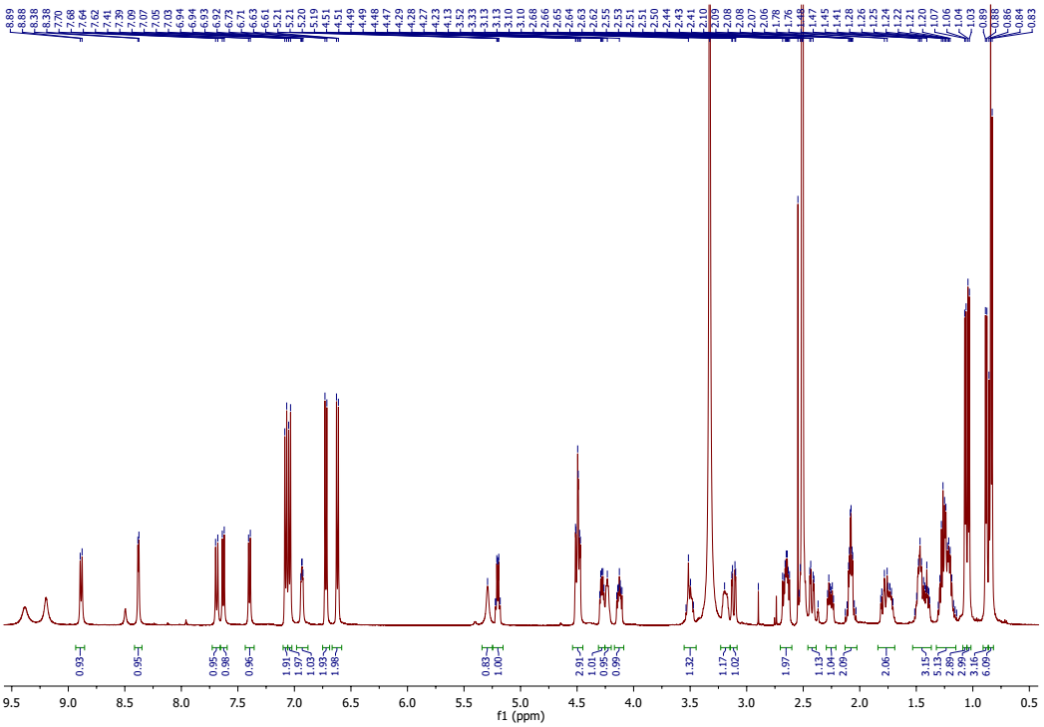

Figure S39. ^{1}H NMR spectrum of compound **10**.

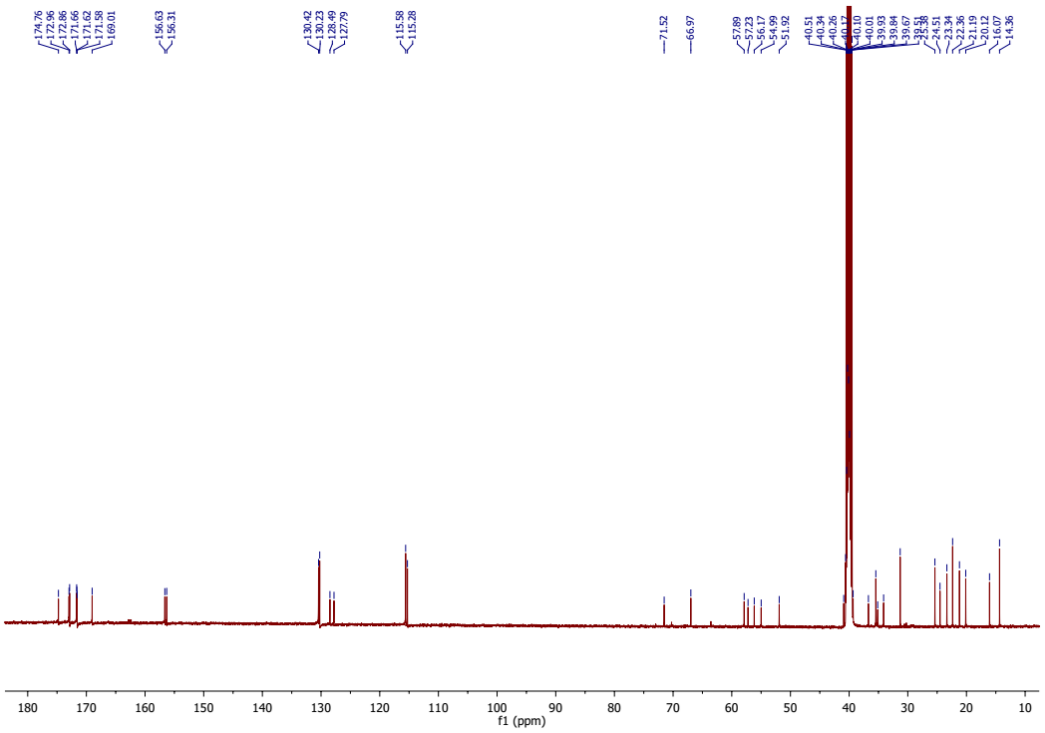

Figure S40. ^{13}C NMR spectrum of compound **10**.

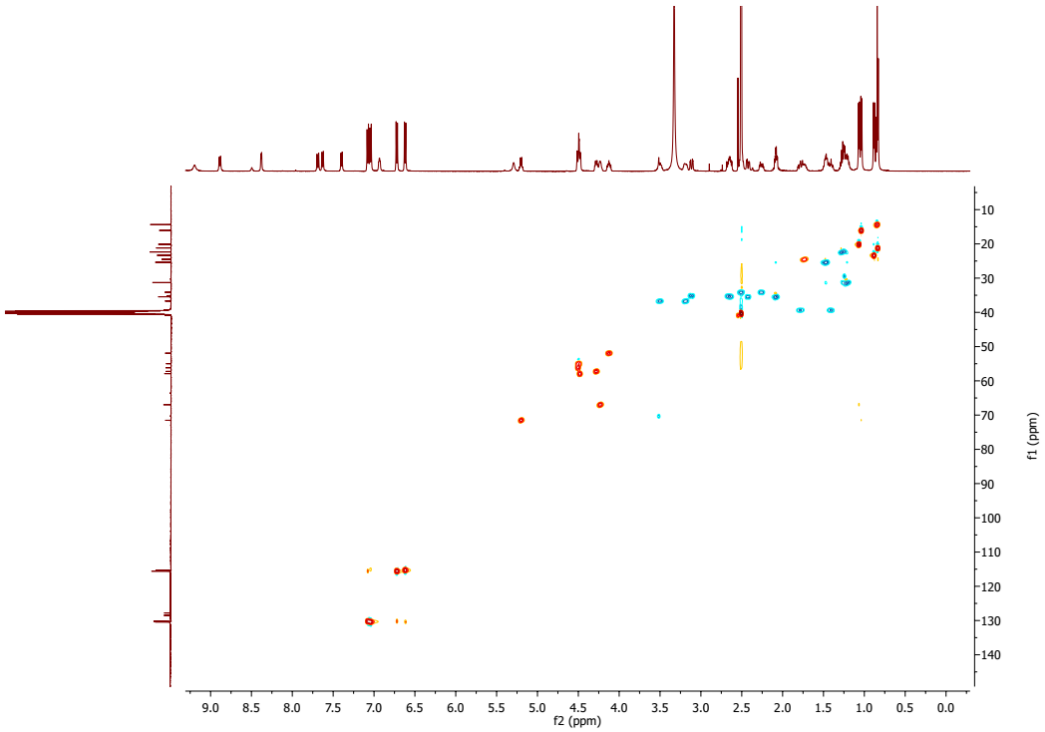

Figure S41. HSQC spectrum of compound **10**.

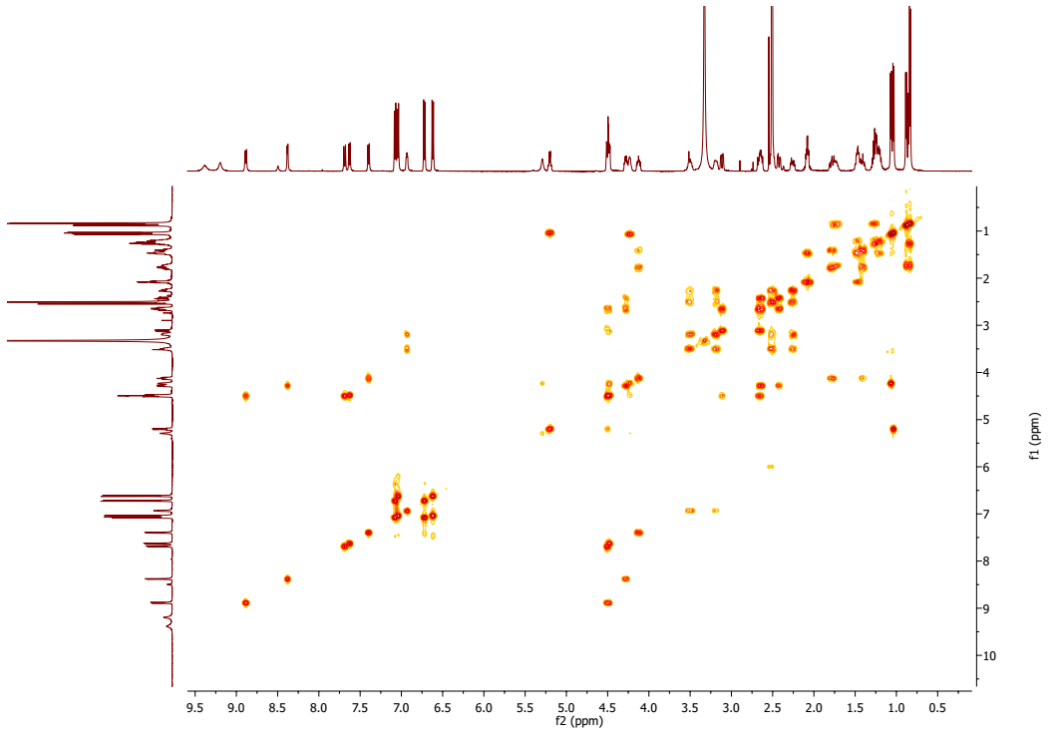

Figure S42. ^{1}H-^{1}H COSY spectrum of compound **10**.

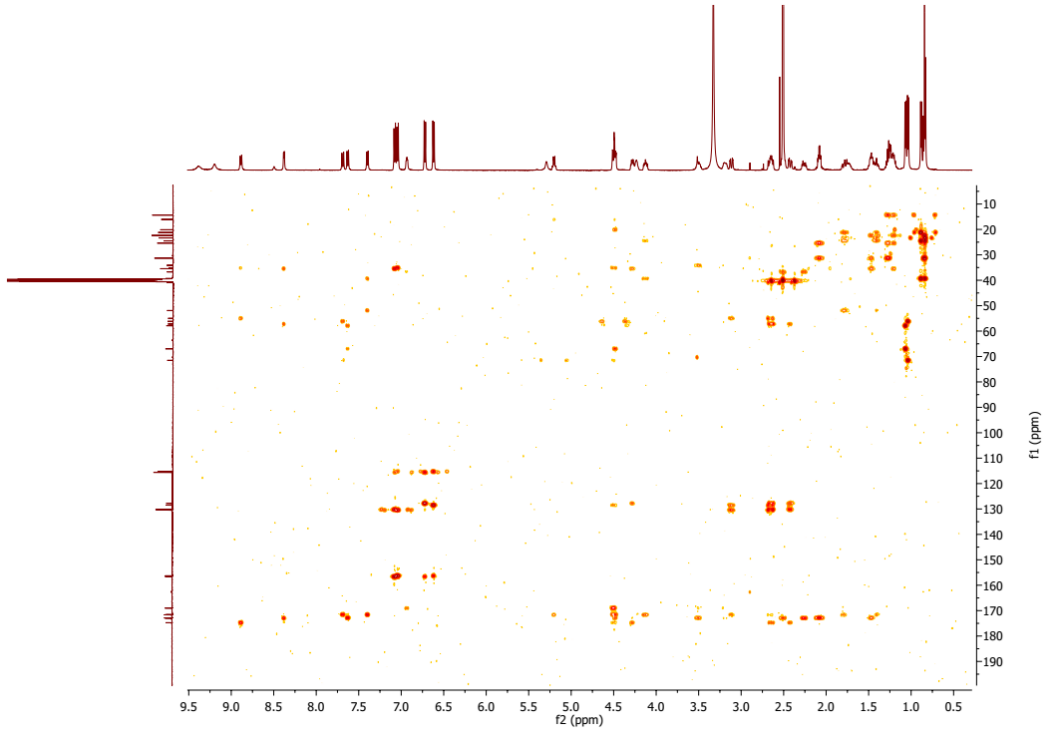

Figure S43. HMBC spectrum of compound **10**.

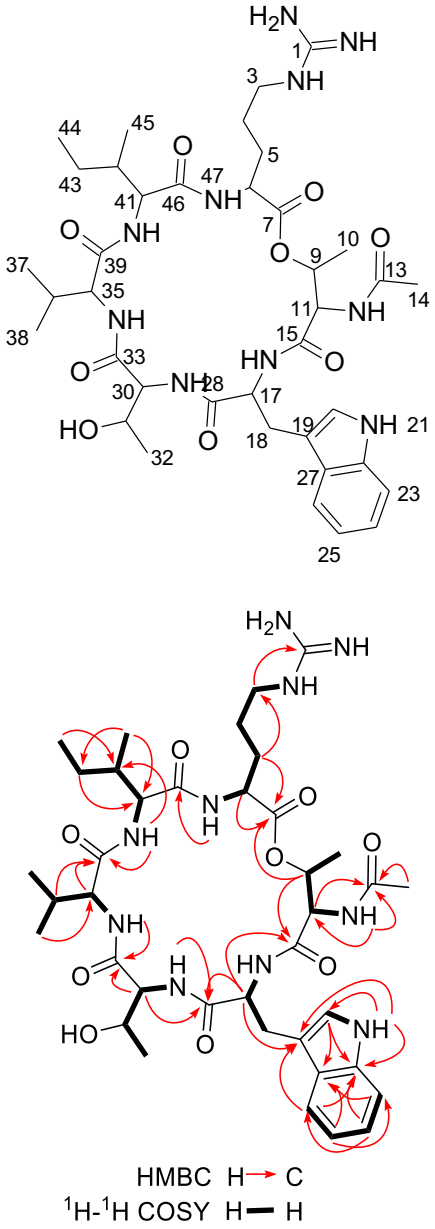

Figure S44. Key HMBC and ^{1}H-^{1}H COSY correlations of compound **26**.

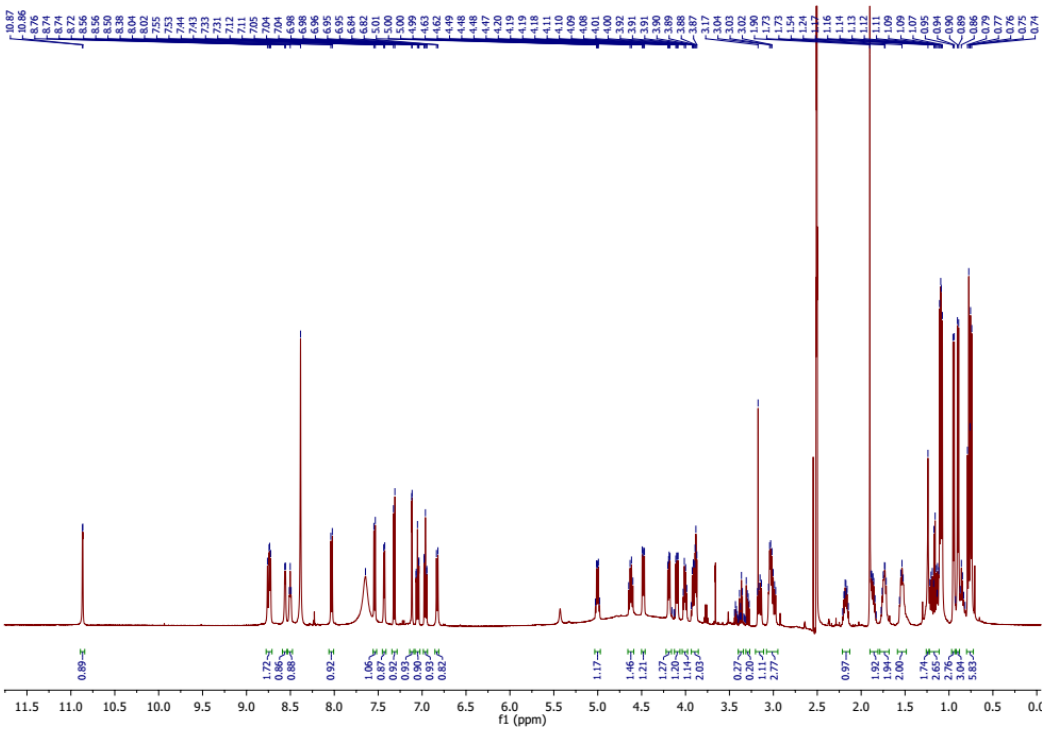

Figure S45. ^{1}H NMR spectrum of compound **26**.

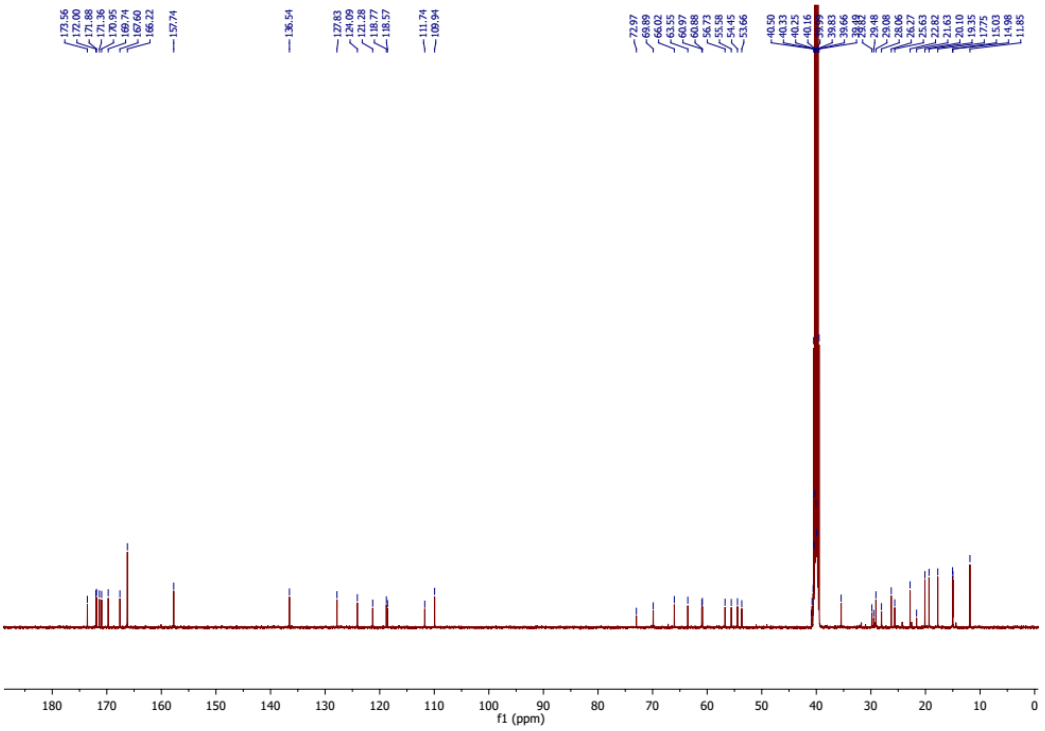

Figure S46. ^{13}C NMR spectrum of compound **26**.

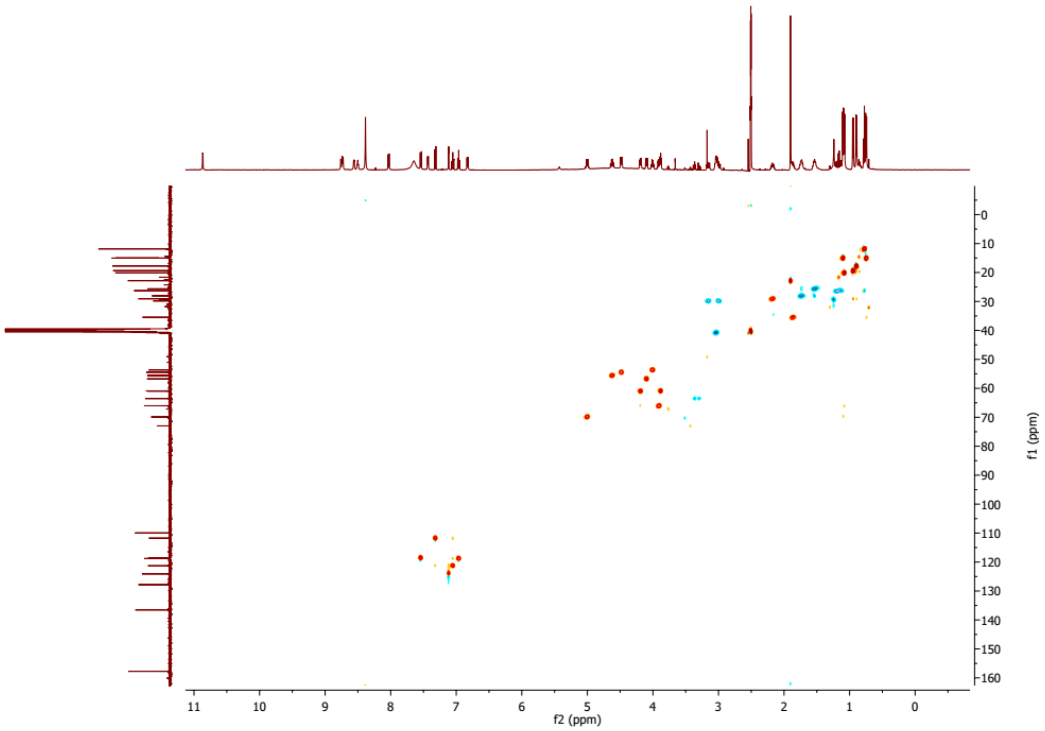

Figure S47. HSQC spectrum of compound **26**.

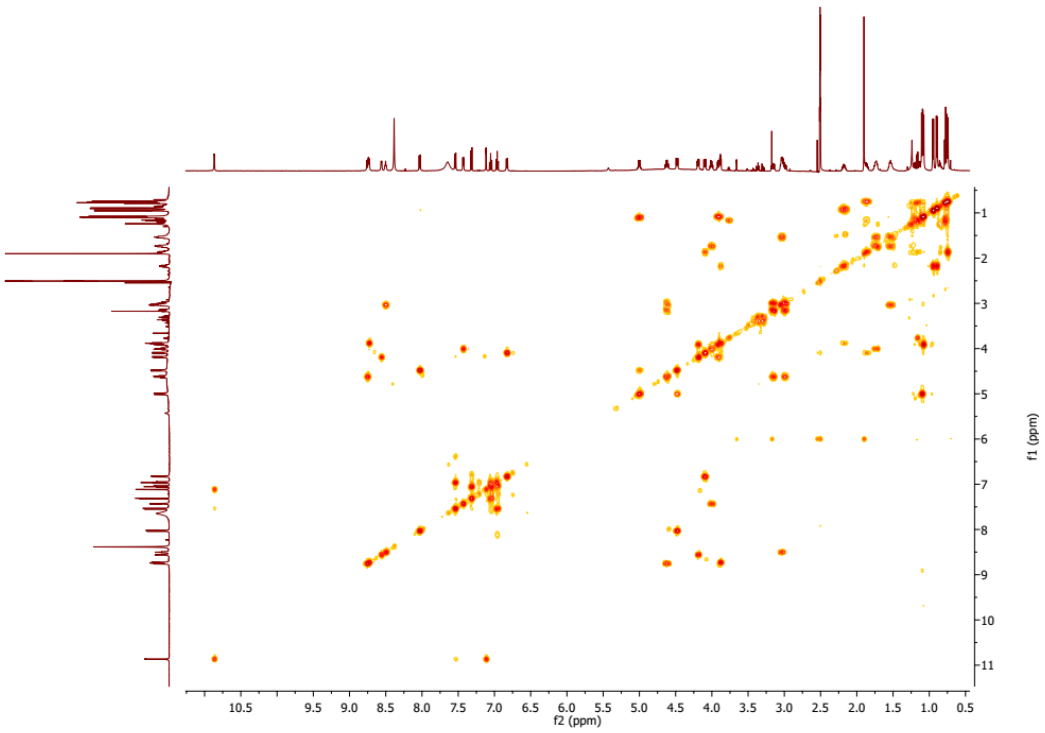

Figure S48. ^{1}H-^{1}H COSY spectrum of compound **26**.

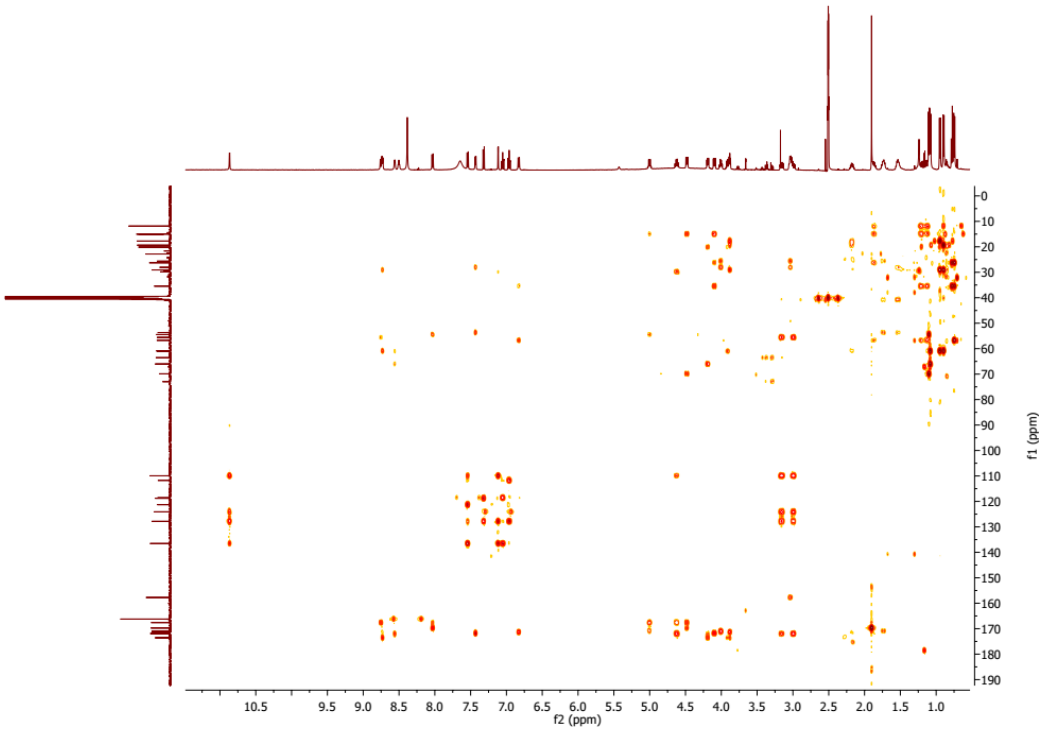

Figure S49. HMBC spectrum of compound **26**.

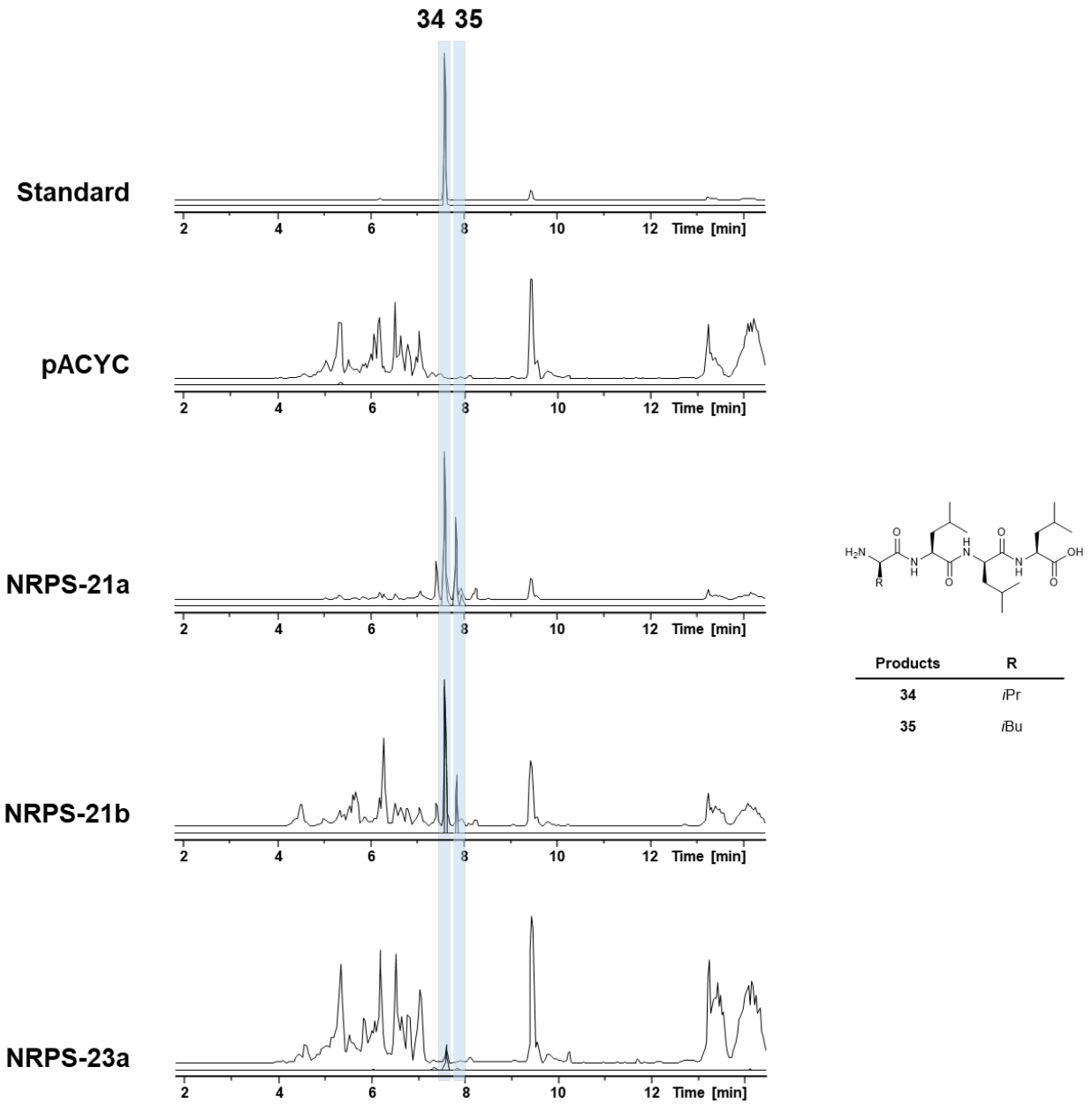

Figure S50. HPLC/MS data refers to Figure 4 (NRPS-21 and -23) of compound **34** and **35** produced in *E. coli* DH10B::*mtaA*. Base Peak Chromatogram (BPC, top) and Extracted Ion Chromatogram (EIC, below) of **34** (*m/z* $[M+H]^+$ = 457.34) and **35** (*m/z* $[M+H]^+$ = 471.35). Chromatograms were compared to an empty vector control and a synthetic standard of compound **34** (*m/z* $[M+H]^+$ = 457.34).

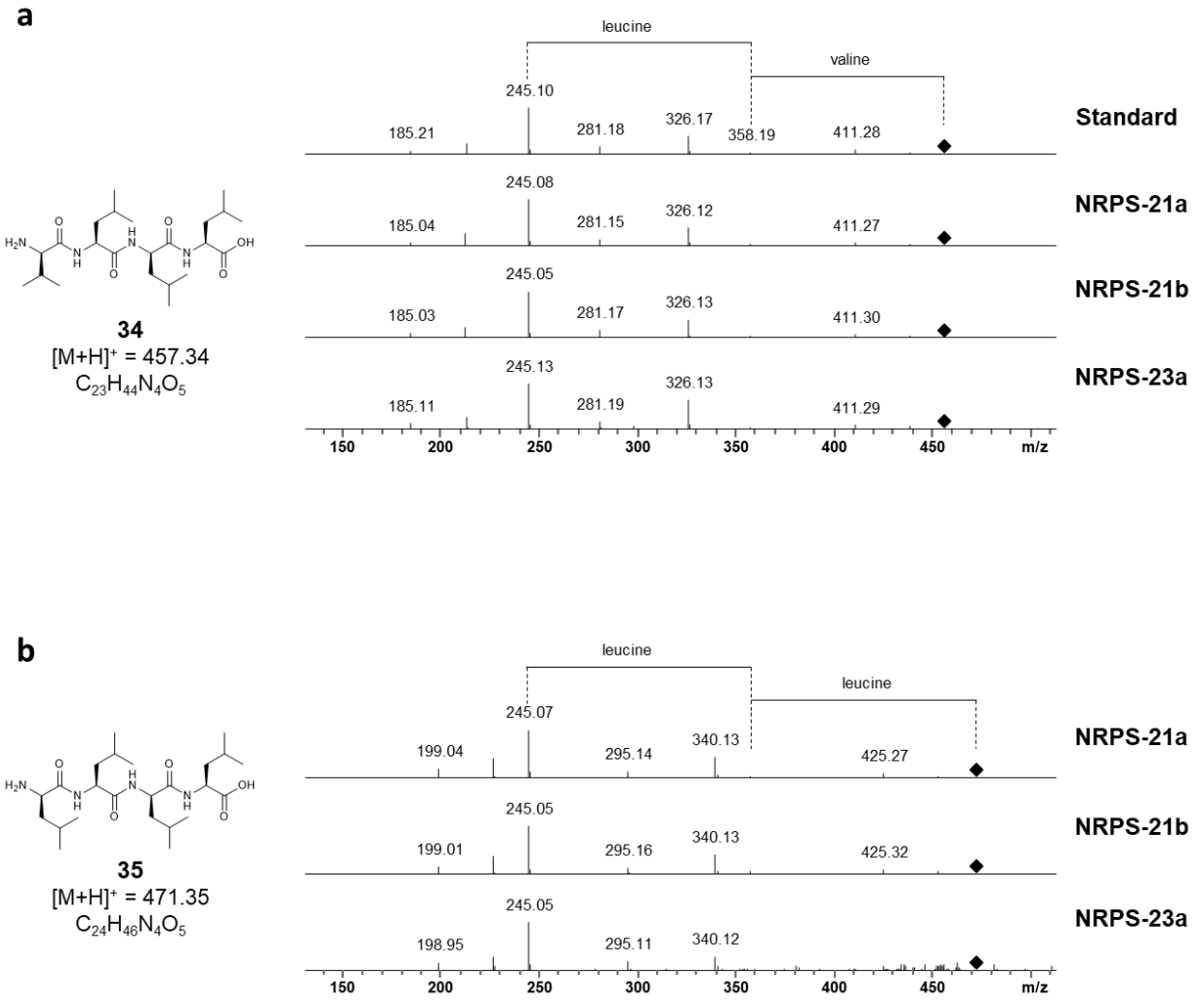

Figure S51. a) HPLC/MS data refers to Figure 4 (NRPS-21 and -23) of compound **34** produced in *E. coli* DH10B::*mtaA*. MS^2 and amino acid fragmentation of compound **34** produced by NRPS-21 and -23 compared to a synthetic standard of compound **34**. **b**) HPLC/MS data refers to Figure 4 (NRPS-21 and -23) of compound **35** produced in *E. coli* DH10B::*mtaA*. MS^2 and amino acid fragmentation of compound **35** produced by NRPS-21 and -23.

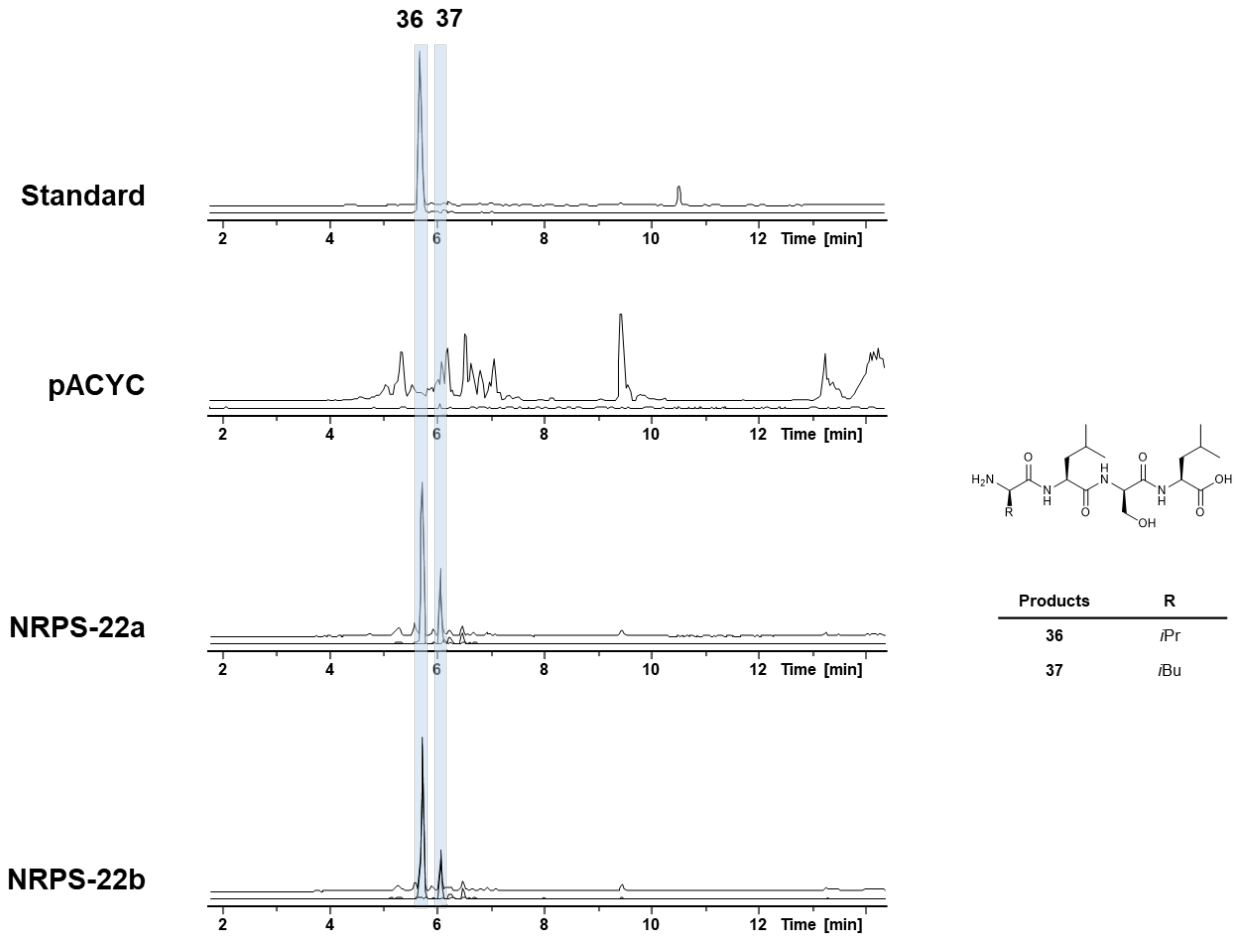

Figure S52. HPLC/MS data refers to Figure 4 (NRPS-22) of compound **36** and **37** produced in *E. coli* DH10B::*mtaA*. Base Peak Chromatogram (BPC, top) and Extracted Ion Chromatogram (EIC, below) of **36** (*m/z* $[M+H]^+$ = 431.28) and **37** (*m/z* $[M+H]^+$ = 445.30). Chromatograms were compared to an empty vector control and a synthetic standard of compound **36** (*m/z* $[M+H]^+$ = 431.28).

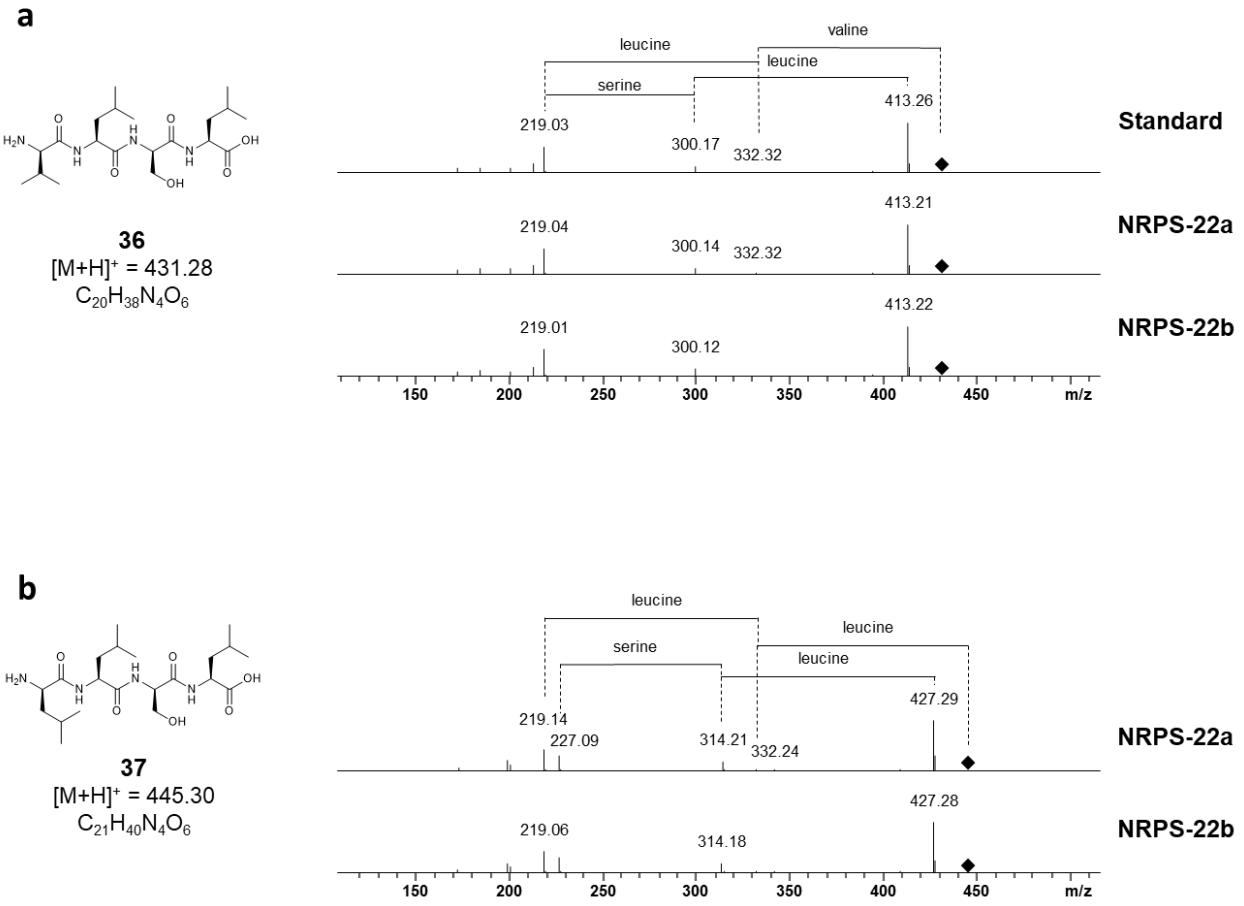

Figure S53. a) HPLC/MS data refers to Figure 4 (NRPS-22) of compound **36** produced in *E. coli* DH10B::*mtaA*. MS^2 and amino acid fragmentation of compound **36** produced by NRPS-22 compared to a synthetic standard of compound **36**. **b**) HPLC/MS data refers to Figure 4 (NRPS-22) of compound **37** produced in *E. coli* DH10B::*mtaA*. MS^2 and amino acid fragmentation of compound **37** produced by NRPS-22.

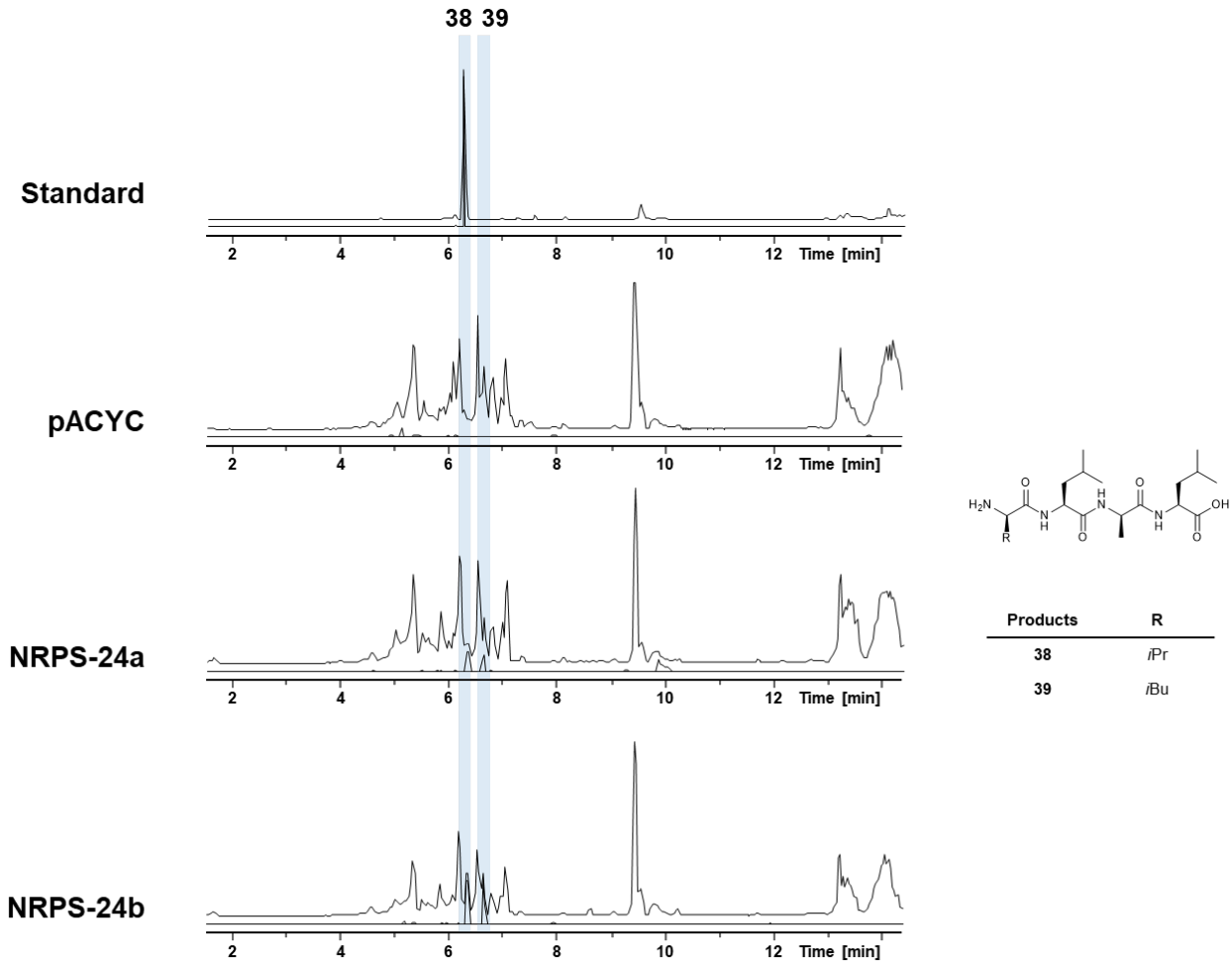

Figure S54. HPLC/MS data refers to Figure 4 (NRPS-24) of compound **38** and **39** produced in *E. coli* DH10B::*mtaA*. Base Peak Chromatogram (BPC, top) and Extracted Ion Chromatogram (EIC, below) of **38** (*m/z* $[M+H]^+$ = 415.29) and **39** (*m/z* $[M+H]^+$ = 429.31). Chromatograms were compared to an empty vector control and a synthetic standard of compound **38** (*m/z* $[M+H]^+$ = 415.29).

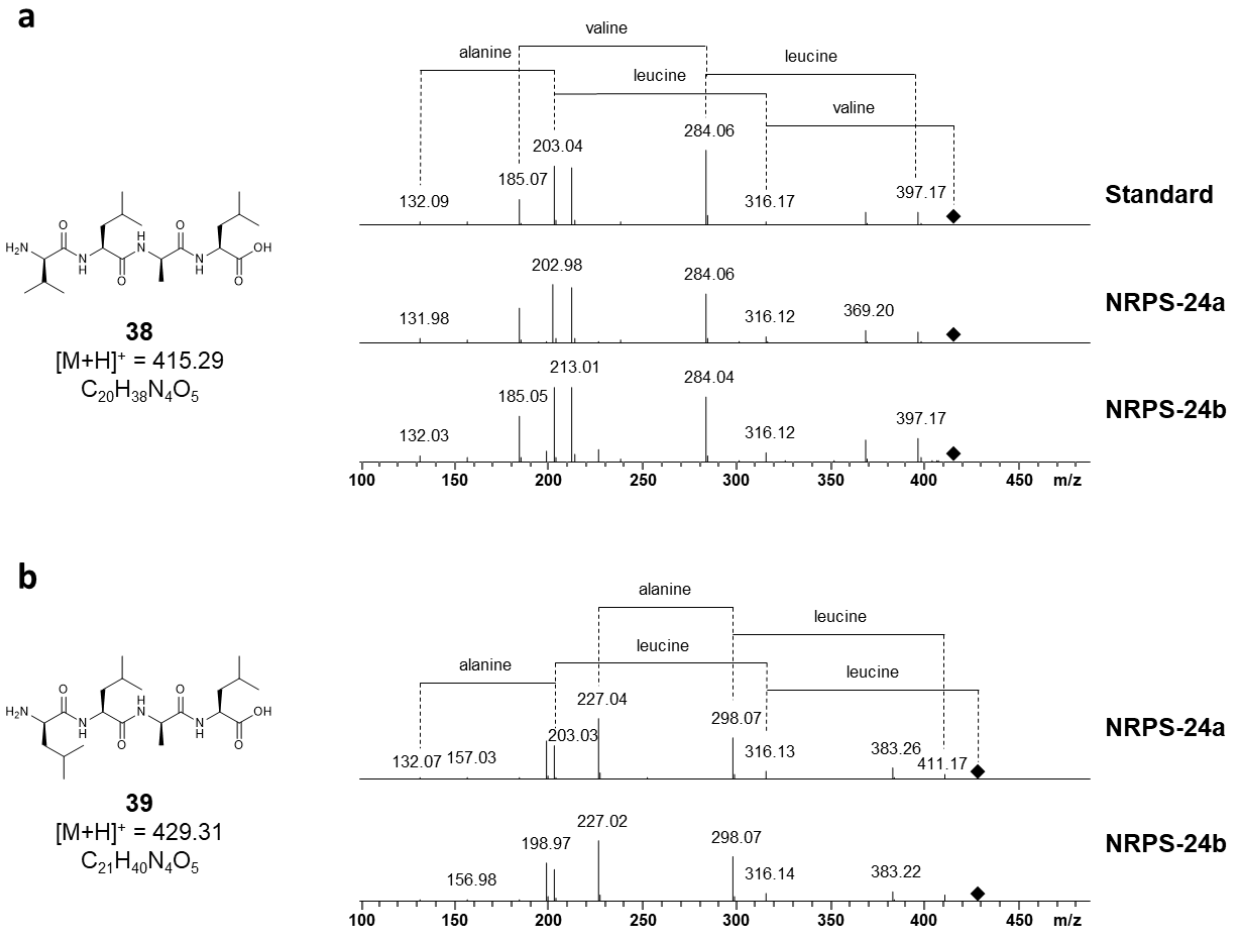

Figure S55. a) HPLC/MS data refers to Figure 4 (NRPS-24) of compound **38** produced in *E. coli* DH10B::*mtaA*. MS^2 and amino acid fragmentation of compound **38** produced by NRPS-24 compared to a synthetic standard of compound **38**. **b**) HPLC/MS data refers to Figure 4 (NRPS-24) of compound **39** produced in *E. coli* DH10B::*mtaA*. MS^2 and amino acid fragmentation of compound **39** produced by NRPS-24.

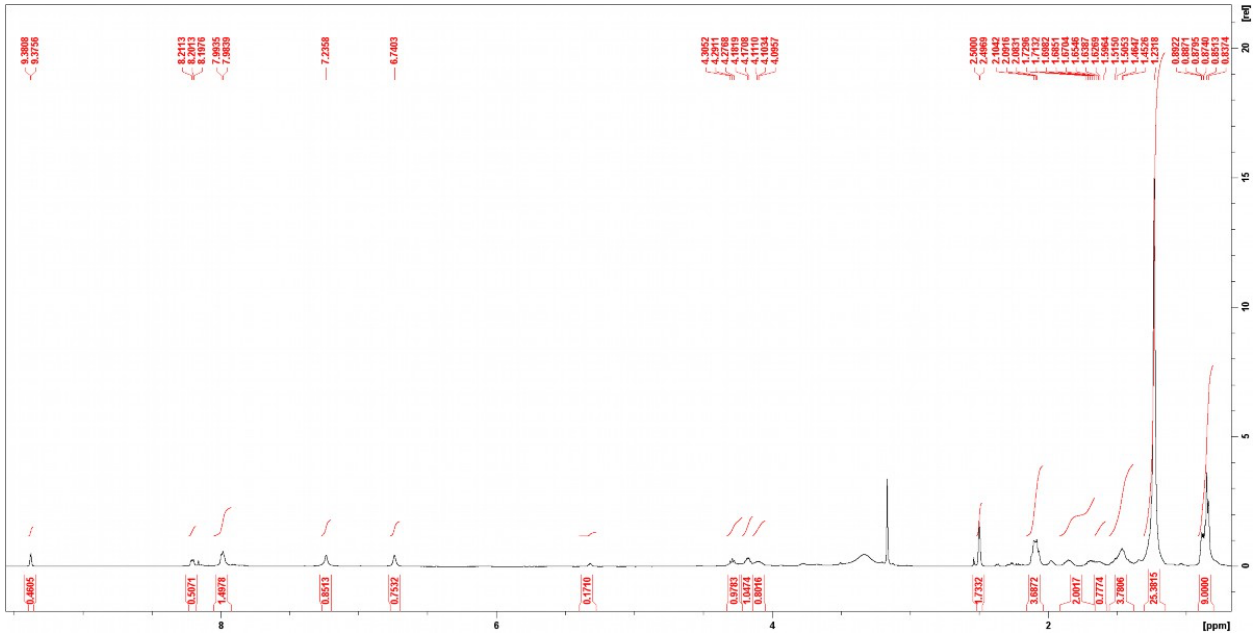

Figure S56. ^{1}H NMR (500 MHz, DMSO-d_6) spectrum compound **41**.

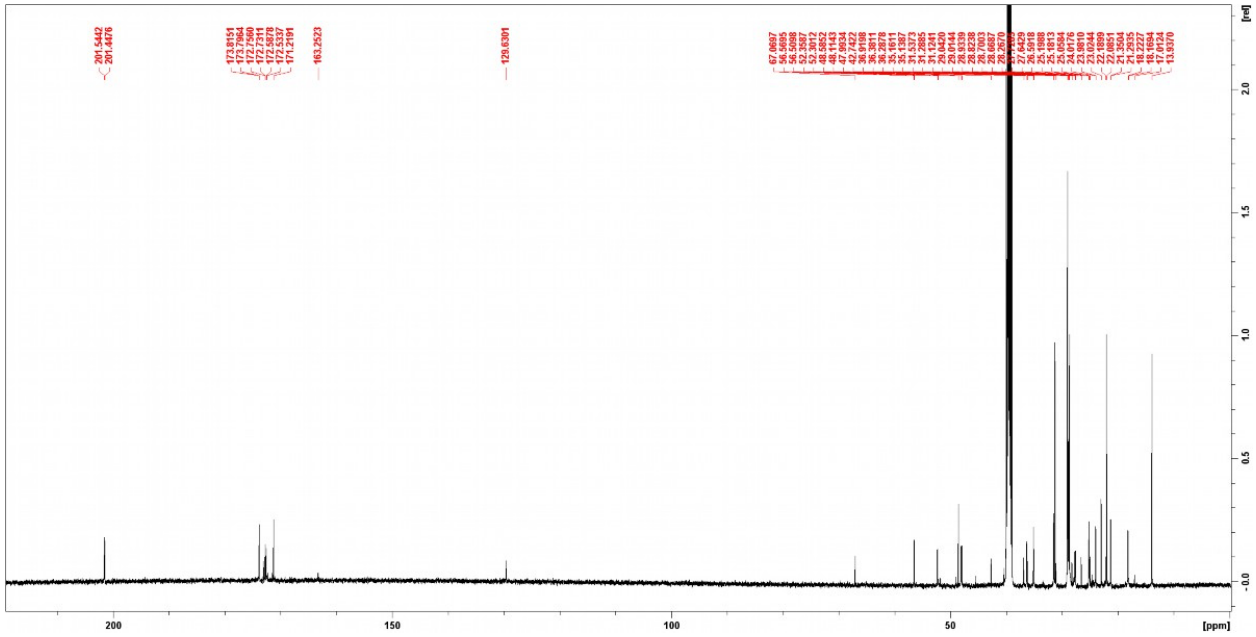

Figure S57. ^{13}C NMR (125 MHz, DMSO-d_6) spectrum compound **41**.

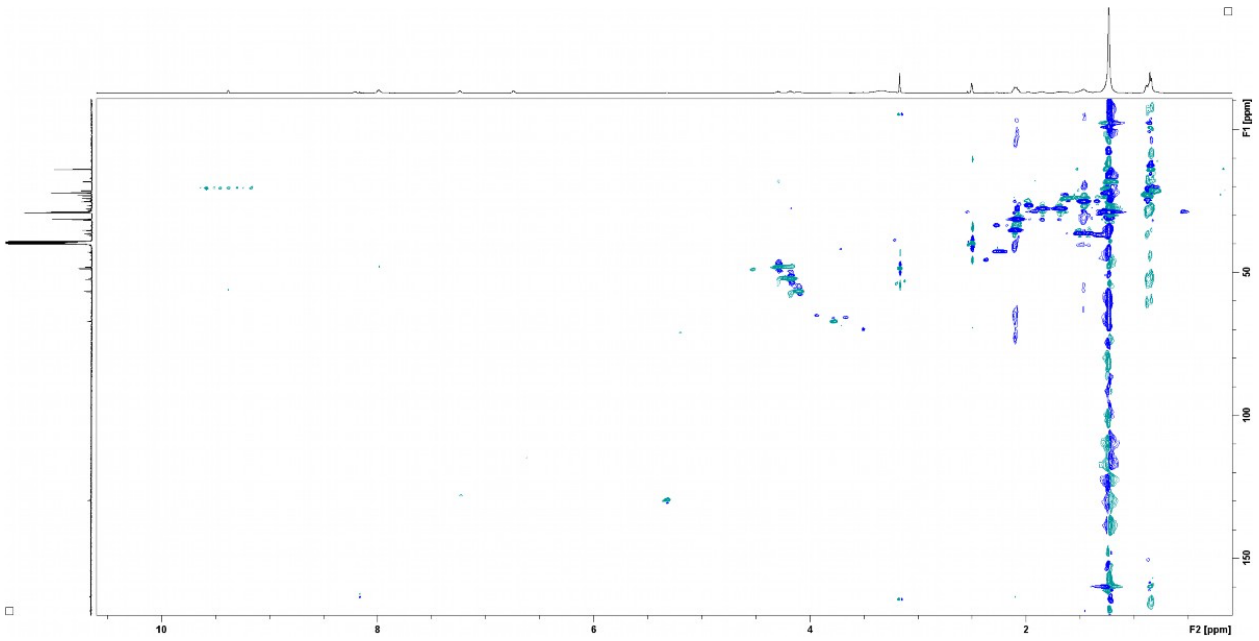

Figure S58. HSQC (DMSO-d6) spectrum of compound **41**.

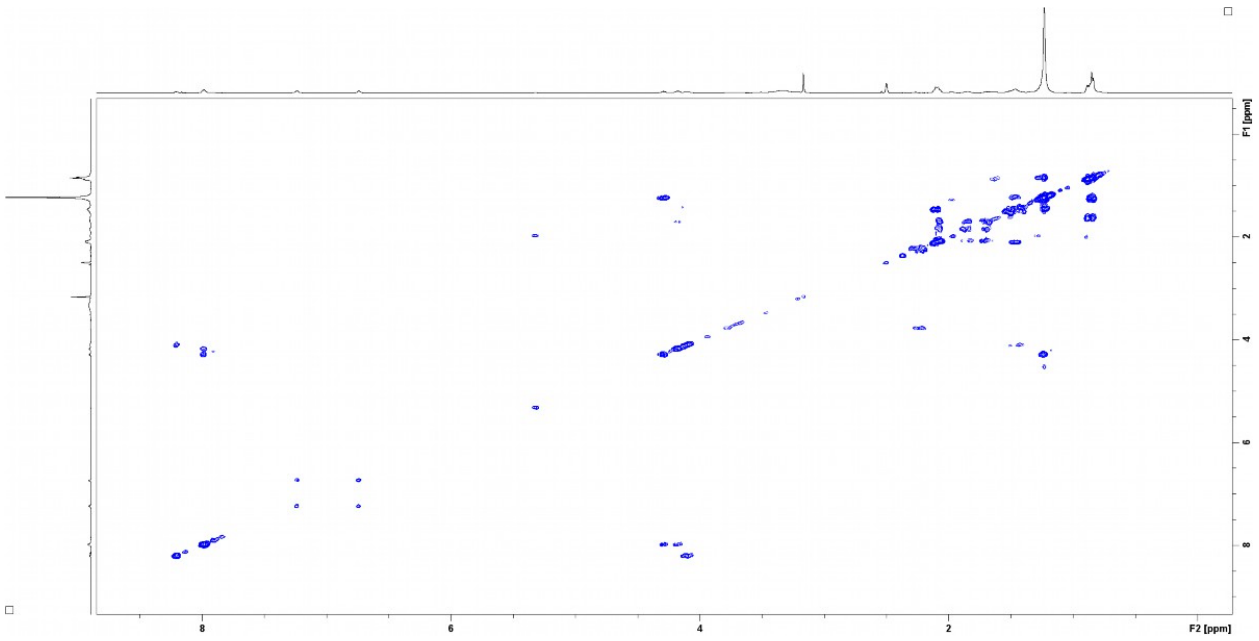

Figure S59. ^{1}H-^{1}H COSY (DMSO-d6) spectrum compound **41**.

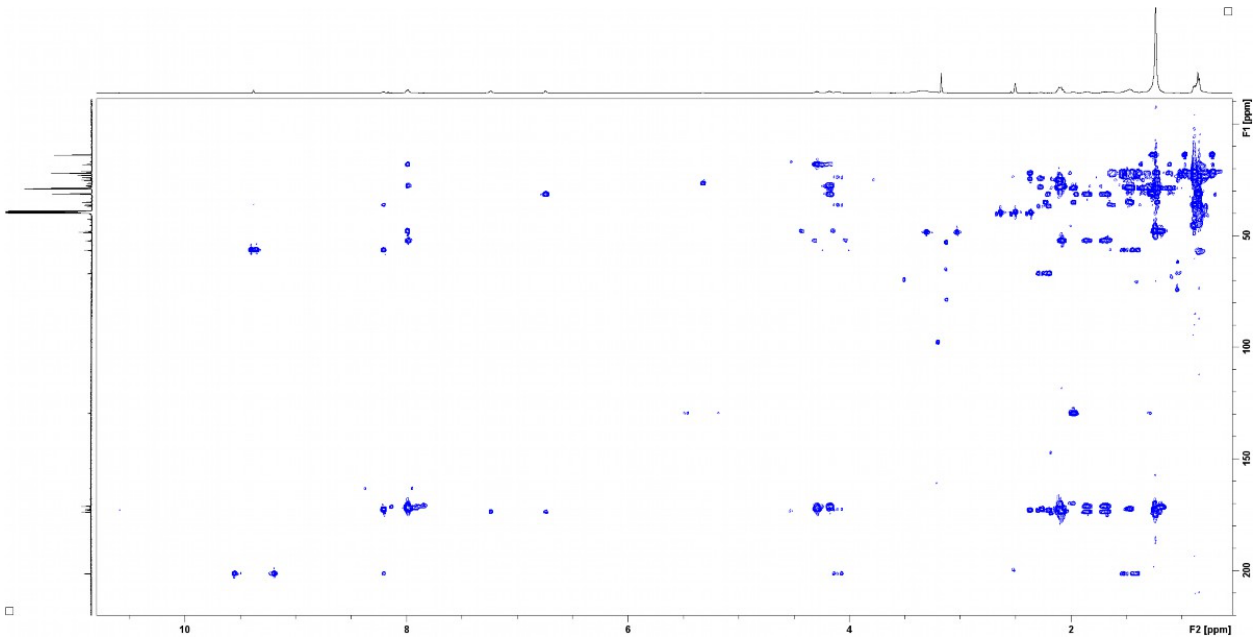

Figure S60. HMBC (DMSO-d6) spectrum compound **41**.

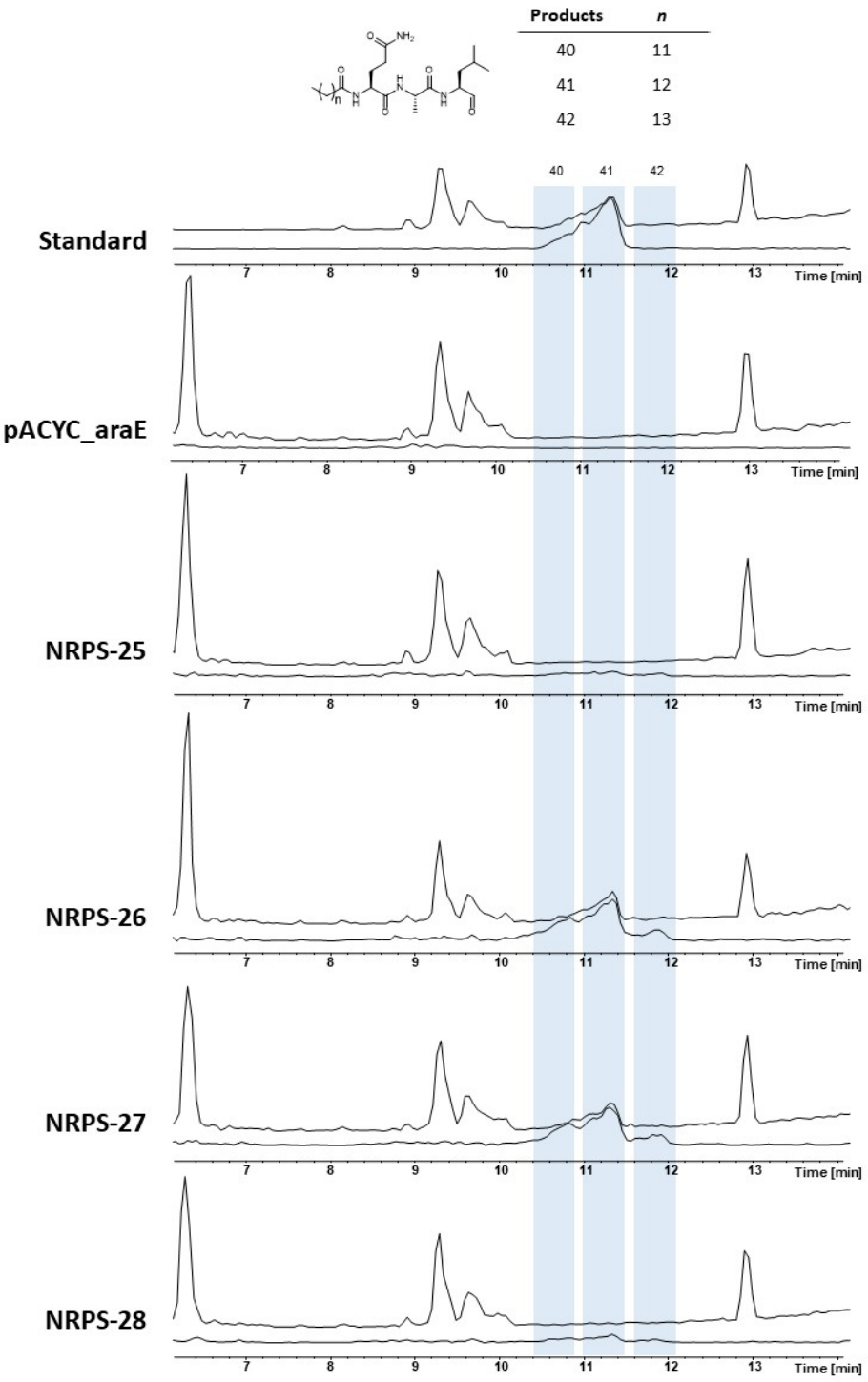

Figure 61. HPLC/MS data refers to Figure 5 (NRPS-25-28) of compound **40**, **41** and **42** produced in *E. coli* DH10B::*mtaA*. Base Peak Chromatogram (BPC, top) and Extracted Ion Chromatogram (EIC, below) of **40** (*m/z* $[M+H]^+$ = 511.38), **41** (*m/z* $[M+H]^+$ = 525.40), **42** (*m/z* $[M+H]^+$ = 539.41). Chromatograms were compared to an empty vector control and a purified compound **42** standard (*m/z* $[M+H]^+$ = 525.40).

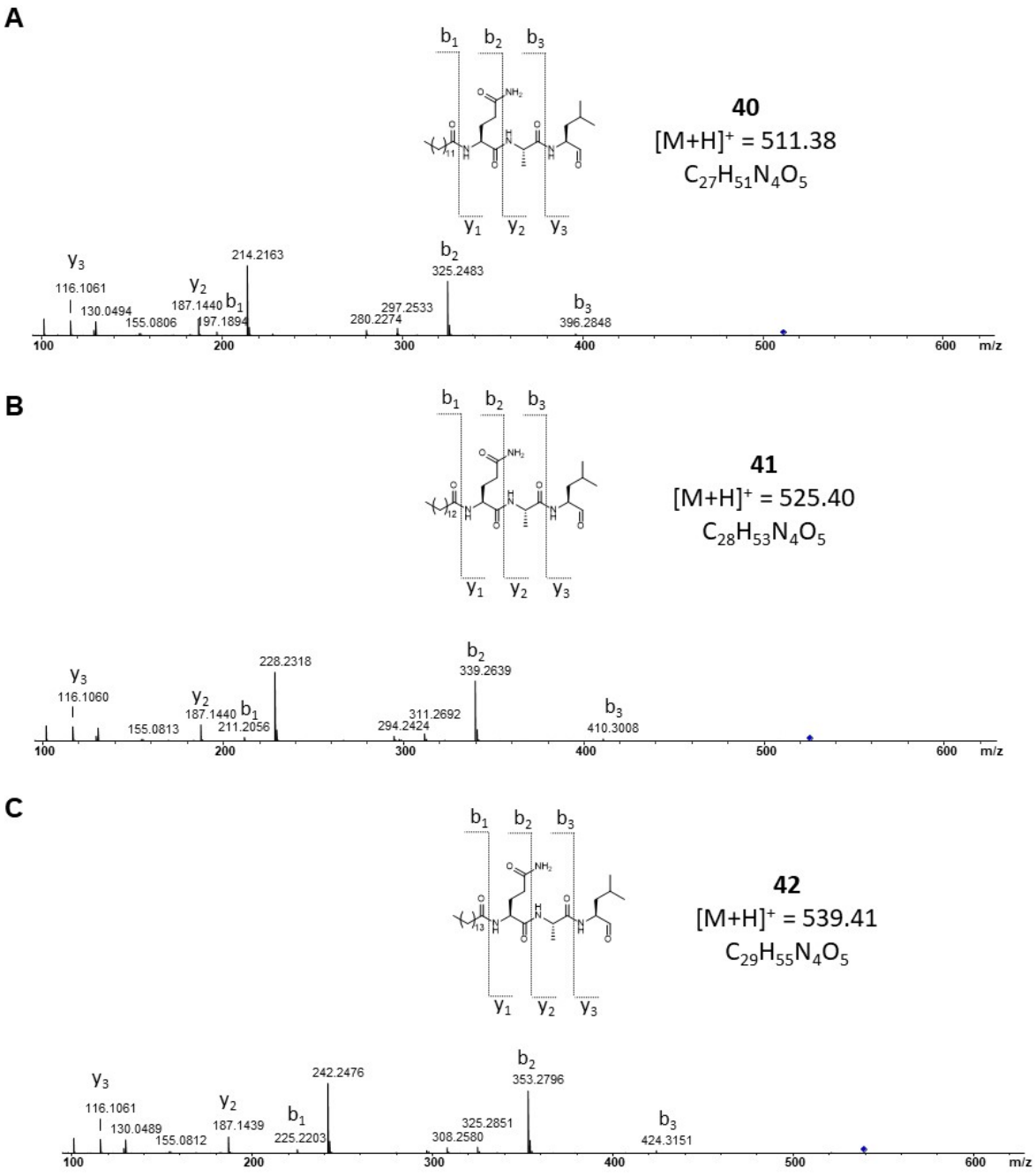

Figure S62. HPLC/MS data refers to Figure 5 (NRPS-26) of compound **40** (A), **41** (B) and **42** (C) produced in *E. coli* DH10B::*mtaA*. Comparison of MS^2 spectra.

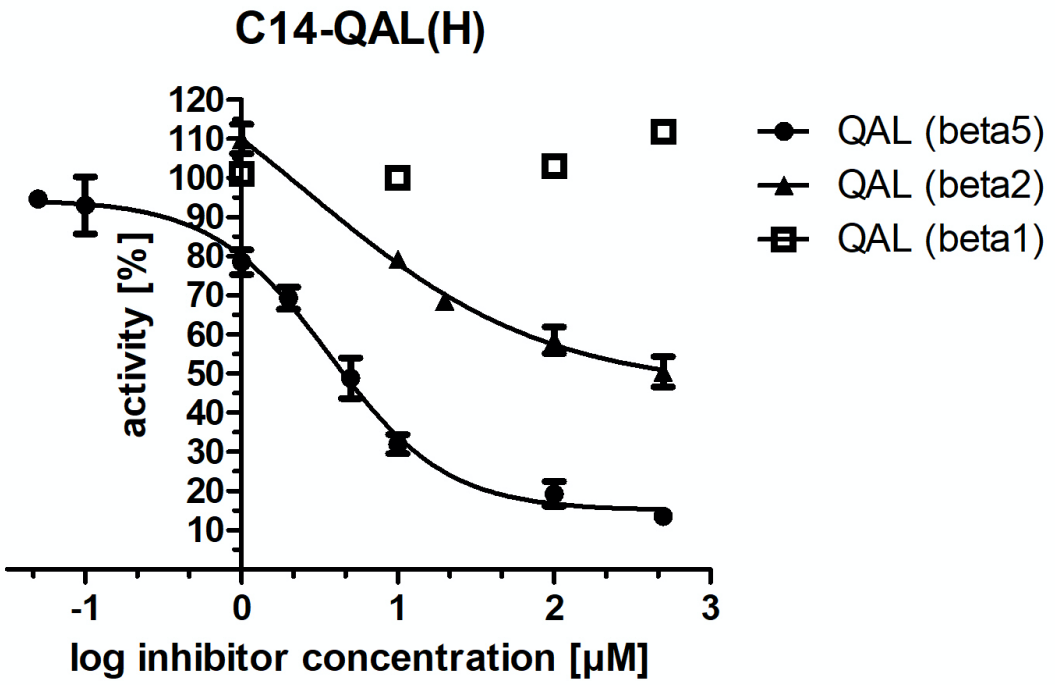

Figure S63. IC_{50} determination of compound **41** (termed as C14-QAL(H)) for subunits beta1, -2 and -5 of yeast 20S proteasome (yCP).

References

1 Bode, E. *et al.* Promoter Activation in Δ hfq Mutants as an Efficient Tool for Specialized Metabolite Production Enabling Direct Bioactivity Testing. *Angewandte Chemie* **131**, 19133-19139, doi:10.1002/ange.201910563 (2019).

2 Bozhueyuek, K. A. J., Watzel, J., Abbood, N. & Bode, H. B. Synthetic Zippers as an Enabling Tool for Engineering of Non-Ribosomal Peptide Synthetases**. *Angewandte Chemie* **133**, 17672-17679, doi:10.1002/ange.202102859 (2021).

3 Gallastegui, N. & Groll, M. Analysing properties of proteasome inhibitors using kinetic and X-ray crystallographic studies. *Methods Mol Biol* **832**, 373-390, doi:10.1007/978-1-61779-474-2_26 (2012).

4 Groll, M. & Huber, R. Purification, crystallization, and X-ray analysis of the yeast 20S proteasome. *Methods Enzymol* **398**, 329-336, doi:10.1016/S0076-6879(05)98027-0 (2005).

5 Kabsch, W. *XDS*. *Acta Crystallographica Section D Biological Crystallography* **66**, 125-132, doi:10.1107/s0907444909047337 (2010).

6 Schneider, T. R. & Sheldrick, G. M. Substructure solution with SHELXD. *Acta Crystallogr D Biol Crystallogr* **58**, 1772-1779, doi:10.1107/s0907444902011678 (2002).

7 Huber, E. M. *et al.* A unified mechanism for proteolysis and autocatalytic activation in the 20S proteasome. *Nature Communications* **7**, 10900, doi:10.1038/ncomms10900 (2016).

8 Emsley, P., Lohkamp, B., Scott, W. G. & Cowtan, K. Features and development of *Coot*. *Acta Crystallographica Section D Biological Crystallography* **66**, 486-501, doi:10.1107/s0907444910007493 (2010).

9 Edgar, R. C. MUSCLE: multiple sequence alignment with high accuracy and high throughput. *Nucleic Acids Res* **32**, 1792-1797, doi:10.1093/nar/gkh340 (2004).

10 Capella-Gutierrez, S., Silla-Martinez, J. M. & Gabaldon, T. trimAl: a tool for automated alignment trimming in large-scale phylogenetic analyses. *Bioinformatics* **25**, 1972-1973, doi:10.1093/bioinformatics/btp348 (2009).
11 Maddison, W. & Maddison, D. R. Mesquite: A modular system for evolutionary analysis. *Evolution* **62**, 1103-1108 (2008).
12 Revell, L. J. phytools: an R package for phylogenetic comparative biology (and other things). *Methods in Ecology and Evolution* **3**, 217-223, doi:10.1111/j.2041-210X.2011.00169.x (2012).
13 Durfee, T. *et al.* The Complete Genome Sequence of *Escherichia coli* DH10B: Insights into the Biology of a Laboratory Workhorse. *Journal of Bacteriology* **190**, 2597-2606, doi:10.1128/jb.01695-07 (2008).
14 Schimming, O., Fleischhacker, F., Nollmann, F. I. & Bode, H. B. Yeast Homologous Recombination Cloning Leading to the Novel Peptides Ambactin and Xenolindicin. *ChemBioChem* **15**, 1290-1294, doi:10.1002/cbic.201402065 (2014).
15 Goldman, B. S. *et al.* Evolution of sensory complexity recorded in a myxobacterial genome. *Proceedings of the National Academy of Sciences* **103**, 15200-15205, doi:10.1073/pnas.0607335103 (2006).
16 Krug, D. *et al.* Discovering the hidden secondary metabolome of Myxococcus xanthus: a study of intraspecific diversity. *Appl Environ Microbiol* **74**, 3058-3068, doi:10.1128/AEM.02863-07 (2008).
17 Kissoyan, K. A. B. *et al.* Natural C. elegans Microbiota Protects against Infection via Production of a Cyclic Lipopeptide of the Viscosin Group. *Current Biology* **29**, 1030-1037.e1035, doi:10.1016/j.cub.2019.01.050 (2019).
18 Petersen, L. M. & Tisa, L. S. Influence of temperature on the physiology and virulence of the insect pathogen Serratia sp. Strain SCBI. *Appl Environ Microbiol* **78**, 8840-8844, doi:10.1128/AEM.02580-12 (2012).
19 Joyce, S. A. & Clarke, D. J. A hexA homologue from Photorhabdus regulates pathogenicity, symbiosis and phenotypic variation. *Molecular Microbiology* **47**, 1445-1457, doi:10.1046/j.1365-2958.2003.03389.x (2003).
20 Tobias, N. J. *et al.* Natural product diversity associated with the nematode symbionts Photorhabdus and Xenorhabdus. *Nature Microbiology* **2**, 1676-1685, doi:10.1038/s41564-017-0039-9 (2017).
21 Behsaz, B. *et al.* Integrating genomics and metabolomics for scalable non-ribosomal peptide discovery. *Nature Communications* **12**, doi:10.1038/s41467-021-23502-4 (2021).
22 Lorenzen, W., Ahrendt, T., Bozhüyük, K. A. J. & Bode, H. B. A multifunctional enzyme is involved in bacterial ether lipid biosynthesis. *Nature Chemical Biology* **10**, 425-427, doi:10.1038/nchembio.1526 (2014).
23 Kegler, C. & Bode, H. B. Artificial Splitting of a Non-Ribosomal Peptide Synthetase by Inserting Natural Docking Domains. *Angewandte Chemie* **132**, 13565-13569, doi:10.1002/ange.201915989 (2020).
24 Fuchs, S. W., Proschak, A., Jaskolla, T. W., Karas, M. & Bode, H. B. Structure elucidation and biosynthesis of lysine-rich cyclic peptides in Xenorhabdus nematophila. *Organic & Biomolecular Chemistry* **9**, 3130, doi:10.1039/c1ob05097d (2011).
25 Vo, T. D., Spahn, C., Heilemann, M. & Bode, H. B. Microbial Cationic Peptides as a Natural Defense Mechanism against Insect Antimicrobial Peptides. *ACS Chemical Biology* **16**, 447-451, doi:10.1021/acschembio.0c00794 (2021).
26 Sievers, F. & Higgins, D. G. Clustal Omega for making accurate alignments of many protein sequences. *Protein Sci* **27**, 135-145, doi:10.1002/pro.3290 (2018).
27 Blin, K. *et al.* antiSMASH 6.0: improving cluster detection and comparison capabilities. *Nucleic Acids Res* **49**, W29-W35, doi:10.1093/nar/gkab335 (2021).
28 Niehs, S. P. *et al.* Genome Mining Reveals Endopyrroles from a Nonribosomal Peptide Assembly Line Triggered in Fungal–Bacterial Symbiosis. *ACS Chemical Biology* **14**, 1811-1818, doi:10.1021/acschembio.9b00406 (2019).
29 Wang, X. *et al.* Discovery of recombinases enables genome mining of cryptic biosynthetic gene clusters in Burkholderiales species. *Proc Natl Acad Sci U S A* **115**, E4255-E4263, doi:10.1073/pnas.1720941115 (2018).
30 Isogai, A. *et al.* Structural Analysis of New Syringopeptins by Tandem Mass Spectrometry. *Bioscience, Biotechnology, and Biochemistry* **59**, 1374-1376, doi:10.1271/bbb.59.1374 (1995).